Stressful environments:

Motility and catecholamine response in *Vibrio cholerae*

Dissertation zur Erlangung des

Doktorgrades der Naturwissenschaften

Fakultät Naturwissenschaften

Universität Hohenheim

Institut für Mikrobiologie

vorgelegt von

Dipl.-Biol. Petra Halang

aus München, Deutschland

Stuttgart, 2014

Dekan: Prof. Dr. Heinz Breer

Referent: Prof. Dr. Julia Fritz-Steuber

Korreferent: Prof. Dr. Wolfgang Hanke

Eingereicht am: 26.02.2014

Tag der mündlichen Prüfung: 03.07.2014

Eidesstattliche Versicherung gemäß § 7 Absatz 7 der Promotionsordnung der Universität Hohenheim zum Dr. rer. nat.

- Bei der eingereichten Dissertation zum Thema **"Stressful environments: Motility and catecholamine response in *Vibrio cholerae*"** handelt es sich um meine eigenständig erbrachte Leistung.
- Ich habe nur die angegebenen Quellen und Hilfsmittel benutzt und mich keiner unzulässigen Hilfe Dritter bedient. Insbesondere habe ich wörtlich oder sinngemäß aus anderen Werken übernommene Inhalte als solche kenntlich gemacht.
- Ich habe nicht die Hilfe einer kommerziellen Promotionsvermittlung oder –beratung in Anspruch genommen.
- Die Bedeutung der eidesstattlichen Versicherung und der strafrechtlichen Folgen einer unrichtigen oder unvollständigen eidesstattlichen Versicherung sind mir bekannt.

Die Richtigkeit der vorstehenden Erklärung bestätige ich: Ich versichere an Eides Statt, dass ich nach bestem Wissen die reine Wahrheit erklärt und nichts verschwiegen habe.

Die vorliegende Arbeit wurde im Zeitraum vom 15.07.2010 bis zum 30.09.2013 am Institut für Mikrobiologie, Universität Hohenheim unter der Leitung von Frau Prof. Julia Fritz-Steuber angefertigt.

Petra Halang

To Stephan

Abstract

The human pathogen *Vibrio cholerae* is able to inhabit a variety of environments. These include especially aquatic ecosystems, but the human intestine as well. *V. cholerae* is thus tolerant to a wide range of salinity and pH. Motility is achieved by a sodium driven polar flagellum. The affinity for Na^+ to run the flagellum is determined by the stator complex PomAB, which is embedded in the cell membrane within the flagellar motor. A critical aminoacid residue for the binding of Na^+ is aspartate 23 within the transmembrane helix of PomB. A mutation of this aminoacid residue leads to an immotile phenotype of *V. cholerae*.

It was thus of interest to investigate if other polar or acidic aminoacid residues within PomB are important for the passage of Na^+. Two potential candidates are serine at position 26 and aspartate at position 42 of PomB, both aminoacid residues are conserved within sodium driven flagellar stator complexes. To characterize the pathway of Na^+ through the PomAB channel, the influence of chloride salts (Na^+ and K^+) and the pH on the motility of *V. cholerae* was studied. Motility decreased at elevated pH but increased if a chaotropic chloride salt was added, which excludes a direct Na^+ and H^+ competition in the process of binding to the conserved PomB D23 residue. Cells expressing the PomB S26A/T or D42N variants lost motility at low Na^+ concentrations but regained motility in the presence of 170 mM chloride. The swimming speeds of individual cells were also analyzed and revealed that S26 located within the membrane helix of PomB is required to promote very fast swimming of *V. cholerae*. Loss of hypermotility was observed with the S26T variant of PomB which was partially restored by lowering the pH of the external medium. Modification of PomA and PomB by N,N'-dicyclohexylcarbodiimide indicates the presence of protonated carboxyl groups in the hydrophobic regions of the two proteins. Na^+ did not protect PomA and PomB from this modification. It could be demonstrated that the motility of *V. cholerae* is influenced by the pH and osmolality of

the medium and thus, the aminoacid residues – S26 and D42 together with D23 – of PomB have a function in the passage of Na^+ into the cell. The H^+ rather than the Na^+ concentration determines the efficiency of the motor, indicating the presence of a catalytical important hydrogen bond network in the motor channel. It is proposed that D23, S26 and D42 of PomB are part of an ion-conducting pathway formed by the PomAB stator complex.

As mentioned above, *V. cholerae* is a pathogen which settles the human intestine. As other pathogens are able to respond specifically to the stress associated mammalian hormones epinephrine and norepinephrine it was of an interest to investigate the influence of these hormones on growth and motility of *V. cholerae*. The response to epinephrine and norepinephrine is mediated by the QseC sensor protein. The genome of *V. cholerae* comprises a gene which is homolog to *qseC* from *E. coli*. Growth and swarming of *V. cholerae* was enhanced in the presence of 0.1 mM epinephrine or norepinephrine. qRT-PCR experiments revealed increased expression of the genes encoding the putative sensor kinase *qseC* and *pomB*, a component of the flagellar motor complex under the influence of catecholates. HPLC measurements of bacterial supernatant revealed that norepinephrine is completely degraded or metabolized after 48 h in the presence of *V. cholerae*, concomitant with the appearance of another, unidentified compound. On the other hand, *V. cholerae* seemed to stabilize epinephrine. After 48 h, 0.46 % of the epinephrine added at the beginning of the growth experiment was retained. Again, a yet unidentified compound was detected. The experiments conducted in this work strongly indicate the presence of a catecholate receptor in *V. cholerae*.

Zusammenfassung

Das für den Menschen pathogene Bakterium *Vibrio cholerae* ist in der Lage eine Vielzahl von unterschiedlichen Lebensräumen zu besiedeln. Diese beinhalten vor allem aquatische Ökosysteme, aber auch den menschlichen Dünndarm. *V. cholerae* ist daher in der Lage sich einem breiten pH Bereich und unterschiedlichen Salzkonzentrationen in der Umgebung anzupassen. Beweglich wird *V. cholerae* durch den Besitz eines polaren Flagellums, welches durch Na^+ angetrieben wird. Die Affinität für Na^+ wird festgelegt durch den membranständigen Statorkomplex PomAB, welches innerhalb des Flagellenmotors liegt. Ein wichtiger Aminosäurerest für die Bindung von Na^+ ist hierbei das Aspartat 23 in der transmembranen Helix von PomB. Eine Mutation dieser Aminosäure führt zu einem immotilen Phänotyp von *V. cholerae*.

Es war daher von Interesse, andere polare oder saure Aminosäuren innerhalb von PomB zu untersuchen, die ebenfalls wichtig sein könnten für den Transport von Na^+. Zwei mögliche Kandidaten sind hierbei das Serin an Position 26 und das Aspartat an Position 42 von PomB. Beide Aminosäuren sind innerhalb der natriumbetriebenen Statorkomplexe konserviert. Um den Weg des Na^+ durch den PomAB Kanal zu charakterisieren, wurde der Einfluss von Chloridsalzen (Na^+ und K^+) im Medium und der pH des Mediums auf die Beweglichkeit von *V. cholerae* untersucht. Die Beweglichkeit nimmt unter erhöhtem pH ab, nimmt aber wieder zu, wenn chaotrope Chloridsalze dem Medium beigefügt wurde. Dies schließt eine direkte Konkurrenz um die Bindung an dem konservierten D23 in PomB zwischen Na^+ und H^+ aus. Zellen, die PomB S26A/T oder D42N Varianten exprimieren, waren unbeweglich bei niedrigen Na^+ Konzentrationen, erlangten ihre Beweglichkeit wieder durch die Zugabe von 170 mM Chlorid. Die Schwimmgeschwindigkeiten einzelner Zellen wurde ebenfalls in dieser Arbeit untersucht. Die Messungen ergaben, dass S26 in der transmembranen Helix von PomB wichtig ist, um sehr schnelle Schwimmgeschwindigkeiten zu erreichen. Hypermotilität in der S26T Variante von PomB konnte teilweise durch das

Absenken des pHs im Medium wiedererlangt werden. Die Modifizierung von PomA und PomB durch N,N'-dicyclohexylcarbodiimide deutet darauf hin, dass in den hydrophoben Regionen der beiden Proteine, protonierte Carboxylgruppen vorhanden sind. Na^+ konnte PomA und PomB nicht vor dieser Modifikation schützen. In dieser Arbeit konnte gezeigt werden, dass die Beweglichkeit von *V. cholerae* durch den pH und die Osmolalität des Mediums beinflusst wird. Die Aminosäuren S26 und D42 zusammen mit D23 von PomB spielen eine Rolle im Na^+ Transport in die Zelle. Außerdem prägt eher die H^+ als die Na^+ Konzentration der Umgebung die Effizienz des Motors, was auf ein katalytisch wichtiges Netz aus Wasserstoffbrückenbindungen hindeutet. Es wird postuliert, dass D23, S26 und D42 von PomB beim Transport von Na^+ durch den PomAB Kanal eine Rolle spielen.

Wie bereits oben erwähnt, ist *V. cholerae* in der Lage, den menschlichen Dünndarm zu besiedeln. Es ist bereits bekannt, dass andere pathogene Mikroorganismen in der Lage sind, auf die Stresshormone Adrenalin und Noradrenalin von Säugetieren zu reagieren. Es war daher von Interesse, den Einfluss dieser Hormone auf das Wachstum und die Beweglichkeit von *V. cholerae* hin zu untersuchen. Das membranständige Sensorprotein QseC erkennt in pathogenen Bakterien die Hormone Adrenalin und Noradrenalin. Und auch *V. cholerae* besitzt ein Gen, welches homolog ist zu *qseC* aus *E. coli*. Das Wachstum und Schwärmverhalten von *V. cholerae* wurde durch die Zugabe von 0.1 mM Adrenalin und Noradrenalin im Medium verstärkt. Außerdem stieg unter Einfluss der Katecholate die Expressionsrate der Gene *qseC*, welches für eine hypothetische Sensorkinase kodiert und *pomB*, welches für ein Protein des Flagellenmotors kodiert. Messungen des bakteriellen Überstandes mittels HPLC ergaben, dass nach 48 h Noradrenalin komplett in ein noch nicht näher charakterisiertes Produkt abgebaut oder von *V. cholerae* metabolisiert wurde. Auf der anderen Seite scheint *V. cholerae* Adrenalin im Medium zu stabilisieren. Nach 48 h konnte noch 0.46 % des zu Beginn der Experimente eingesetzten Adrenalins wiedergefunden werden. Aber auch hier wurde wieder ein noch nicht identifizierter Stoff detektiert. Die Experimente, die in dieser Arbeit durchgeführt wurden, deuten sehr stark darauf hin, dass *V. cholerae* ein Rezeptor für Katecholate besitzt.

Contents

Chapter A

Introduction

1 *Vibrio cholerae* – the causative agent of cholera.

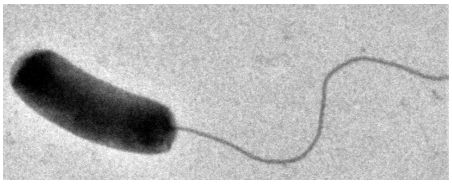

Figure A.1: Electron micrograph of *V. cholerae* O395 N1. Picture was taken by Sebastian Leptihn.

Vibrio cholerae was first described by Filippo Pacini in 1854 as the causative agent of cholera (21) but it was not before 1883 that it got known to the public. At this time, Robert Koch isolated *V. cholerae* out of deceased cholera patients and solved the transmission of the cholera infection. His discoveries and hygiene measures helped fighting the cholera outbreak in Hamburg in 1892 (82).

V. cholerae is a rod shaped, gram negative facultative anaerobe bacteria which belongs to the genus of *Vibrionaceae*. It is halophil and tolerant to alkaline conditions and most common in seawater or brackish water (80). Motility is achieved via a single polar flagellum which is driven by a sodium gradient (73, 102). There are plentiful of different strains of *V. cholerae* but only serotype O1 and O139 cause outbreaks of cholera (52).

This work was performed with an apathogenic *V. cholerae* strain which is regarded as safe to work with in laboratories of safety step 2 (S2 standard) (31). This strain is a derivative of the pathogenic strain *V. cholerae* Ogawa 395 in which the two copies of the *ctxA* genes were deleted (142).

1.1 Cholera – still a major risk for humans' health

Cholera is a severe illness which is triggered by the bacterium *V. cholerae*. It results in acute dehydration, caused by diarrhea and vomiting combined. Without treatment, lethality ranges between 20 % to 70 %. Most outbreaks occur in third world countries with poorly developed potable and sewage water systems (as seen in Fig. A.2). Cholera outbreaks may also appear after natural catastrophes, e.g. in october 2010 after a great earthquake in Haiti. Cholera is still ongoing in Haiti with currently 649.499 cases and over 8.000 deaths reported (updated April 10, 2013) (53).

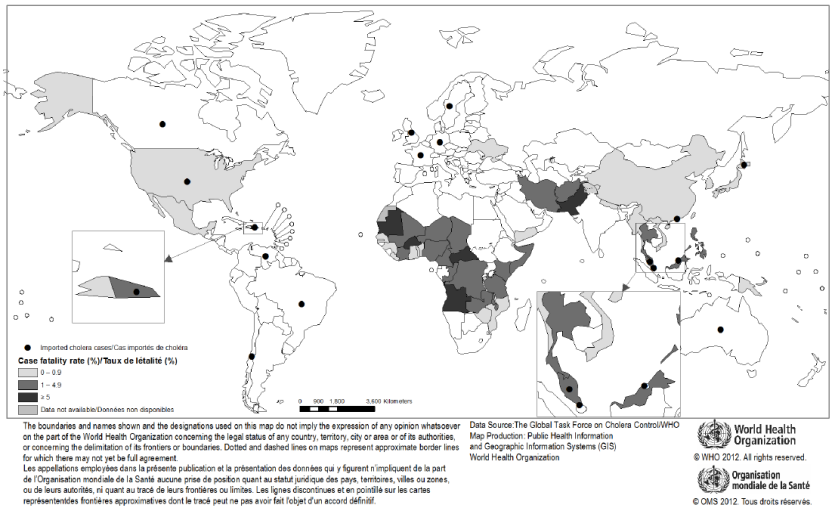

Figure A.2: Countries reporting cholera in 2011. Printed with permission of the WHO.

Most people get infected by consuming water or aliments contaminated with excrement. *V. cholerae* then starts to colonize the small intestine where it attaches itself to the epithelial cells. During reproduction, it secrets an enterotoxin – the cholera toxin (CTX) – which leads to an acute gastroenteritis.

The cholera toxin consists of five B subunits and one A subunit (Fig. A.3). Subunit A features an enzymatic activity and subunit B a targeting function, which binds on the luminal surface of the epithelial cells of the intestine (28, 176, 190). For liberating and activating subunit A, a proteolytic cleavage and a reduction of a disulfide bond is needed (141, 153). Finally in the cytosol, the A subunit catalyzes ADP-ribosylation of a GTP-binding regulatory protein ($G\alpha_s$) (61). As an increase in activation leads to a higher adenylate cyclase activity, the cAMP level rises and leads to an over-activation of protein kinase A which phosphorilates chloride channel proteins. The efflux of chloride

ions results in a secretion of water, Na^+, K^+ and HCO_3^- (167), finally causing diarrhea and vomiting.

1.2 The life cycle of *V. cholerae*

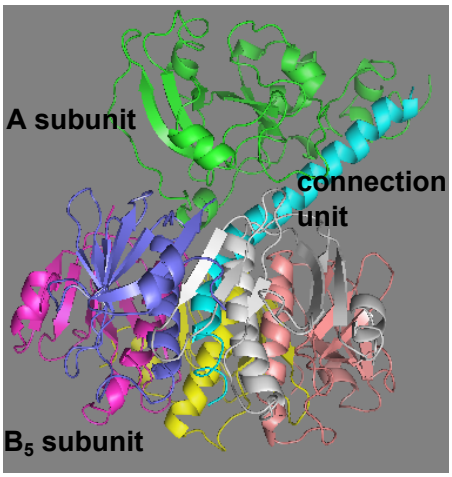

Figure A.3: Crystal structure of the cholera toxin. Subunit A (green) is connected via a connection unit (blue) to the five B subunits. Structure was drawn with Pymol, pdb-file: 1XTC, after (239).

V. cholerae is a natural inhabitant of brackish or seawater where it can be found in planktonic form as single, free swimming cells. But as Costerton and coworkers proposed, bacteria are rarely found in a free swimming phase in aquatic habitats (40). They are more likely to form associations on hard surfaces – either as a bacterial monolayer, forming micro-colonies or as complex organized, three-dimensional structures – named biofilms. It is supposed that biofilms confer an advantage in survival of aquatic microorganisms and support degradation and metabolization of complex compounds (40, 41). *V. cholerae* is known to form biofilms on plants, filamentous green algae, phytoplankton (e.g. cyanobacteria (88)), zooplankton (e.g. copepods (34, 84)), crustaceans and insects or egg masses of chironomid insects (67). As soon as *V. cholerae* participate in the formation of a biofilm, they are predominantly aflagellated and thus immotile.

Three steps are involved in the formation of biofilms. The initial step involves planktonic *V. cholerae* which are able to move directed and actively attach themselves on solid surfaces. After forming micro-colonies or single monolayers (step two) they eventually start building up a three-dimensional biofilm by producing exopolysaccharide (EPS) (225).

There are three well characterized pathways in *V. cholerae* which result in biofilm formation. First of all, there is a phase variation pathway which results in two morphological variants of *V. cholerae* called smooth and rugose. The latter variant is supposed to produce more EPS (33, 233, 234). A second pathway involves quorum-sensing. Deletion of HapR – a transcriptional regulator – also results in an enhanced production of EPS (68, 89, 214, 242). The third pathway is dependent on the polar flagellum. Deletion of *flaA* – which results in an aflagellated phenotype – promotes EPS production and

biofilm formation (226). The same results could be seen with strains which are disrupted in the flagellar motor (111).

Apart from existing in a free-swimming planktonic form or as an association in a biofilm, *V. cholerae* is also able to switch into a viable but non-culturable state when conditions in their surroundings change for the worse or when they form a biofilm (3). In this state, they are exhibiting a coccoid phenotype and it is not possible to reactivate them in conventional culture media (38). Nevertheless they remain potentially pathogenic (37, 38) and it is considered that non-culturable *Vibrios* living in a biofilm contribute mainly to the seasonal epidemics of cholera (1, 2).

1.3 Diversity and chromosomal organization of *V. cholerae*

The strain *V. cholerae* is a very heterogenous group with numerous different serotypes. But as mentioned before, only two serotypes (Inaba (AC) and Ogawa (AB)) and two biotypes (classical and El Tor) of the toxigenic O group 1 *V. cholerae* and serogroup O139 induce the outbreak of cholera (52). While serotype O1 causes the majority of outbreaks, serogroup O139 – which was first described in Bangladesh in 1992 (87) – provokes outbreaks mostly in the Southeast Asian region. Both strains can be identified by agglutination with their specific antiserum (O group 1-specific or O group-139 specific antiserum) against the lipopolysaccharide component of their cell wall, their ability to produce enterotoxins (cholera toxin CTX) and in the case of the O139 serogroup, the presence of a polysaccaride capsule (52, 91). This capsule protects the bacterium from serum bactericidal activity (90) and mediates adherence to epithelial cells (92).

Different factors play an important role in the ability of *V. cholerae* to colonize and initiate cholera in the host. Pathogenic strains possess genes which encode for the cholera toxin (CTX) and the toxin-coregulated pilus (TCP) – a colonization factor (94). These virulence factors are often encoded on bacteriophages (e.g. cholera toxin is encoded on CTXϕ (137, 222)), plasmids, chromosomal islands (e.g. VPI pathogenicity island (105)) or transposons and are able to be moved horizontally (158, 222) or vertically through a bacterial population which results in an increased evolutionary fitness to the bacteria (222).

In 2000 the complete genome of *V. cholerae* El Tor N16961 was sequenced by Heidelberg and coworkers. Genes are divided on two circular chromosomes of different sizes. Chromosome 1 consists of 2.961.146 base pairs, while the smaller chromosome 2 consists of 1.072.314 bp. Strikingly, there are approximately 100 duplications of ORF on each chromosome which were obtained by horizontal or lateral gene transfers. Genes which

are important for virulence of *V. cholerae* reside on chromosome 1. Sequence comparison revealed that chromosome 2 was originally a mega-plasmid which was gathered by an ancestral *Vibrio* species but it still remains unclear why chromosome 2 has not yet been incorporated into chromosome 1 (75).

2 The role of Na^+ or H^+ in membrane bioenergetics

Cells are enclosed compartments separated to their environment by a cellular membrane composed of a lipid bilayer. This membrane barrier ensures that compounds will not diffuse into or out of the cell along a gradient. Nevertheless it is important for the cell to absorb or discard molecules under controlled conditions. Therefore protein complexes are embedded into the cell membrane to perform tasks like the controlled transport of molecules and the creation of a chemical or electrical gradient and its conversion into useful work (47).

2.1 Generation of a sodium or proton motive force

To establish a chemical or electrical gradient along the cell membrane, primary membrane embedded pumps are necessary. These primary transport systems are able to transfer uncharged molecules (to build up a chemical gradient) or charged molecules (to additionally establish a membrane potential) along the cell membrane. These transport systems can be divided into pumps, which serve the cell directly without having a function in energy transduction (e.g. ATP driven importers or exporters, P-type ATPases) or pumps which can energize the cell membrane via an electrochemical ion gradient. This energy is utilized in different cellular processes, e.g. driving the flagellar motor (mechanical), synthesizing ATP (chemical) or gathering of nutrients (osmotic) (47).

Most bacteria use H^+ for these cellular processes, but current findings demonstrate that alkalophilic and thermophilic bacteria are able to use Na^+ as a coupling ion (71, 185, 191). The sodium cycle is also present in marine bacteria (100) and human or animal pathogens (71). Nonetheless, Mulkidjanian and coworkers propose that the sodium motive force is an outdated way of membrane energy metabolism which was gradually replaced in most ecologically niches by the more powerful proton cycle (154).

A schematic illustration of membrane protein complexes, which play a role in the sodium cycle of *V. cholerae* is given in Fig. A.4 (63, 70). Via the flagellar motor (PomAB stator complex) and via symporters in combination with metabolites (e.g. aminoacids), Na^+ enters the cell from the periplasm which leads to an accumulation of sodium in

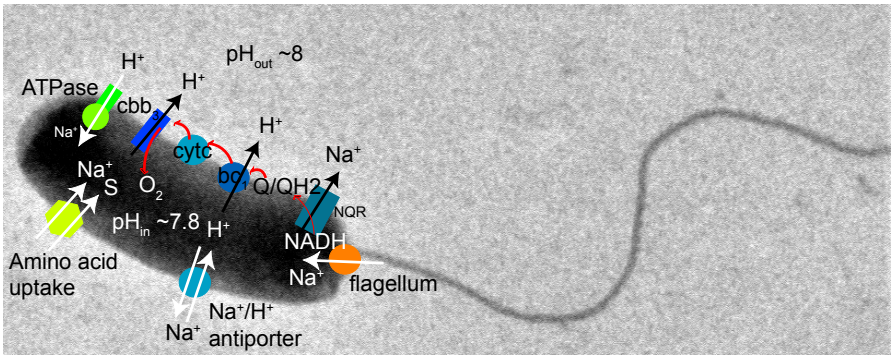

Figure A.4: Sodium and proton transporters in *V. cholerae*. Na^+ can be extruded via the redox driven Na^+-NQR or in exchange for H^+, via specific antiporters. On the other hand, sodium enters the cell via the flagellar stator complex PomAB or in combination with metabolites, e.g. aminoacids via specific symporters (70).

the cell. On the other hand, to maintain a sodium gradient, the membrane is embedded with several exporters. A redox driven sodium pump (Na^+-NQR) removes sodium across the cell membrane from the cytoplasm into the periplasm. Deletion of the *nqr* operon revealed that the Na^+-NQR is not essential for survival of *V. cholerae* but may play an important role in the regulation of sodium homeostasis and cellular sodium regulation (e.g. growth was inhibited at low and high external sodium concentrations) (70). *V. cholerae* maintains three Na^+/ H^+ antiporters (NhaA (217), NhaB (78) and NhaD (49)) which transport sodium from inside the cell into the periplasm in exchange for protons and therefore enable *V. cholerae* to survive in environments with high salinity. In addition *Vibrio* carries the regulator NhaR – a close homolog to NhaR in *E. coli* which is important for the survival at high LiCl and pH conditions (230). Beyond that, genomics predict the presence of four NhaC paralogs, a *mrp* operon, NhaP and MleN homologs as putative sodium transporters (162). For NhaP it could recently be demonstrated that it works as a specific K^+/ H^+ antiporter (172).

2.2 The relationship between virulence and sodium bioenergetics

It is not yet fully understood how motility affects virulence (161) but it is reasonable that the sodium cycle plays an important role in the pathogenicity of *V. cholerae* (70, 71). Strains which are – due to changes in the membrane sodium flux – limited in their motility, show a higher expression of virulence genes and in contrast, hyper-motile strains are less virulent (62). The dissipation of the sodium motive force by ionophores, by mutations in the *nqr* operon or by NQR inhibitors stimulate the expression of the cholera toxin and the toxin coregulated pili (73). These observations are in accordance

with the hypothesis that the role of the cholera toxin may lie in the generation of a sodium rich environment in the intestinal lumen to increase the effectiveness of the sodium cycle in alkalic surroundings (13). In this context membrane embedded receptors might play a role in sensing the activation state of the NQR complex by direct protein-protein interactions or noticing the intracellular sodium level and respectively noticing a change of the sodium gradient across the cell membrane. As an example the membrane embedded receptors TcpP and TcpH should be mentioned which regulate the expression of *toxT* (72). An illustration is given in Fig. A.5.

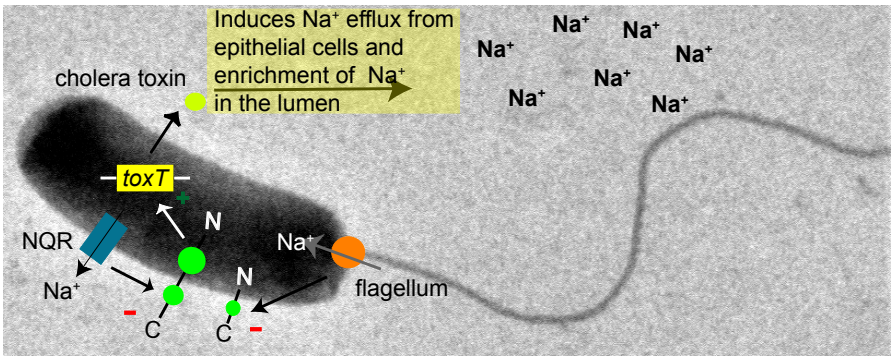

Figure A.5: Schematic illustration of some proteins which might be influenced by altered membrane sodium flux. (63, 70) Under physiological conditions the expression of *toxT* is repressed. The membrane embedded regulators TcpP and TcpH might sense changes in the membrane sodium flux or the level of the sodium gradient across the membrane during colonization and activate expression of *toxT*. Cholera toxin will be released into the host intestinal lumen which will result in an efflux of sodium ions from the epithelial cells. A sodium rich environment in the intestinal lumen increases the effectiveness of the sodium cycle in alkaline surroundings (13).

3 The flagellum – or how motility is achieved in bacteria

It is essential for bacteria to be able to move, either away from a repellent or towards an attractive environment (7, 50). Motility is achieved via extracellular helical filaments – called flagella, which can be rotated clockwise (CW) or counterclockwise (CCW) (23). The number of flagella and their formation differ from species to species (150) and depends on the habitat in which the cells reside (231). They can be localized at the poles (mono- or bipolar) or evenly spread over the cell surface (peritrich). Besides their role in motility, flagella also possess a function in biofilm formation (170), adhesion (58) and colonization of host organisms (86) or sensing environmental conditions (e.g. viscosity or moisture) (24, 132, 223).

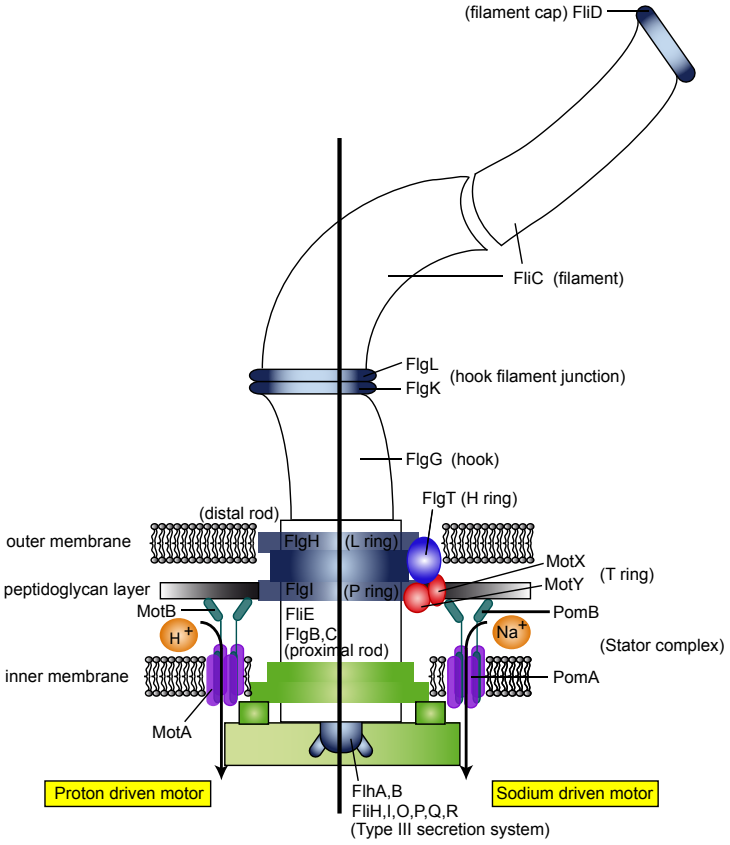

Figure A.6: Schematic illustration of a flagellum occurring in gram negative bacteria. A proton driven motor can be seen at the left side, while the sodium driven motor is illustrated on the right side. In contrast to the proton driven motor complex, the sodium driven possesses additional proteins: MotX and MotY, which build up the T ring (133, 134, 135) and FlgT (and potential other proteins) which compose the H ring (32, 131, 204, 205).

3.1 The structure and function of the flagellar complex

The bacterial flagellum consists of three distinct parts: the flagellum, a 15 nm to 20 nm hollow filament, which is build up by flagellin proteins. The hook, which connects the filament to the motor complex and finally the membrane embedded motor complex, which is based on a rotor and a stator complex (Fig. A.6). The flagellar complex consists of over 40 proteins which are regulated in a hierarchical manner (99, 136). Flagellar assembly takes place from the inside out. It starts with the membrane embedded basal body, succeeded by the hook and completed by the filament (145). First, the Sec system is used to integrate membrane embedded proteins into the bacterial cell wall (MS rings, stator proteins, PL rings). The other flagellar proteins, which are located outside the cell (e.g. hook, flagellins) are exported via the type III export system, which resides inside the flagellar motor complex (129).

The flagellum is driven either by a proton or a sodium gradient (see Chap. A, 2.1). The mechanism, how the ion flux is converted into torque still remains unclear. Nevertheless, it is known that two components of the motor complex are essential for

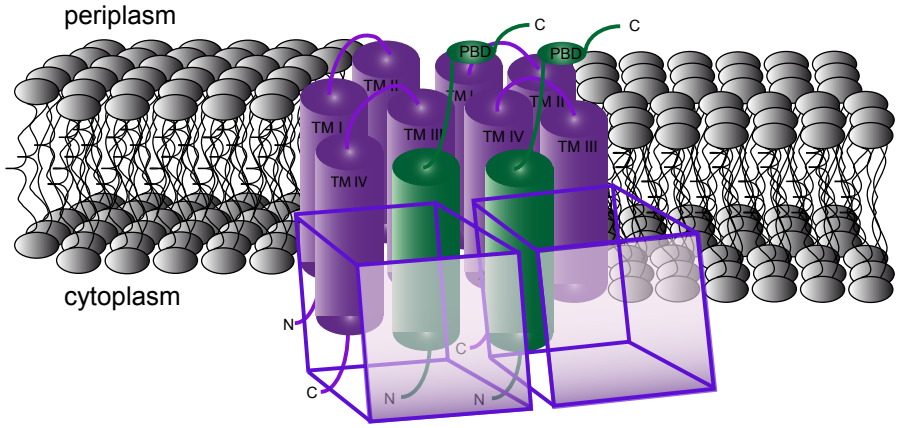

Figure A.7: Model of the flagellar stator complex. It is assumed that four MotA/PomA (purple) and two MotB/PomB (green) form a flagellar stator complex. It is supposed that ions are guided from the periplasma into the cytoplasm via a channel, built by helices III and IV of MotA/PomA and the single transmembrane helix of MotB/PomB (26, 175).

torque generation. First of all, the flagellar switch complex and second, the stator complex, which defines the specificity to either proton or sodium ions.

Each stator complex is composed of four MotA (PomA) and two MotB (PomB) subunits (25, 181, 197, 201, 237) which surround the MS ring (123, 146) (MotAB is commonly denoted to proton driven motors, while PomAB confers to sodium driven motors). The stator complex ($MotA_4B_2$ or $PomA_4B_2$) forms accordingly two channels for the passage of ions (27). Subunit A possesses four transmembrane helices and a large cytoplasmic loop between helix II and III while subunit B consists of one transmembrane helix and a large periplasmic domain which harbors a peptidoglycan-binding motif at the C-terminus. It is postulated that helices III and IV of the A subunit and the single transmembrane helix of subunit B are in close proximity to form an ion channel (232), as can be seen in Fig. A.7.

The C terminal part of subunit B – which is essential for stator function – reaches into the periplasmic space and attaches itself to the peptidoglycan layer with its special peptidogylcan binding motif, which increases the stability of the stator complex in the cell membrane (22). The number of stator units ranges between 11 - 12, depending on the species. With regard to the high rotational speeds – 1700 Herz – which were determined for the sodium dependent polar flagellum of *V. alginolyticus*, it was first assumed that the rotor and stator complexes of the flagellar motor might form a tight and stable complex (130). Nonetheless it could be demonstrated that stator complexes dynamically associate with or dissociate from the motor without disrupting the flagellar rotation (113), helping

oneself from a reservoir of membrane embedded, inactive stator precomplexes (60, 213). The concentration of either proton or sodium ions may contribute to the selection of either $MotA_4B_2$ or $PomA_4B_2$ stator complexes in species with different stator systems, e.g. *Shewanella oneidensis* (165).

It is supposed that upon ion influx, conformational changes occur in the cytoplasmic loop of subunit A bringing the cytoplasmic loop in close proximity to FliG. Charged residues of the cytoplasmic loop (see grey labeled aminoacids in Fig. A.8) may interact with charged residues, residing in the C-terminal domain of FliG (124, 236, 240, 241). FliG is part of the first mentioned component of the torque generating machinery – the switch complex – which is essential for torque generation and the assembly of the flagellum (63).

Much effort was brought up on elucidating the working model of the motor complex, how torque is being generated and how the ion specifity is defined. Chimeric motor complexes were constructed and point mutations in charged aminoacids were inserted, investigating their effect on motility. It could be demonstrated that the formerly sodium dependent motor of *V. cholerae* could be converted to a proton dependent motor by exchanging the stator components (10, 63), just as shown for *E.coli* (12, 189). Ergo, the specifity to either proton or sodium ions is defined by the stator components of the flagellar motor.

3.2 In search for the cation translocation pathway through the flagellar motor complex

The flagellar stator complex confers the ion specifity of the motor but it is not yet fully understood how this is achieved. Purification and immunoprecipitation studies on PomA and PomB confirmed interaction between these proteins (175, 237). Cross-linking studies in which aminoacids of the periplasmic loops between helices I and II ($loop_{I-II}$) and helices III and IV ($loop_{III-IV}$) were substituted for cysteines revealed that $loop_{I-II}$ is not accessible to SH-modifying reagents. This suggests that $loop_{I-II}$ lies beneath other proteins – e.g. PomB, MotX, MotY – or is deeply embedded in the pore region of the channel. It is assumed that $loop_{I-II}$ is irrelevant in sodium conduction. In contrast, $loop_{III-IV}$ lies accessible in the periplasma and mutations within this region impair motility (11). These findings suggest that helices III and IV of PomA and the single transmembrane helix of PomB compose a pore for sodium translocation. As a consequence it is a major point to identify aminoacid residues which contribute to the passage of Na^+.

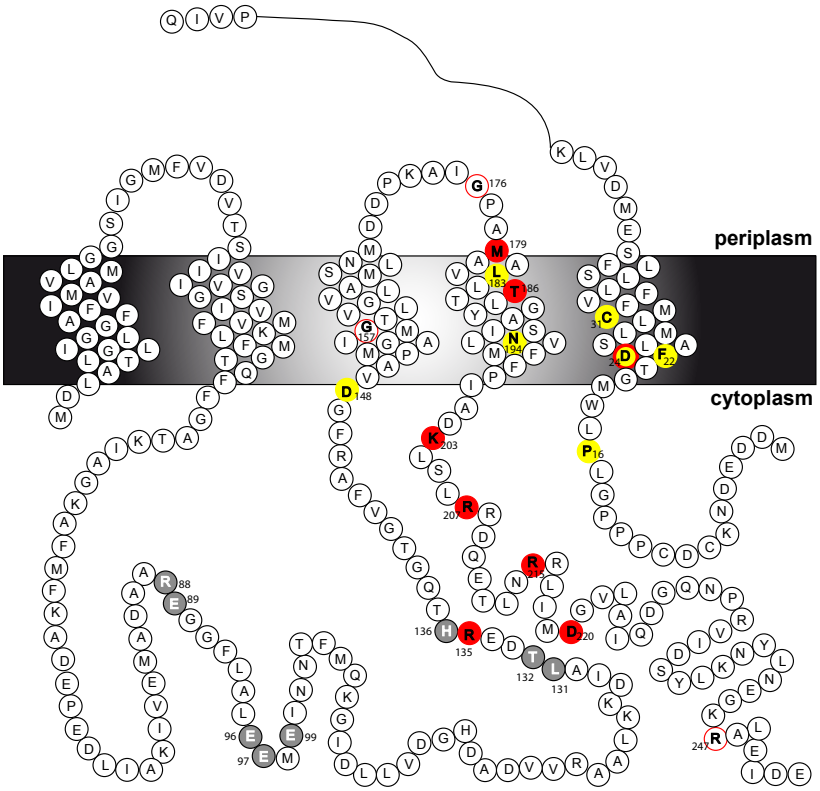

Figure A.8: Putative topology model of the PomAB complex of *V. alginolyticus* with aminoacid code, (after (11, 102, 200, 206)). PomA is composed of four transmembrane helices with two short periplasmic loops connecting helices I and II and helices III and IV. A large cytoplasmic loop is connecting helices II and III. Red or yellow colored residues display mutated aminoacids. Mutations in red coded aminoacid residues confer an immotile phenotype due to disturbed complex formation of PomA/B (G176, K203) or disrupted ion conduction (D24). Grey marked aminoacid residues in the cytoplasmic loop might play a role in the interaction with the C-terminal part of FliG (200).

The putative topology of PomA and PomB of *V. alginolyticus* – with aminoacid code – is illustrated in Fig. A.8 (after (11, 102, 200, 206)). Colored (yellow/ red) residues confer to mutated aminoacids. Mutations in aminoacids, coded in red, result in an immotile phenotype of *V. alginolyticus* either due to disturbed complex formation of PomA/B (G176, K203) or disrupted ion conduction (D24). The aspartate is highly conserved in sodium dependent stator complexes and a mutation of D23 also results in an immotile phenotype of *V. cholerae*, while complementation with a glutamate restores motility (220).

Terauchi and coworkers propose a model of the ion flux pathway based on mutagenesis analysis and motility assays performed under the influence of phenamil, a sodium channel

blocker. In a first step the sodium ion enters the channel via the periplasmic side by connecting to L183 of PomA and C31 of PomB. In a following step the sodium ion binds to a pocket build by N194 of PomA and D24 of PomB. After this step an event of generating torque has to occur in which the sodium ion has to be released into the cytoplasm. At this step F22, which is located on the cytoplasmic side in PomB might play an important role (206). The charged residues in the large cytoplasmic loop between helices II and III of PomA (grey colored residues in Fig. A.8) might contribute to torque generation by interacting with the C-terminal region of FliG (200). But nevertheless the mechanism of ion translocation and torque generation still remains obscure.

3.3 Genome organization of flagellar genes and their regulation

The assembly of the flagellar complex is highly ordered, beginning with the insertion of the membrane embedded proteins, followed by the extracellularly localized flagellar proteins. Therefore it is important that the expression of flagellar genes is carried out in an organized manner.

The genes encoding for flagellar proteins lie on several clusters on the bacterial chromosome. It is known for *E.coli* and *Salmonella* that their approximately 50 genes encoding for flagella associated proteins are clustered in 15 to 17 operons (103, 109). The flagella associated genes of *V. cholerae* are organized on three distinct loci on the chromosome (75).

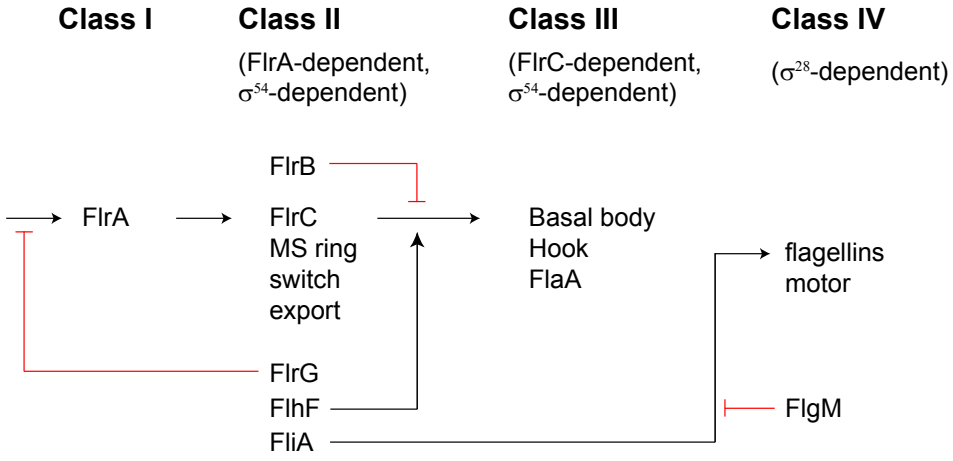

Figure A.9: Proposed model of regulation of the flagellar transcription hierarchy in the polar flagellated *V. cholerae*. The master regulator FlrA controls transcription of the subsequent flagellar genes. FlhG regulates expression of the transcription factor FlrA, while the 2CS FlrBC and FlhF starts transcription of the Class III genes. The anti-σ^{28} factor FlgM is a negative regulator of the Class IV genes (39).

A closer look will be given on the flagellar transcriptional hierarchy of *V. cholerae*, a schematic model after (39) of the flagellar transcription hierarchy is illustrated in Fig. A.9. The flagellar genes can be divided in four distinct classes according to their point in time of expression. Class I comprises only one gene, *flrA* – the master regulator of flagellar gene transcription. FlrA is a σ^{54} associated transcriptional activator which triggers expression of class II genes. Class II consists of genes encoding for the flagellar MS ring, the switch complex and the export apparatus. This class also encloses the two-component-system FlrBC and the regulator FlhF which activate the expression of Class III genes, coding for the basal body, the hook and the for motility essential flagellin FlaA (99). The σ factor FliA of Class II positive regulates the expression of non essential flagellins (*flaBCD*) and genes encoding the motor complex.

The expression of flagellar promoters is negatively regulated by the Class II transcription factor FlhG which represses the transcription of the master regulator FlrA. Deletion of *flhG* resulted in a multi-flagellated phenotype. The genes of Class IV are controlled by the anti-σ^{28} factor FlgM, which is a negative regulator (39, 135, 199).

4 Bacterial chemotaxis

It is important for bacteria to sense and respond to changes in their surroundings, e.g. temperature (thermotaxis), light (phototaxis), salinity (osmotaxis), oxygen (aerotaxis) and changes in the composition of metabolites or other signaling molecules (chemotaxis) (14, 221). These changes can be detected by membrane embedded receptors and result in a change in gene transcription and/ or active movement towards or away from a certain environmental condition. The receptors can be divided in the thoroughly characterized one- and two-component-systems (195, 211) and the only recently discovered extracytoplasmic function (ECF) σ factors (193).

Motility is regarded as one important part of bacterial pathogenicity. Directed motility is achieved by a network of signal sensing (via two-component-systems) and their effect on the flagella motor.

4.1 The role of the histidine-aspartate phosphorelay (HAP) system in motility

The HAP system is composed of two components, a dimeric histidine protein kinase (HPK) and a response regulator (RR). Signal transduction runs via a *trans*-phosphorylation of a histidine residue in one of the two monomers of the HPK by the γ-phosphoryl

group of an ATP. This phosphate is subsequently shifted to an aspartate of the RR, which activates the RR's output domain. The structures of the HPKs and RRs are quite conserved. Most of the HPKs possess a N-terminal region with at least two transmembrane domains. Their periplasmic linker sequence is important for sensing extracytoplasmic signals. The C-terminal part, which resides in the cytoplasm is build up by different domains: a linker (HAMP domaine, (histidine kinase, adenylyl cyclases, methyl-binding proteins)), a dimerization and a kinase domain. The kinase domain is important for the interaction with its cognate RR. Exceptions of the before mentioned HPKs, are for example CheA and NtrB, which lack the periplasmic and the transmembrane domain.

The chemosensory system is thoroughly studied and characterized in *E. coli*. Findings of highly homologue chemotaxis proteins in *V. cholerae* indicate that the chemosensory system works the same way (30). Receptors, (dimeric methyl-accepting chemotaxis proteins (MCPs)), are embedded in the inner membrane of *E. coli* and may interact either with a periplasmic binding protein (PBP) or in the cytoplasm with the signaling domain of CheA/W. CheW plays here an important role in complex formation and signal transduction from the MCP to the HPK CheA. Decline in the amount of attractants leads to a lesser binding to the MCPs, which animates CheA *trans*-autophosphorylation. As a result, the concentration of phosphorylated CheY in the cytoplasm rises. Binding of CheY-P at the flagellar motor causes the counterclockwise rotation of the flagellum to stop and change into a clockwise rotation (see lower part of Fig. A.10). The cells can be observed, changing from a smooth straight swimming to a tumbling, which results in a change in direction towards a more convenient surrounding.

4.2 The phosphoenolpyruvate (PEP) dependent carbohydrate phosphotransferase systems (PTSs)

Another important mechanism in bacteria is the possibility to transfer different carbohydrates into the cell via the phosphoenolpyruvate dependent carbohydrate phosphotransferase systems. The PTSs play an important role in the regulation of multiple other metabolic pathways in the bacterial cell and they are also tightly connected to the chemotaxis system and thus motility of cells. A simplified schematic model of the PTS is illustrated in the upper part of Fig. A.10.

In general the mechanism works as follows: Cytoplasmic distributed phosphoenolpyruvat (PEP) donates its phosphate. This phosphate is then transferred to a carbohydrate, which results in an uptake of carbohydrate-phosphate and leaves pyruvate inside the cell. The phosphotransferase system with its proteins is best investigated in *E. coli* and

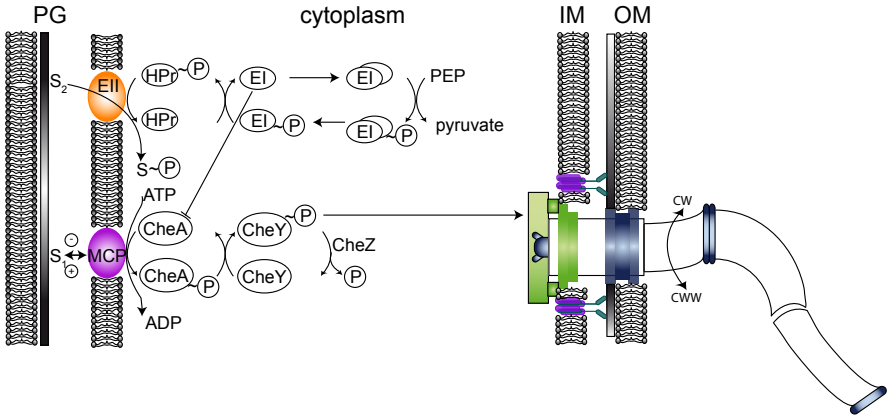

Figure A.10: A simplified illustration of effectors of motility of *E.coli*. An initial step in chemotactic signaling is the percipience of signals (S_1) by membrane embedded chemoreceptors (MCPs) (lower part of the image). The histidine kinases CheA will be autophosphorylated when the concentration of attractants in the surrounding medium decreases. The phosphate will be then transferred to the response regulator CheY, which binds in its phosphorylated state to FliM, the flagellar switch protein. This causes the flagellum to switch from CCW rotation to a clockwise rotation and eventually leads the cell to stop and re-adjusting swimming direction to more promising regions. To achieve directed swimming, CheY-P gets dephosphorylated by CheZ. Chemotaxis and therefore motility is tightly connected to transport of substrates (S_2), e.g. carbohydrates into the cell. The pathways therefore are the phosphoenolpyruvate (PEP) dependent carbohydrate phosphotransferase systems (PTSs) (upper part of the illustration). They consist of a substrate specific, membrane embedded receptor (EII) which gets phosphorylated via EI, a PEP-dependent histidine kinase and HPr, a phosphohistidine carrier protein. High amount of dephosphorylated EI is likely to inhibit phosphorylation of CheA and consequently keeps the cell on a straight swimming track (30, 125, 221).

S. typhimurium. The proteins involved in PTS are the soluble and cytoplasmic localized proteins EI and HPr which contribute in the phosphorylation of any carbohydrates in a cell. In contrast to that the membrane embedded protein EII is highly specific for a carbohydrate, e.g. for glucose or mannitol. EII can either consist of a single protein with three domains (A, B and C) or as a protein complex of two or more proteins. In this complex at least one protein is membrane bound, the rest is soluble. The protein domains B, C contribute in the transfer of the phosphate to the carbohydrate, while domain C forms a translocation channel (169).

But how does the PTS influence the chemotaxis system and motility in bacteria? Unphosphorylated EI of the PTS prevents autophosphorylation of the chemotaxis protein CheA. The high concentration of carbohydrates in the surrounding results in a higher transport rate of the carbohydrate and therefore the amount of phosphorylated EI decreases. Unphosphorylated EI results in suppressed autophosphorylation of CheA. This

causes a decline in phosphorylated CheY, which enables the cell to prolong swimming in a straight direction (30, 125, 221).

In summary, motility in bacteria is a complex field, with many components influencing bacterial movement e.g. composition of the environment (distribution of nutrition) and the ability to generate energy to run the flagellar motor (H^+ or Na^+ gradient).

5 Studying motility behavior of bacteria

An experimentally easy approach to visualize abnormalities in the motility behavior of bacteria is the investigation of strains on softagar plates. Typically, such plates contain 0.25 % agar (w/v), providing a semi-solid medium with a viscosity that allows motile bacteria to swim through. If a single colony is stabbed on a softagar plate and this plate is then incubated for several hours, the bacteria form a swarming ring whose diameter is a measure for the ability to swarm. These experiments reflect the motility of cells within a colony, therefore describing a multi-cellular entity. Motility of cells in softagar depends on various factors, first of all the medium composition (wetness or dryness, distribution of nutrient) and secondly the cell density, which influences the communication between cells by quorum sensing (194). Another approach of investigating the motility of cells is by tracking of single cells in liquid medium using microscopy and video recording. The advantage of this method is the detection of the swimming behavior of single cells in media where nutrient and signaling factors are evenly distributed. In this study, motility of *Vibrio cholerae* strains which carry mutations in the single transmembrane helix of PomB was studied. PomB interacts with PomA, forming a $PomA_4PomB_2$ complex, which is an essential part of the stator of the flagellar motor of *V. cholerae* (65, 208, 235). This flagellar motor uses – in contrast to flagellar motors driven by the H^+ motive force – Na^+ as coupling cations *V. cholerae* (85, 101, 203). *V. cholerae* Δ*pomAB* strains expressing PomB-S26A or PomB-S26T variants were in the focus of this work. It has been suggested that the exchange of serine (conserved for Na^+ flagellar motors) for a threonine (conserved for H^+ motors) might influence the ion specificity of bacterial motors (206).

6 Microbial Endocrinology – how stress affects health

For centuries it has been known – based on empiric observations more than scientific experiments – that stress enhances the probability to get infected with pathogenic microorganisms. Under stress the body pours the catecholamine hormones epinephrine

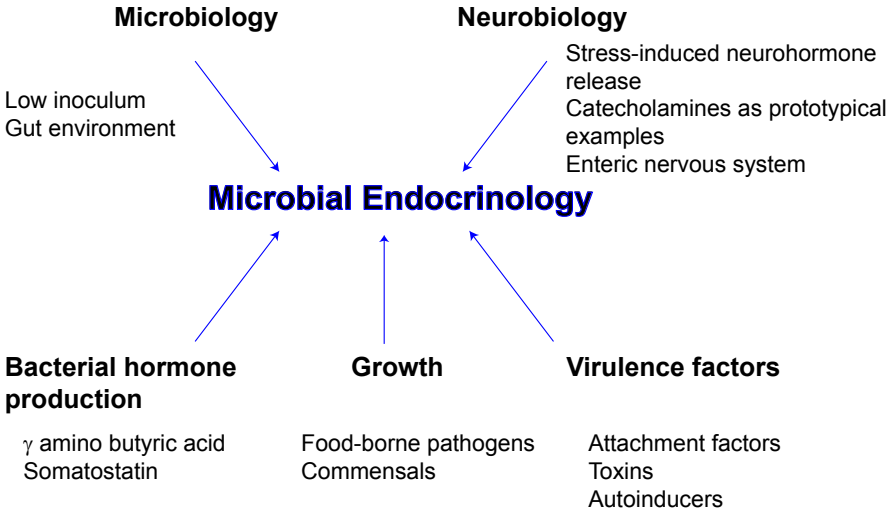

Figure A.11: Microbial endocrinology combines the fields microbiology and mammalian physiology and neurobiology. Commensal bacteria and food-borne pathogens are subject to a diversity of neuroendocrine hormones. Microbes are able to detect and respond to changes in the neuroendocrine environment of the host. Picture adapted from (126).

and norepinephrine which trigger the *fight or flight* reaction in humans. Nevertheless the exact mechanism on how the infection progress is accomplished and how pathogen microorganisms profit on stressed host, remained obscure. First observations revealed that patients who were treated with purified epinephrine – and not adequate sterilized syringes – were more susceptible to bacterial sepsis. From the 1980s on, by and by more hormonal compounds and their receptors were detected in microorganisms which possess identical or closely identical structure to mammalian hormones (115, 116). Up from 1992 on, extensive studies were accomplished on how endocrine hormones influence bacterial growth (128). Well characterized organisms are for example pathogenic enterohemorrhagic *E. coli* (EHEC) (83) or *S. enterica* Serovar Typhimurium (18, 19).

The quite recently established field of microbial endocrinology comprises an intersection of the scientific fields mammalian physiology, neurobiology and microbiology (126), as shown in Fig. A.11, dealing with microbiology – growth of bacteria in the gut environment, microbe host interaction, production of bacterial hormones, like GABA or somatostatin and bacterial virulence factors – and neurobiology (release of hormones under stress conditions and the enteric nervous system).

6.1 The human body – a hostile environment for pathogenic bacteria

The human body is settled with a variety of microorganisms. These can be divided in three classes. There are the commensal microorganisms which feed from the same nutrition as their host but without harming him. Secondly, there is the group of mutualistic microorganisms where both – bacterium and host – benefit and the third group comprises pathogenic bacteria (45). It is estimated that the human body consists of approximately 10^{13} human cells and inherits 10^{14} prokaryotic cells, which make up the endogenous bacterial flora (83). While commensal microorganisms live in symbiosis with their host, the host organism develops different strategies to fend off pathogenic bacteria. The human body comprises two different systems of immune defense. First, the unspecific immune defense, including anatomic or physiological barriers (epithel cells), phagocytosis, inflammations or defense via the complement system. The second immune defense strategy is the specific immune defense via specific antibodies or lymphocytes.

Yet another defense system, which belongs to the unspecific immune defense mechanism is the establishment of an iron deprived environment in the body, as iron is essential for different cellular processes in bacterial cells, e.g. the respiratory chain, and it is therefore an important nutritional element for growth (174). This environment is achieved by special iron binding proteins, called transferrin and lactoferrin. These bind Fe(III) with high affinity to its C- and N-terminus and transfer it to iron depending cells. Under stressful situations the body pours the catecholamines epinephrine and norepinephrine, which are able to form complexes with iron. A method to scavenge this iron from iron-norepinephrine complexes is the possession of specific proteins, e.g. the neutrophil gelatinase-associated lipocalin (NGAL) (144).

6.2 Pathways of iron acquisition in bacteria

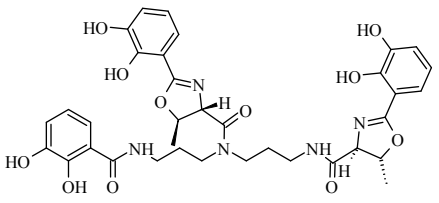

Figure A.12: Chemical structure of vibriobactin, a sideropohre of *Vibrio*. Siderophores bind iron with the free OH-groups of the aromatic ring.

Iron is important for different processes in the bacterial cell, and with the exception of lactobacilli (6, 164, 227) which use manganese and cobalt as biocatalysts instead, all microorganisms so far rely on iron. Microorganisms encounter difficulties in the assimilation of iron, first of all, iron is distributed as insoluble hydroxo complexes in nature, as the biological relevant state of iron is the ferrous form which is rather unstable and secondly, the iron uptake has

to be regulated via special transport systems to avoid the formation of hydroxy radicals in the cell.

Iron uptake systems of gram negative bacteria are illustrated in Fig. A.13 but not all systems have to be present in one microorganism. Bacteria are able to secrete iron binding small molecules or oligopeptides, called siderophores into their surrounding. The expression of genes involved in iron uptake is regulated by the concentration of iron in the cell. Siderophores possess a high affinity for Fe^{3+} and form very stable complexes. Vibriobactin, the catecholate siderophore of *Vibrio* for example maintains three bidentate ligands for iron (Fig. A.12). Besides, pathogenic bacteria of the families *Neisseriaceae* and *Pasteurellaceae* do not produce siderophores for the aquisition of iron but are rather able to assimilate iron from the uptake of lactoferrin or transferrin (64). Another method of pathogenic bacteria is the direct uptake of heme or heme-protein complexes (hemoglobin, hemoglobin-haptoglobin, heme-albumin, heme-hemopexin or myoglobin). Heme carrier proteins are located inside the cell of the host, therfore it is necessary for the pathogen microorganism to secrete exotoxins, e.g. hemolysins (*V. cholerae* (196)), cytolysins (110) or proteases (183) to lyse the cells and liberate the heme from its carrier. The uptake of heme involves the TonB system in gram negative bacteria or in the case of gram positive bacteria, a combination of a cell surface protein and an ABC transporter.

The uptake of iron in gram positive bacteria involves fewer proteins as these microorganisms possess just one cell membrane. As a consequence they lack the periplasmic iron carrier proteins, iron is bound to a membrane embedded receptor and directly transferred via a membrane associated ABC transporter into the cell (108).

6.3 Use of epinephrine and norepinephrine as bacterial pseudosiderophores

As mentioned above, bacteria are able to produce small molecules – siderophores – to sequester iron from the surrounding. These siderophores are grouped according to the nature of their binding site. One group consists of siderophores which bind iron to their catechol site. These catechol siderophores contain structural similarities to the catecholamines epinephrine and norepinephrine, which are effector compounds proceeded from tyrosine. Both of them possess a benzene ring with two adjacent hydroxyl groups and an amine side chain, which resides opposite of the benzene ring (Fig. A.14). Epinephrine and norepinephrine work as hormones in stress-related responses (e.g. *fight or flight* stress response in higher animals (77)), as neurotransmitter in the central nervous system or neurotransmitter in the autonomic nervous system. Under stress, the

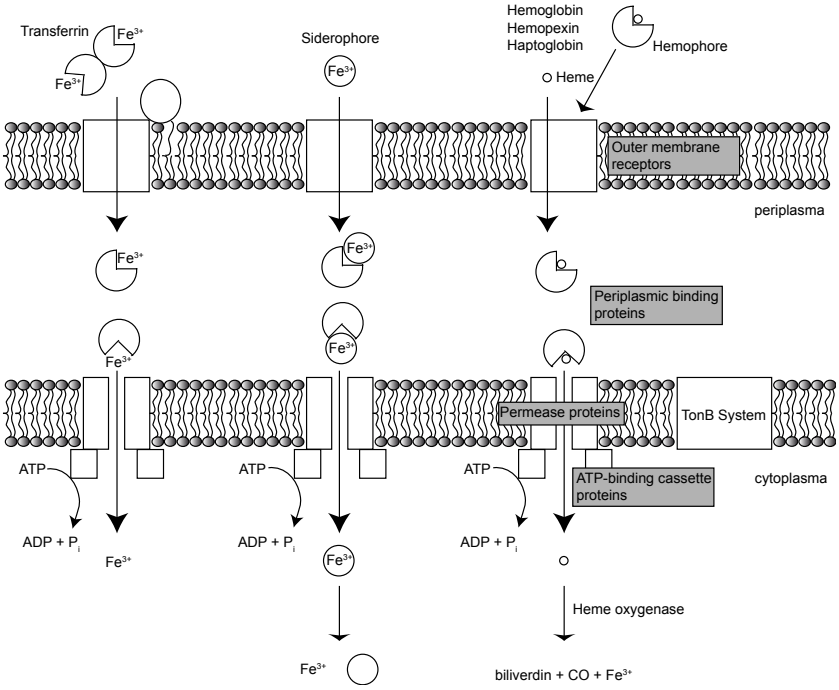

Figure A.13: Iron uptake systems of gram negative bacteria. With the possession of an inner and an outer membrane, iron uptake systems of gram negative bacteria require a receptor embedded in the outer membrane, periplasmic binding proteins which accept the transferred iron and permease protein complexes which lie in the inner membrane. The passage of iron across the outer membrane requires the action of the TonB system and transfer across the inner membrane requires ATP (108).

concentration of epinephrine and norepinephrine rises to $2\,\mathrm{nM\,L^{-1}}$ and $20\,\mathrm{nM\,L^{-1}}$ respectively, with a half-life of approximatly 1 min (79). Experiments revealed that stress related traumata (e.g. from surgery (5)) or territorial and social stress (well investigated in mice and rat models) lead to an increased infection rate with pathogenic bacteria (17, 215). It could also be demonstrated that epinephrine and norepinephrine supports growth (54, 55, 56) and motility (18, 19) of some gram negative bacteria (*E. coli*, *S. enterica* Serovar Typhimurium, *Klebsiella pneumoniae* (20) or *Pseudomonas aeruginosa* (74, 120), and different *Vibrio* species (155)) in bacteriostatic medium (e.g. serum)).

Recently the mechanism was elucidated by which catecholamine hormones bind to the ferrous ion inside the lactoferrin/ transferrin complex. The binding of iron to norepinephrine is illustrated in Fig. A.15. The catecholamines are able to reduce Fe(III) to Fe(II), which results in a lower affinity for transferrin or lactoferrin to Fe(II). The response of the gut flora after a stress event may take 24 h or more as the removal of iron from lactoferrin by catecholamines takes about 24 h (174).

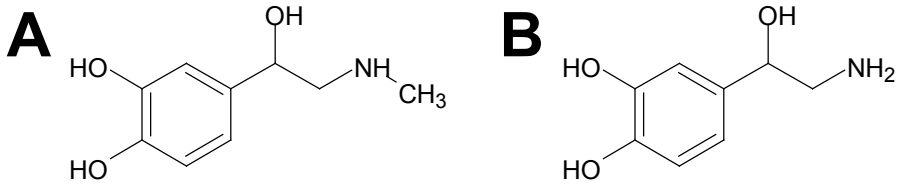

Figure A.14: Structure of the catecholamines epinephrine (A) and norepinephrine (B). As seen in this illustration, the catecholamines epinephrine and norepinephrine both feature one bidentate ligand for iron.

It could be demonstrated for *E. coli* that norepinephrine works as transcription factor, enhancing the expression of the siderophore enterobactin and as a direct consequence iron uptake (29). Structural similarities between bacterial siderophores and the catecholamine hormones and the availability of epinephrine and norepinephrine in the host gut prove that pathogenic bacteria are able to use these compounds as pseudosiderophores for the uptake of iron.

6.4 Inter-kingdom signaling: how bacteria communicate with their host

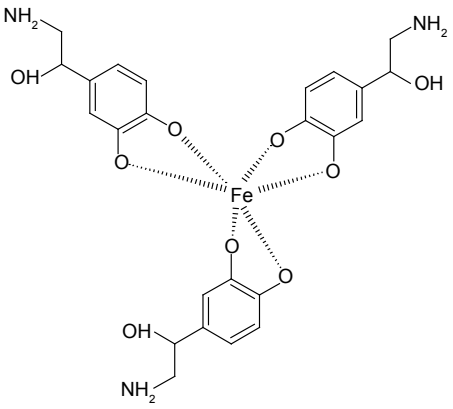

Figure A.15: Norepinephrine can be used as bacterial pseudosiderophore. Three molecules of norepinephrine are able to form a complex with iron. Picture after (174).

Bacteria are able to communicate by secreting small molecules into the environment, called autoinducers (AI). The mechanism of this cell-to-cell signaling is called *quorum sensing* (QS). This form of communication can occur within the same species or in bacteria of different genera. QS enables bacteria to behave rather like a multicellular entity than individual cells, thus helping them in overwhelming the host defenses (43). The first bacteria species in which QS was characterized was *Vibrio fischeri*, a marine bacterium that colonizes different marine animals. At high cell densities, *V. fischeri* secretes an AI, a homoserine lactone, which eventually diffuses back into the cytoplasm where it binds to LuxR. This LuxR-AI complex is an activated transcription factor which induces the transcription of the *lux* operon and consequently leads to light production (184, 194). A general overview about the mechanism is given in Fig. A.16.

So far, the mechanism of *quorum sensing* has been elucidated for numerous bacteria, especially human pathogens (e.g. EHEC/ EPEC, *Samlonella*, *Enterococcus faecalis*, *V. cholerae* and so on). QS plays here a major role in flagella synthesis and motility, resistance to human complement, biofilm formation or the production of virulence factors (93).

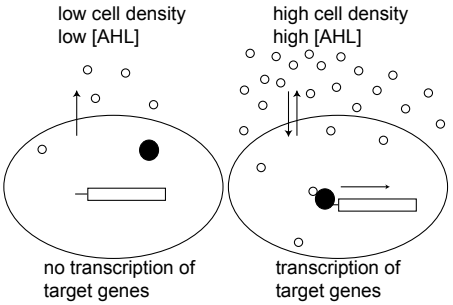

Figure A.16: Schematic illustration of the mechanism of *quorum sensing*. At low cell density, the bacterial cell is secreting autoinducers (○), the transcriptional regulator (●) is at this moment inactive. As the cell density rises, the amount of secreted AIs increases, which can also be taken up by other cells. Inside the cell, the AI activates a transcription factor which binds to the promoter sequence of its target gene and initiates transcription (43).

Bacteria are not only capable of communicating among themselves. There is also strong interaction between bacteria and host. Bacteria can also modulate mammalian cell-signal transduction or vice versa, bacterial gene expression pattern can be influenced by host hormones. Steroid hormones of the host are able to cross the bacterial membrane while peptide or amine hormones bind to membrane embedded receptors of bacteria. Here, the focus lies on the detection of epinephrine and norepinephrine via QseBC. This two component system has been extensively studied in *E. coli* (192) and *S. enterica* Serovar Typhimurium (18, 19). QseC is a membrane embedded sensor kinase which gets phosphorylated upon binding either the bacterial autoinducer AI-3 or one of the mammalian hormones epinephrine and norepinephrine. The phosphate of QseC is then transferred to the cognate response regulator which initiates transcription of different virulence asociated genes, like the master regulator for flagella synthesis *flhDC*, the Shiga toxin *stxAB* and the LEE genes.

Homologs to the QseC receptor have also been found in *S. enterica* Serovar Typhimurium, *V. parahaemolyticus* and *Francisella tularensis* (83). QseC of *S. enterica* Serovar Typhimurium plays a major role in the colonization of the swine gastrointestinal tract. While deletions of *qseB* (response regulator) or *qseBC* (two-component system: histidine kinase (QseC) and its cognate response regulator (QseB)) revealed no altered motility phenotype compared to the wild type, motility was reduced in the *qseC* (histidine kinase) mutant. This led to the conclusion that QseB is a negative regulator of bacterial motility (19).

The field of microbial endocrinology elucidates the bacteria-host communication via mammal hormones and their influence on virulence (colonization of the host by pathogens

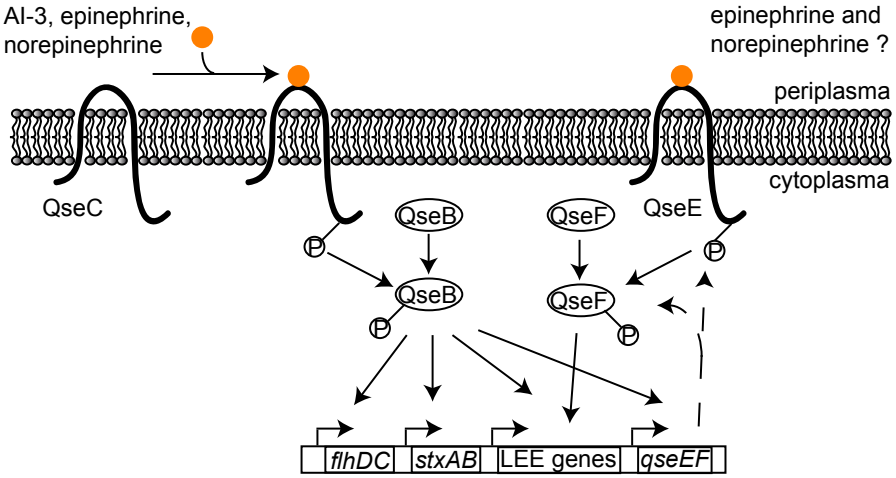

Figure A.17: Percipience of catecholamine hormones in enterohemorrhagic *Escherichia coli* (EHEC). The catecholamines epinephrine and norepinephrine and the autoinducer AI-3 bind to the membrane embedded receptor QseC, which results in its autophosphorylation. QseC then transfers its phosphate to its cognate response regulator QseB which triggers a signal cascade which eventually results in transcription of different virulent associated genes (83).

or the expression of toxins). The current findings confirm observations that humans or productive livestock which encountered stressful situations – these are connected with the discharge of the catecholamine hormones epinephrine and norepinephrine – are more likely to get infected with pathogenic bacteria.
As converse argument, it is evident that bacteria are able to cross-talk with their host. It could be demonstrated that bacteria are able to sense epinephrine or norepinephrine with the membrane embedded receptor QseC which leads to an altered gene expression in virulence associated genes. Furthermore they are able to get access to iron, which is bound to lactoferrin or transferrin which enhances their growth.

7 Aim of this work

V. cholerae is motile by means of its polar flagellum, which is driven by sodium ions. The affinity for Na^+ to run the flagellum is determined by the stator complex PomAB, which is embedded in the cell membrane within the flagellar motor.

The first part of this work focus on the characterization of the PomAB stator complex. The importance of different polar or charged aminoacid residues within PomB on motility will be investigated. There are two possible mechanisms how Na^+ will be transported through the PomAB channel. First of all, Na^+ might directly bind to D24,

a critical aminoacid residue (as it was postulated by Sudo *et al.* (198)) or a hydrogen–bond–network, build by certain aminoacid residues (D23, S26) within the PomAB channel might faciliate the passage of Na^+ from the periplasm into the cytoplasm.

The second part of this work will focus on the effect of epinephrine and norepinephrine on growth and motility of *V. cholerae* and the identification of a putative sensor protein, which is able to detect catecholates. It could be shown that different pathogenic microorganisms are able to detect and respond to catecholates due to the possession of a membrane embedded sensor kinase (QseC). Despite earlier findings, where it could be shown that the *V. cholerae* strain RIMD2203102 does not respond to catecholates (155), it could be shown that *V. cholerae* responds to both epinephrine and norepinephrine.

Chapter B

Results

1 The function of the Na^+driven flagellum of *V. cholerae* is determined by osmolality and pH

Petra Halang, Sebastian Leptihn, Thomas Meier, Thomas Vorburger, Julia Steuber

Journal of Bacteriology, 195(21):4888–4899, 2013

Vibrio cholerae is motile by its polar flagellum, which is driven by a Na^+-conducting motor. The stators of the motor, composed of four PomA and two PomB subunits, provide access for Na^+ to the torque-generating unit of the motor. To characterize the Na^+ pathway formed by the PomAB complex, the influence of chloride salts (Na^+ and K^+) and pH on the motility of *V. cholerae* was studied. Motility decreased at elevated pH but increased if a chaotropic chloride salt was added, which excludes a direct Na^+ and H^+ competition in the process of binding to the conserved PomB D23 residue. Cells expressing the PomB S26A/T or D42N variants lost motility at low Na^+ concentrations but regained motility in the presence of 170 mM chloride. Both PomA and PomB were modified by N,N'-dicyclohexylcarbodiimide (DCCD), indicating the presence of protonated carboxyl groups in the hydrophobic regions of the two proteins. Na^+ did not protect PomA and PomB from this modification. This study shows that both osmolality and pH have an influence on the function of the flagellum from *V. cholerae*. It is proposed that D23, S26, and D42 of PomB are part of an ion-conducting pathway formed by the PomAB stator complex.

1.1 Identification of critical aminoacid residues within the transmembrane helix of PomB

As described in Chap. A, 3.1, the stator complex in flagellar motors of bacteria consists of four PomA and two PomB proteins.

It is assumed that helices III and IV of PomA are close to the single transmembrane helix of PomB and form a sodium conducting channel across the bacterial cell membrane. Which aminoacids of the PomAB complex play a role in binding of sodium ions and contribute to the motility of *V. cholerae* is not yet fully understood. Vorburger *et al.* showed that a conserved aspartate at aminoacid position 23 of PomB is essential for motility in *V. cholerae* (220). One of the question that will be addressed in this chapter is the identification of other aminoacids in the transmembrane helix of PomB, which as well contribute to the passage of Na^+.

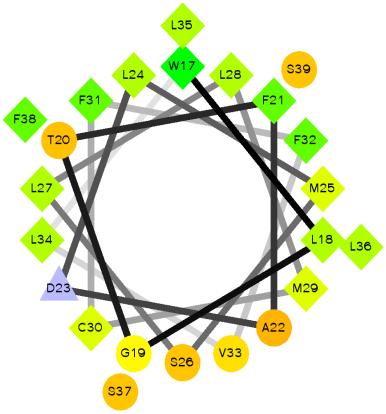

Figure B.1: Helical wheel projection of the transmembrane helix of PomB from *V. cholerae*. Helical wheel projection of PomB was performed using a script by Armstrong and Zidovetzki (8). The aminoacid sequence of PomB of *V. cholerae* with accession number gi:51241597 ranging from W17 to S39 was used as template. Hydrophilic residues are displayed as circles, hydrophobic residues as diamonds and negatively charged residues are shown as triangles. Green colored icons are in accordance to 100 % hydrophobicity, while 0 % hydrophobicity is displayed in yellow. Charged residues are shown in blue.

A helical wheel projection was performed with the predicted transmembrane helix of PomB using HMMTOP (209, 210). The helix ranged from tryptophan at position 17 to serine at position 39. As demonstrated in Fig. B.1, serine 26 – which is a polar aminoacid – is on the same helical side as the conserved aspartate 24. It faces the inside of the Na^+ transmembrane channel. Hence, serine 26 may play a role in the guidance of Na^+ across the cell membrane. A secondary structure prediction also revealed that at the periplasmic side an aspartate, which is conserved in sodium driven PomB proteins, lays in close proximity to the entrance of the sodium channel. It therefore may participate in the initial binding of sodium. Side-directed mutagenesis in *pomB* was performed to investigate the roles of these two specific aminoacids in sodium translocation.

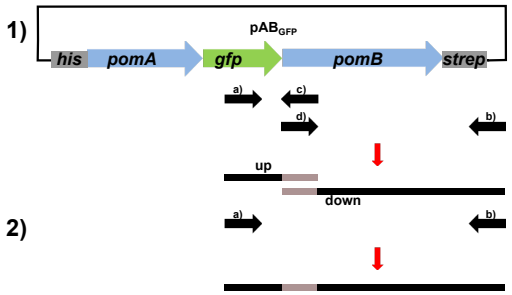

Figure B.2: Schematic illustration of a two step PCR reaction, for amplification of GFP-PomB variants. In a first step (1), the up and down fragments were amplified, with pAB$_{GFP}$ as template sequence. The forward primer WS-013-GFPend f (a) and specific reverse primers (c) for the introduction of single point mutations in *pomB* were needed to replicate the up fragment. Specific forward primers (d) and the reverse primer VcmotBRIII (b) were applied to amplify the down fragment. In a second PCR reaction (2), the up and down fragments were fused to a 1092 bp fragment containing the designated mutations. For this step, the primer pair WS-013-GFPend f (a) and VcmotBRIII (b) was used.

1.2 Construction of plasmids carrying PomB with mutated S26 or D42

Mutations in the nucleotide sequence of *pomB* were inserted by using a two step PCR reaction (15) using pAB as template and one pair of complementary oligonucleotides accommodating the codon for the desired mutation (S26A: VCb90V-S26A and VCb50R-S26A, S26T: VCb90V-S26T and VCb50R-S26T, D42N: *pomB*-D42N fwd and *pomB*-D42N rev) and two flanking oligo-nucleotides (VC*motAV*III and VC*mot*BRIII) matching the sequence of the wild type genes. In a first step the up and down fragments were amplified and fused in a second PCR reaction using primer pair VC*motAV*III and VC*mot*BRIII. The resulting 1762 bp PCR fragments and vector pAB were restricted using enzymes NdeI and XhoI. Ligation of purified fragments and pAB vector fragment were performed at room temperature for 3 h resulting in pAB-S26A, pAB-S26T and pAB-D42N. The plasmids were transformed immediately into chemical competent *E. coli* XL10 Gold as described in Chap. D, 3.5.1. Plasmids were isolated from *E. coli* XL10 Gold as described in Chap. D, 4.7.1 and transformed into electro competent *V. cholerae* Δ*pomAB* as described in Chap. D, 3.5.2.

1.3 Construction of plasmids carrying GFP labeled PomB variants

One point which has to be addressed, is the correct insertion of mutated PomB into the stator complex of the flagellar rotor. To answer this question, the superfolder green fluorescent protein (GFP) (166) was fused to the N-terminus of PomB wt and variants in order to visualize PomB at the cell pole of *V. cholerae* with fluorescence microscopy.

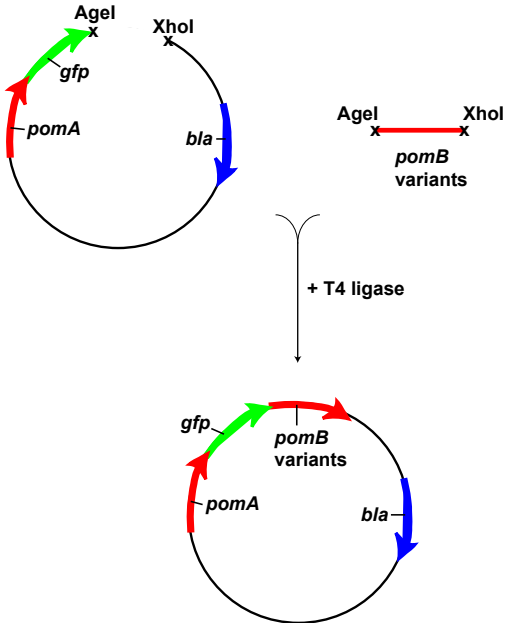

Figure B.3: Construction of pAB$_{GFP}$-PomB variants. Plasmid pAB$_{GFP}$ and PCR fragments with inserted mutations were cut at restriction sites AgeI and XhoI (red crosses). After purification, the fragments were ligated into pAB$_{GFP}$, resulting in plasmids pAB$_{GFP}$ -D23E, -D23N, -S26A, -S26T or -D42N and transformed into *E. coli* XL10 Gold or TOP10.

The procedures are illustared in Fig. B.2 and Fig. B.3.

Point mutations in the aminoacid sequence of PomB were inserted performing a two step PCR reaction (15) using FINNZYMES Phusion™ High-Fidelity DNA Polymerase (NEB). Glutamate at position 23 was exchanged against aspartate or asparagine, serine at position 26 was replaced by alanine or threonine and glutamate at position 42 was substituted for asparagine. In a first PCR reaction the up and down fragments of GFP-PomB were amplified from plasmid pAB$_{GFP}$ using the forward primer WS-013-GFPend f with either the reverse primers Vcb49R-D23E, Vcb49R-D23N, Vcb50R-S26A, Vcb50R-S26T or pomB-D42N-rev for the up fragment. The down fragments were amplified using either the forward primers VCb82V-D23E, VCb82V-D23N, VCb90V-S26A, VCb90V-S26T or pomB-D42N fwd in combination with the reverse primer VcmotBRIII rev. Up and down fragments were purified as described in Chap. D, 4.7.2 and used for a second PCR reaction to amplify fragments GFP-PomB-D23E, -D23N, -S26A, -S26T and -D42N using primer pair WS 013-GFPend f and VcmotBRIII, resulting in a 1092 bp fragment – containing the designated mutations – which was as well purified. pAB$_{GFP}$ and the GFP-PomB fragments were cut using restriction enzymes AgeI and XhoI, additionally pAB$_{GFP}$ was treated with CIP. The purified restriction products were ligated with the enzyme T4 DNA ligase (NEB) at room temperature for three hours, which results in plasmids pAB$_{GFP}$-D23E, -D23N, -S26A, -S26T and -D42N.

1.4 GFP labeled PomB localizes at the cell pole of *V. cholerae* Δ*pomAB*

In previous studies, Fukuoka and coworkers postulated that a point mutation in the critical aspartate 24 in PomB of *V. alginolyticus* results in a loss of motility due to a defect in the flagellar stator assembly (59). They lean their assumption on the observations that GFP labeled PomB-D24N did not localize at the cell pole in the same amount GFP-PomB wild type did.

To confirm a proper assembly of the stator components in the flagellar motor, the superfolder green fluorescence protein was fused to the N-terminus of PomB and PomB variants. These plasmids were then transformed into the strains *V. cholerae* Δ*pomAB* and *V. cholerae* Δ*fliG*. The *fliG* deletion mutant served as control for deficient stator assembly. It has been shown that this component of the flagellar switch complex is essential for flagellar assembly. A loss of FliG results in an aflagellated phenotype of *V. cholerae* (63). It is assumed that PomA and GFP-PomB will not integrate into the cellular membrane or the flagellar motor. Fluorescence signals are neither expected in the membrane nor at the cell poles.

As experiments, in which low concentrations of arabinose (0.4 mM and 1 mM) were added to the cultivation media did not result in a distinct fluorescence signal within the cells (data not shown), a concentration of 10 mM was chosen. A quantitative analysis was performed by counting a minimum of 305 cells (PomB-wt: 500, -D23E: 322, -D23N: 342, -S26A: 500, -S26T: 500, -D42N: 305). The results are summarized in Tab. B.1. The PomB-D23N variant does does not show a significant difference compared to the wild type. The stator complex assembles in the flagellar motor at the cell pole.

The resulting images from the fluorescence microscopy are shown in Fig. B.4. All cells show a distinct fluorescence signal of GFP-PomB and GFP-PomB variants either at one cell pole or both. Even when no polar signal was detected, the cell membranes exhibit an even fluorescence signal. As mentioned in Chap. A, 3.1, the PomAB complex enters the cell membrane as inactive stator complexes, where they migrate towards the cell pole, to assemble there into the flagellar motor. Despite a mutation in the aminoacid sequence of PomB, the flagellar stator complex (PomAB) is transported into the cell membrane and assembled into the flagellar motor. As expected the control experiments with the aflagellated *V. cholerae* Δ*fliG* complemented with plasmids encoding for PomA and GFP-PomB and GFP-PomB variants show no or very slight fluorescence signals in the cytoplasm (Fig. B.5). Due to the lack of FliG, the flagellum will not be assembled. So it is most likely, that overexpressed PomA and GFP-PomB wild type (and variants) will soon be degraded by proteases. In these experiments 0.4 mM and 10 mM arabinose

Localization	One pole	Two poles	Membrane associated	Number
wild type GFP-PomB	197 (39.4%)	222 (44.4%)	81 (16.2%)	500 (100%)
GFP-PomB-D23E	128 (39.8%)	184 (57.1%)	10 (3.1%)	322 (100%)
GFP-PomB-D23N	101 (29.5%)	225 (65.8%)	16 (4.7%)	342 (100%)
GFP-PomB-S26A	232 (46.4%)	161 (32.2%)	107 (21.4%)	500 (100%)
GFP-PomB-S26T	259 (51.8%)	191 (38.2%)	50 (10.0%)	500 (100%)
GFP-PomB-D42N	117 (38.4%)	106 (34.8%)	82 (26.9%)	305 (100%)

Table B.1: Cellular localization of GFP-PomB in *V. cholerae* Δ*pomAB* co-expressing wild type PomA and GFP-PomB wild type and variants.

were used as inducer concentrations.

The ability of *V. cholerae* Δ*pomAB* complemented with plasmids coding for PomA and GFP-PomB and GFP-PomB variants to swarm was investigated using a motility assay on 0.25 % softagar plates containing 0.4 mM, 1 mM and 10 mM arabinose. Single colonies were stabbed into the agar with a toothpick and the plates were incubated for 22 h at 30 °C. The diameters of the colonies were measured and illustrated in Fig. B.6 D. The use of different final inducer concentrations did not result in a significantly altered motility behavior (Fig. B.6 A-C) but a decrease in motility can be clearly seen when cells are expressing GFP labeled PomB or PomB variants. Swarming diameters reach a size of approximately 0.25 cm, while the swarming ring of *V. cholerae* coding for wild type PomB reaches a size of approximately 1.5 cm. These results indicate that the green fluorescent protein impairs either the passage of Na^+ through the stator complex into the cell or the transfer of torque. GFP-labeled PomB is sufficient to confirm the polar localization of PomB variants but not to investigate the impact of mutations within PomB.

1.5 Purification of *V. cholerae* membranes containing PomA GFP-PomB wild type and variants.

For the isolation of membranes containing PomA GFP-PomB wt (and GFP-PomB variants) of *V. cholerae*, cells were cultivated as described in Chap. D, 5. The cells were harvested and the membranes containing PomA GFP-PomB wild type or GFP-PomB

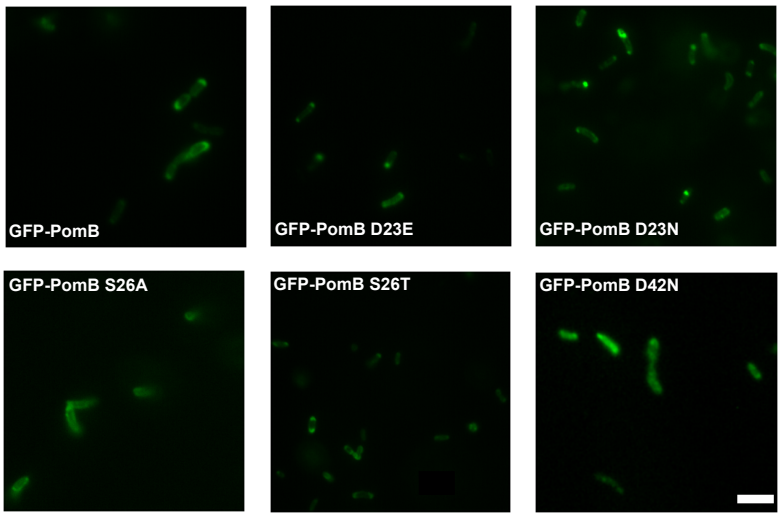

Figure B.4: GFP-PomB wt and variants localize at the cell pole of *V. cholerae* Δ*pomAB*. Expression of PomA and GFP-PomB wt and variants were started using 10 mM arabinose. After five hours, polar localization (signals on one or both poles) of GFP-PomB and GFP-PomB variants was analyzed by counting a minimum of 305 cells. Bar indicates 5 µm.

variants were isolated as described in Chap. D, 6. Gradient centrifugation of membranes yielded a brown band (Fig. B.7), which was used for further analysis by SDS-PAGE and Western blotting.

Protein concentration was determined as described in Chap. D, 10.2. For SDS-PAGE analysis a total of 200 µg of protein was loaded. Proteins were separated on a 10 % SDS-PAGE by electrophoresis as described in Chap. D, 10.3. After separation, GFP-labeled PomB wild type and variants were visualized using a TyphoonTrio System (GE healthcare) with excitation wavelength of 488 nm and 526 nm emission filter. As molecular standards the Precision Plus Protein WesternC Standards (BioRad) were used. The final band positions and the respective intensities are shown in Fig. B.8. The obtained fluorescence image (A) are in complete agreement with the corresponding western blot analysis (B) of the gel. GFP-PomB and all investigated variants are present in approximately equal amount (intensity of the bands) and same size (y-position of the bands) in the cell membrane. Uninduced whole cells of *V. cholerae* were used as a negative control. They show no fluorescent signal (Fig. B.8 A) and no detection in western blot analysis (Fig. B.8 B). The upper bands in Fig. B.8 B result from detection of the biotinylated α subunit of the oxaloacetate decarboxylase in *V. cholerae* by the Strep-Tactin-HRP conjugate.

These results (Fig. B.8) demonstrate, that a single point mutation in the aminoacid

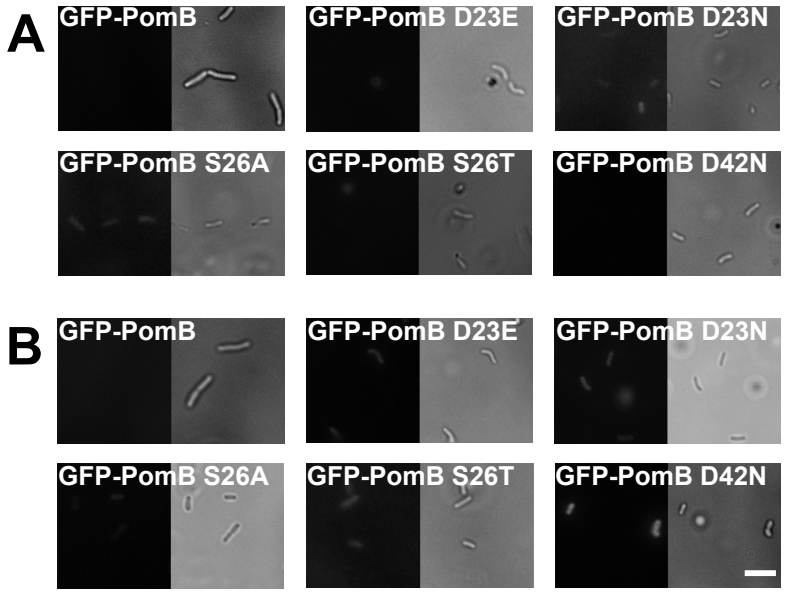

Figure B.5: *V. cholerae* Δ*fliG* shows no polar localization of GFP-PomB wt and variants. Cells were grown aerobically in liquid medium containing 0.4 mM (A) or 10 mM (B) arabinose. After five hours, 20 µL culture were spotted on poly-L-lysine covered glass slides and inspected using a fluorescence microscope to observe GFP-PomB and GFP-PomB variants. DIC images are shown on the right side of the corresponding fluorescence image. Bar indicates 5 µm.

sequence of PomB will not lead to an altered motility behavior due to disrupted stator complexes. It could be demonstrated that GFP-labeled PomB and PomB variants were integrated into the cell membrane. This conclusion is completely in line with the results of the experiments of Chap. D, 1.4.

1.6 Motility of *V. cholerae* Δ*pomAB* complemented with plasmid encoded PomA and PomB wt and variants relies on osmolality and pH

To find out whether the activity of the flagellum depends on the concentration of Na^+ and H^+, the motility of *V. cholerae* Δ*pomAB* co-expressing wild type PomA and variants of PomB was investigated on motility plates at pH 7.0, 8.0 and 9.0 in either rich or salt based minimal medium, and at different Na^+ concentrations ($[Na^+]$). The concentration of Na^+ ions of the media was determined by AAS, as described in Chap. D, 10.1. A decrease in the proton concentration in the media did not lead to a stimulation of swarming of *V. cholerae* expressing wild type PomB on softagar plates (Fig. B.9 and Fig. B.10), but rather reduced motility both at low and high Na^+ concentrations. At

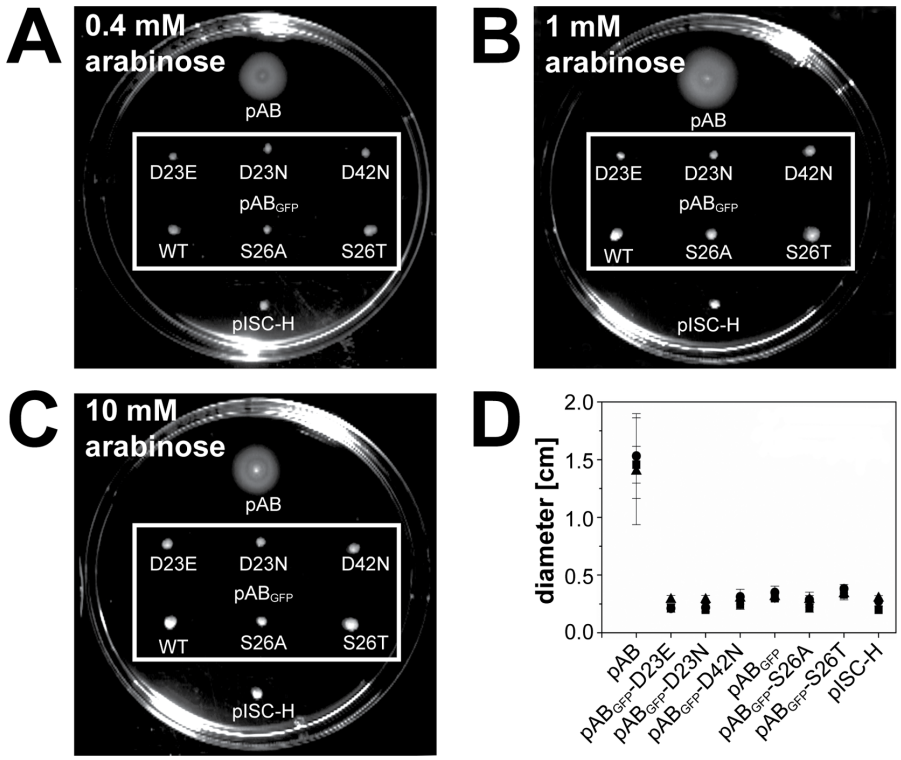

Figure B.6: Swarming of *V. cholerae* Δ*pomAB* transformed with plasmids coding for PomA and GFP-PomB (wt and variants). Swarming assays were performed on LB softagar plates pH 7 (0.25% agar supplemented with 0.4 mM (A), 1 mM (B) or 10 mM (C) arabinose and incubated at 30 °C for 22 h. (D) After 22 h, diameters were measured. In total, ten experiments for each condition were performed and the average of eight experiments was calculated (highest and lowest values were omitted). ■: 0.4 mM arabinose; •: 1 mM arabinose; ▲: 10 mM arabinose. Strains transformed with pAB encoding for PomA and PomB (indicating regular swarming), or with the empty vector pISC-H (exhibiting no motility), served as controls.

the lowest [Na^+] tested (1.6 mM in minimal medium), and at pH 9.0, motility of cells expressing wild type PomB was lost. Lowering the pH to 7.0 at this [Na^+] led to an increase in motility which reached roughly 50 % of motility observed at high [Na^+] at pH 7.0 (Fig. B.10). The stimulation of motility of cells expressing wild type PomB by Na^+ (170 mM, added as NaCl) was observed both on rich and minimal medium at pH 7.0, 8.0 and 9.0. However, this increase in motility was also achieved when NaCl was replaced by KCl. Under extreme conditions (pH 9.0 and 1.6 mM Na^+ in minimal medium) when cells were immotile, addition of 170 mM KCl rescued motility to the same extent as observed with 170 mM NaCl (Fig. B.10). Similar results were obtained when the carboxylic group at position 23 in PomB was maintained in the D23E variant.

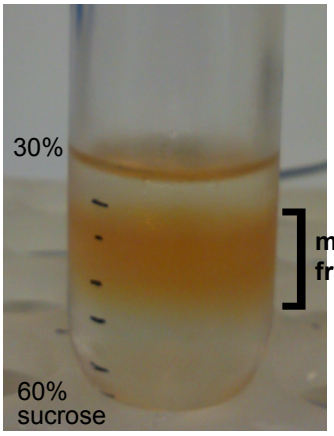

Figure B.7: Purification of isolated membranes using sucrose gradient centrifugation. Gradient ranged from 30 % to 60 % sucrose (w/v). After centrifugation, a clear, brownish fraction was visible which contains the purified membranes. Protein concentration was determined using a BCA assay. The concentration of proteins in the upper and lower fraction was below the detection level. The purified membranes were used for further analysis (SDS-PAGE and western blot).

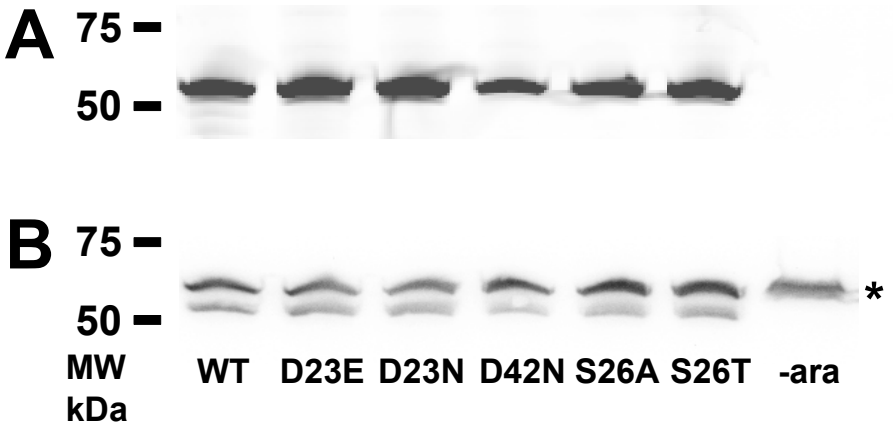

Figure B.8: Detection of GFP-PomB variants in membranes from *V. cholerae* Δ*pomAB* purified by sucrose density centrifugation. A total of 200 µg membrane protein per lane were loaded on an SDS-PAGE gel and subjected to electrophoresis. (A) In gel fluorescence of GFP-PomB wt and variants. Control (lane to the very right): uninduced whole cells. Molecular standard: Precision Plus Protein WesternC Standards (BioRad). (B) Western blot analysis of the gel from (A) blotted on a nitrocellulose membrane. GFP-PomB (with C-terminal Strep-tag) was visualized using Strep-Tactin-HRP and ECL. The upper bands result from detection of the biotinylated subunit α of *V. cholerae* oxaloacetate decarboxylase by the Strep-Tactin-HRP conjugate.

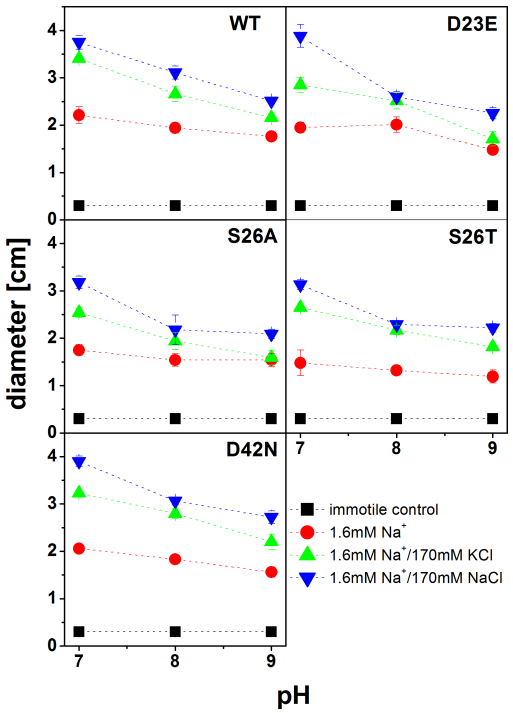

Figure B.9: The influence of pH and salt on swarming of *V. cholerae* Δ*pomAB* expressing PomB variants in LB medium. *V. cholerae* Δ*pomAB* was transformed with plasmids encoding for His6-PomA (wt) together with PomB-Strep (wt) or its D23E, S26A, S26T and D42N variants. The diameter of the swarming rings was determined after 21 h. Mean values from 8 experiments per data point are shown. No swarming was observed with cells transformed with the empty expression vector or with cells expressing the D23N variant of PomB.

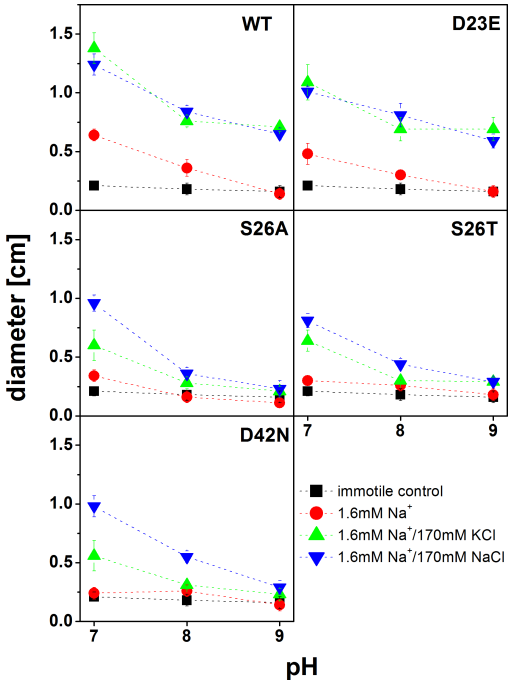

Figure B.10: The influence of pH and salt on swarming of *V. cholerae* Δ*pomAB* expressing PomB variants in minimal medium. *V. cholerae* Δ*pomAB* was transformed with plasmids encoding for His6-PomA (wt) together with PomB-Strep (wt) or its D23E, S26A, S26T and D42N variants. The diameter of the swarming rings was determined after 45 h. Mean values from 8 experiments per data point are shown. No swarming was observed with cells transformed with the empty expression vector or with cells expressing the D23N variant of PomB.

When M9 minimal medium buffered with 10 mM Tris and glucose as carbon source was used, we again observed slight stimulation of motility of cells expressing wild type PomB compared to PomB-D23E at pH 7.0 (Fig. B.10). In these experiments, the diameters of swarming rings were measured after 45 h at 30 °C.

1.7 Flagellation state of *V. cholerae* Δ*pomAB* expressing PomA and wild type PomB or PomB variants was confirmed by transmission electron microscopy

Cells harboring plasmids coding for PomA and wild type PomB (or PomB variants) were cultivated and prepared for inspection under a transmission electron microscope (LEO 912AB; Zeiss) as described in Chap. D, 8. Micrographs of cells were recorded with an magnification of x630.

V. cholerae Δ*pomAB* pAB	+ Flagellum	- Flagellum	Number
pH7			
wt	132	25	157
-D23E	121	23	144
-D23N	125	22	147
-S26A	128	15	143
-S26T	140	14	154
-D42N	126	23	149
pH8			
wt	135	27	162
-D23E	118	40	158
-D23N	142	7	149
-S26A	115	36	151
-S26T	116	38	154
-D42N	112	39	151

Table B.2: Statistical analysis of the flagellar state of *V. cholerae* Δ*pomAB* complemented with plasmids encoding for PomA and wild type PomB or PomB variants. A minimum of 143 cells for each condition were counted.

As expected most of the cells showed a polar flagellum (Fig. B.11) when cultivated in sodium limited minimal medium at pH 7.0 or pH 8.0. A quantitative analysis (Tab. B.2) also revealed no significant differences in the state of flagellation between the different strains. These results proofed that the diminished motility which was observed under

sodium limited condition on swarming plates (Fig. B.10) was not due to a lack of flagellation.

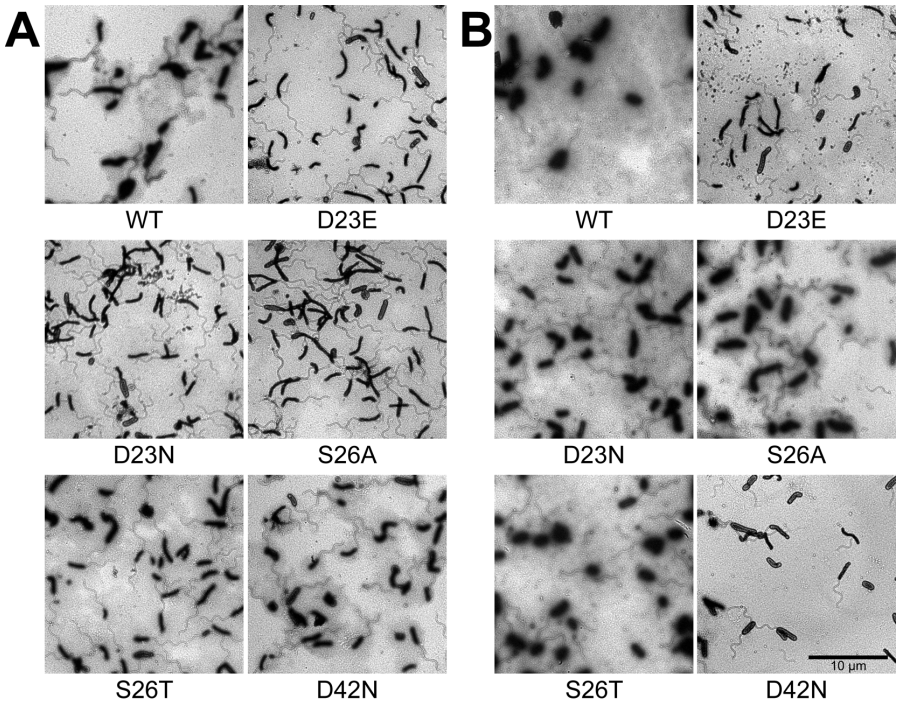

Figure B.11: Electron micrographs of *V. cholerae* Δ*pomAB* complemented with plasmids pAB coding for His-PomA and PomB wt and variants. Most of the cells show flagellation when grown on sodium limited M9 Minimal Medium supplemented with 10 mM arabionose at pH7 (A) or pH8 (B). Pictures were taken by Sebastian Leptihn using a Transmission Electron Microscope (LEO 912AB, Zeiss, Germany) at 80 kV. Bar indicates 10 µm.

1.8 Na^+ does not protect PomAB from modification by ^{14}C-DCCD

DCCD (N,N'-dicyclohexylcarbodiimide) is a reagent, which exclusively modifies carboxylic groups of aminoacids in hydrophobic environments. This reaction setup has been successfully used in the identification of different critical residues of protein complexes which are essential for binding Na^+ (e.g. modification of the c_{11} ring from the ATP synthase of *Ilyobacter tartaricus* (140) or the modification of NQR from *Klebsiella pneumoniae* (216)). To identify critical carboxylates of the PomAB stator complex which are essential for the binding of Na^+ or H^+, the influence of Na^+ on the modification of the PomAB or the PomAB-D23N complex by ^{14}C-DCCD was performed as described in (65). These experiments were performed by Thomas Vorburger.

The autoradiogram of the PomAB complex after modification with ^{14}C-DCCD at pH 6.0, 7.0 or 8.0 in the presence of 15 µM or 50 mM Na^+ and subsequent separation of the PomAB subunits by SDS-PAGE are shown in Fig. B.12 A. In a hydrophobic environment both subunits were labeled by ^{14}C-DCCD, which indicates the presence of at least one protonated, carboxylic residue. The addition of 50 mM Na^+ did not protect PomA or PomB from the reaction with ^{14}C-DCCD, although PomB inherits a carboxylic residue (D23) in its transmembrane region. As a positive control, the c-ring of *I. tartaricus* was included, which was – as expected – labeled by ^{14}C-DCCD in an sodium free environment, while it was protected from labeling by the addition of 50 mM sodium. To stimulate binding of Na^+ to the PomAB complex, 50 mM Na^+ was added to PomAB 10 min prior to the addition of ^{14}C-DCCD, and the pH was raised to 8.5, which facilitates the deprotonation of carboxylic groups (Fig. B.12 B). At alkaline conditions the overall modification of PomAB with ^{14}C-DCCD was reduced, but clearly, Na^+ did not have any effects on the rates of the protein modification. Interestingly, modification of wild type PomB was enhanced compared to the PomB-D23N variant at pH 7.5 and 8.5 (Fig. B.12 B), suggesting that D23 contributed to the reaction with ^{14}C-DCCD. Kinatic analysis of the modification of PomA and PomB with ^{14}C-DCCD at pH 7.5 revealed that both proteins were modified at a similar rate. Interestingly, at pH 8.5 PomA was no longer modified by ^{14}C-DCCD (Fig. B.12 C, D).

1.9 Tracking motility of single cells using light microscopy

Investigating motility of bacteria on softagar plates gives no insight on the swimming behavior of a single cell in liquid cultivation medium. As mentioned in the introduction, motility is influenced by different factors like chemotaxis and condition of the substrate (e.g. wetness or dryness of the agar plate). One has to take into account that the increase of the diameter of the swarming ring is not only dependent on the motility of the single cells but also on the growth speed of the colony. Swarming assays only give an rough estimation of the bacterial swimming speed. On account of this, velocity of single cells were determined by recording their movement in liquid media. This setup gives a precise determination of the actual speed without the distortion due to growth or agar composition.

The swimming speeds of *V. cholerae* cells producing wild type PomAB in liquid LB medium at different proton and salt concentrations were also determined (see Fig. B.13). In accord with the observed pH-dependent swarming behavior on solid medium, there was a decrease in motility with increasing pH at all salt concentrations investigated

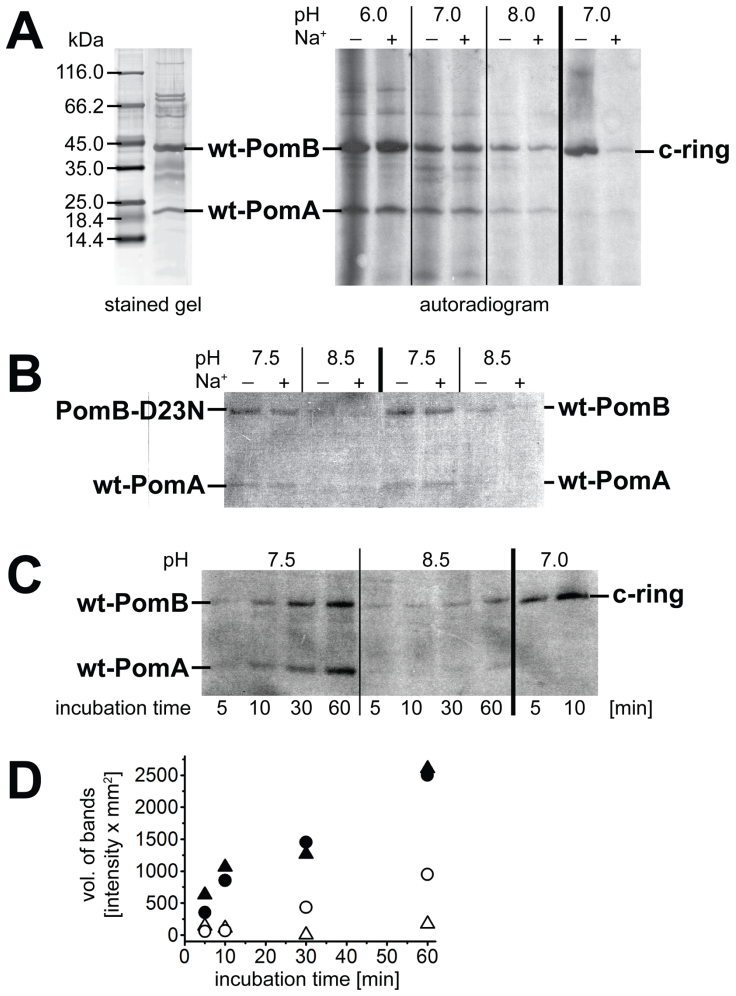

Figure B.12: SDS-PAGE of the PomAB complex and modification with ^{14}C-DCCD. (A) Left panel: SDS-PAGE of PomAB (2.2 µg in Cymal-5) stained with silver. Right panel: Autoradiogram of PomAB and the c-ring separated by SDS-PAGE after modification with ^{14}C-DCCD in the presence or absence of Na^+. PomAB (in Triton X-100, 6 µg per lane) was allowed to react with ^{14}C-DCCD for 1 h in the presence of 50 mM Na^+ (+) or absence Na^+ (-). The c-ring of the ATPase (4 µg per lane) served as control. (B) Comparison of the modification state of PomAB (6 µg) and the PomAB-D23N (6 µg) variant with ^{14}C-DCCD in the presence of 50 mM Na^+ (+) or absence of Na^+ (-). The pH was adjusted with MOPS/Tricine. After 10 min of incubation at room temperature, ^{14}C-DCCD was added and incubation was prolonged for 30 min. Reaction mixtures were diluted in SDS loading buffer and subjected to SDS-PAGE, shown is the autoradiogram of the SDS-PAGE. (C, D) Time course of ^{14}C-DCCD modification of PomA and PomB at pH 7.5 or 8.5 without added Na^+. (C): autoradiogram of the corresponding SDS-PAGE gel. Per lane, 6 µg wild type PomAB were loaded after reaction with ^{14}C-DCCD for indicated times. The pH was adjusted with MOPS/Tricine. The residual Na^+ concentration in the reaction mixtures was less than 15 µM. As a control, 4 µg of c-ring were incubated for 5 or 10 min with ^{14}C-DCCD. (D): quantification of the radioactivity incorporated into PomA at pH 7.5 (▲) or pH 8.5 (△), and into PomB at pH 7.5 (•) or pH 8.5 (○). Experiments were performed by Thomas Vorburger.

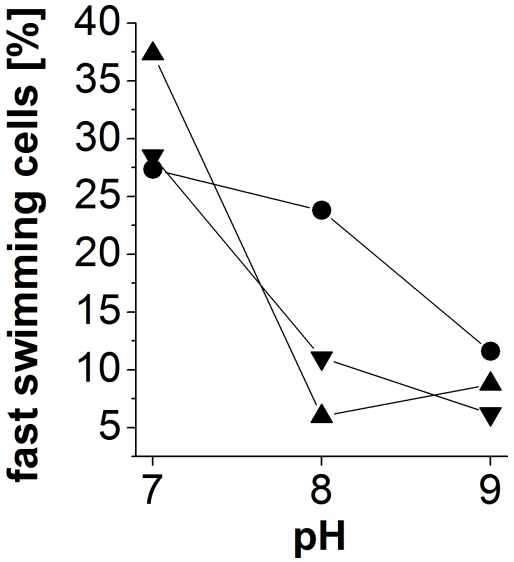

Figure B.13: Influence of external pH and salt on swimming speed of a *V. cholerae* Δ*pomAB* producing PomAB. The swimming speed of single cells was determined by recording their movement. A minimum of 200 tracks of individual cells was analyzed for each condition of pH and salt. Only bacteria exhibiting a swimming speed of $\geq 4\,\mu m\,s^{-1}$ were included in the analysis, and these represent 100 % of the motile cells under the indicated condition. Data points represent the fraction of fast-swimming cells exhibiting motilities between $18\,\mu m\,s^{-1}$ to $30\,\mu m\,s^{-1}$ as a percentage of the total number of motile cells at the indicated condition. ▼: 11 mM Na^+ and 170 mM NaCl; ▲: 11 mM Na^+ and 170 mM KCl; •: 11 mM Na^+.

(Fig. B.9). Notably, the percentage of motile cells at low ionic strength (11 mM Na^+ added) and pH 8.0 was higher than that under conditions with 170 mM NaCl or KCl, and the addition of salts did not stimulate the motility of cells at pH 9.0. In summary, the results show that the osmolality of the external medium rather than its Na^+ concentration determines the performance of the flagellum.

2 Serine 26 in the PomB subunit of the flagellar motor is essential for hypermotility of *Vibrio cholerae*

Petra Halang, Thomas Vorburger, Julia Steuber

Manuscript under revision, PLOS ONE

Vibrio cholerae is motile by means of its single polar flagellum which is driven by the sodium-motive force. The stator complex within the flagellar motor, consisting of subunits PomA and PomB converts the electrochemical sodium ion gradient into torque. Charged or polar residues within the membrane part of PomB could act as ligands for Na^+, or stabilize a hydrogen bond network by interacting with water within the putative channel between PomA and PomB. By analyzing a large data set of individual tracks of swimming cells, we show that S26 located within the membrane helix of PomB is required to promote very fast swimming of *V. cholerae*. Loss of hypermotility was observed with the S26T variant of PomB which was partially restored by lowering the pH of the external medium. This study identifies S26 as a second important residue besides D23 in the PomB channel. The H^+ rather than the Na^+ concentration determines the

efficiency of the motor, indicating the presence of a catalytical important hydrogen bond network in the motor channel.

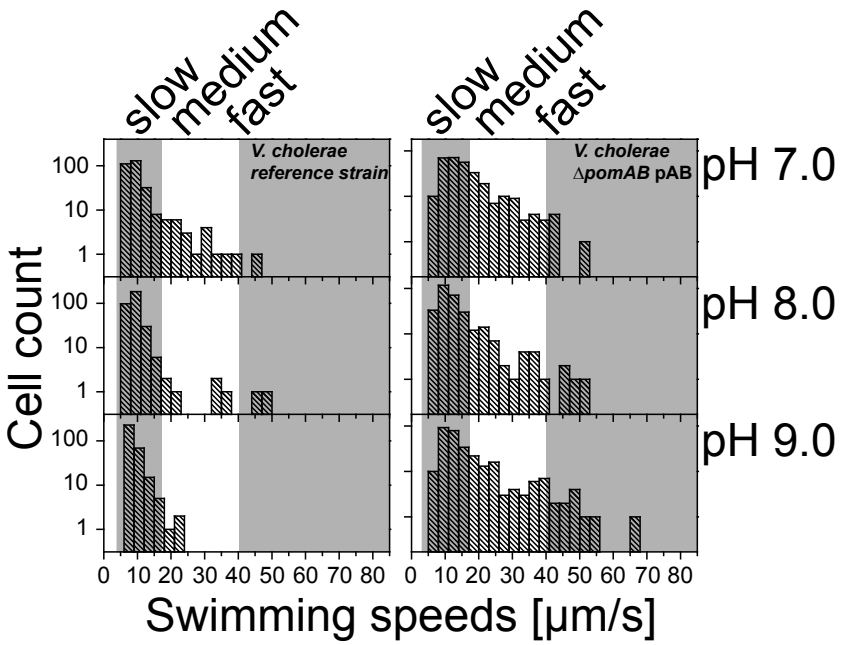

Figure B.14: Influence of pH on the distribution of swimming speeds of the *V. cholerae* reference strain and *V. cholerae* Δ*pomAB* expressing *pomA* and *pomB in trans*. Cells were grown in LB medium containing 171 mM NaCl. A minimum of 305 tracks (pH 7.0: 305; pH 8.0: 326 and pH 9.0: 320) (reference strain = WT; left panel) and 316 tracks (pH 7.0: 323; pH 8.0: 316 and pH 9.0: 322) (*V. cholerae* Δ*pomAB* transformed with plasmid pAB; right panel) per pH condition were analyzed. Tracking results of individual cells were assigned to three main classes of velocities (slow, medium and fast).

2.1 Tracking live *V. cholerae* cells by differential interference contrast microscopy.

An important prerequisite for the tracking of swimming cells by light microscopy is a clear contrast between the individual cells and their surrounding space. In a previous study, the use of a fluorescent dye (MitoTracker®, invitrogen™) to visualize *V. cholerae* cells by their fluorescence signal upon excitation with light of a distinct wavelength was described (220). The advantage of this method is that it produces images of single cells which, at 200-fold magnification, appear as bright, point-shaped objects in front of a dark background. Such objects cannot only be safely detected by spot detection algorithms, they can also be tracked quite easily by tracking algorithms provided by

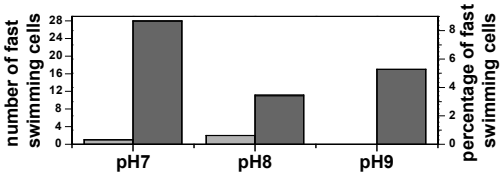

Figure B.15: Number and percentage of fast swimming *V. cholerae* reference strain and *V. cholerae* Δ*pomAB* expressing *pomA* and *pomB in trans*. Cells were grown in LB medium containing 171 mM NaCl. A minimum of 305 tracks (pH 7.0: 305; pH 8.0: 326 and pH 9.0: 320) (■: reference strain = WT) and 316 tracks (pH 7.0: 323; pH 8.0: 316 and pH 9.0: 322) (■: *V. cholerae* Δ*pomAB* transformed with plasmid pAB) per pH condition were analyzed. The number of fast swimming cells is also given as percentage to the whole amount of swimming cells.

commercially available image processing software like Volocity® (Perkin Elmer, USA) or Imaris® (Bitplane AG, Switzerland). However, there are disadvantages. One is that it could be observed that immotile cells produce significantly stronger fluorescent signals than motile cells do, and that these stronger signals tend to overlay the weaker signals of swimming cells, especially those of fast swimming cells. This particularly becomes a problem when a small fraction of fast swimming cells is to be analyzed in the presence of a considerable number of non-swimming cells. Another disadvantage is that the fluorescence signal from MitoTracker® stained cells bleaches out quite rapidly, preventing the recording of video sequences over longer periods of time. The method described here enabled us to analyze the distribution of velocities of a large number of individual cells.

2.2 Overexpression of the PomA and PomB stator components shifts the distribution of velocities towards higher swimming speeds.

Experiments were performed as described in Chap. D, 3.3.3. A minimum of 305 tracks (for pH 7.0) was analyzed. The majority of the analyzed cells of the *V. cholerae* reference strain exhibited swimming speeds in a range between 4 µm s^{-1} to 17 µm s^{-1} (Fig. B.14). The greatest speed measured (48 µm s^{-1}) was observed with *V. cholerae* grown in LB medium buffered to pH 8.0. Most of the cells clustered in a range of 4 µm s^{-1} to 17 µm s^{-1} at all proton concentrations of the medium tested. Only a small subset of cells exhibited high velocities at pH 7.0 and 8.0, while the majority fell into the medium and slow swimmer classes. When the pH was raised to 9.0, hypermotile behavior was completely lost. A different distribution of swimming speeds was observed with *V. cholerae* Δ*pomAB* expressing wild type PomA and PomB, leading to increased amounts of $PomA_4PomB_2$ stator complexes (65). Here, cells reached swimming speeds up to 74 µm s^{-1} (pH 7.0).

Even at pH 9.0, the *V. cholerae* Δ*pomAB* strain, lacking chromosomally encoded PomA and PomB proteins but transformed with the vector encoding for *pomA* and *pomB*, exhibited higher motilities than the reference strain (Fig. B.14). The number of fast swimming cells and the percentage to the whole number of swimming cells is given in Fig. B.15.

2.3 S26 in PomB is critical for fast swimming of *V. cholerae* cells.

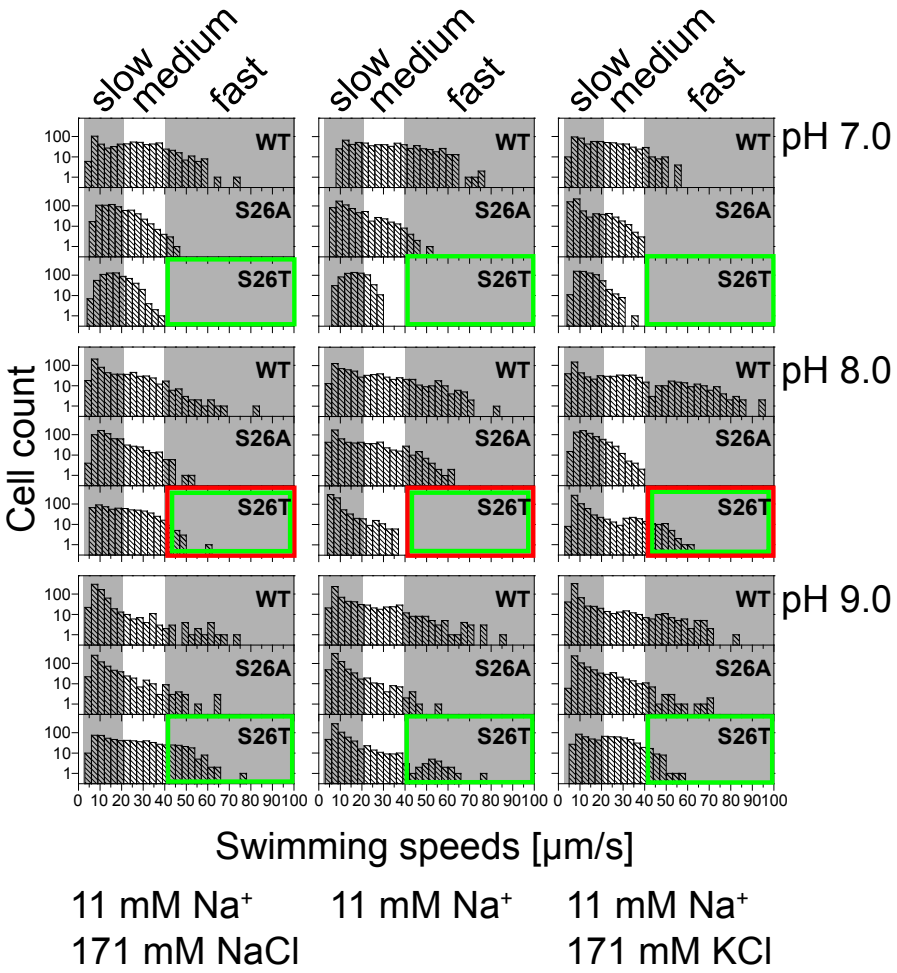

Figure B.16: Influence of pH on the distribution of swimming speeds of the *V. cholerae* Δ*pomAB* complemented with plasmids coding for PomA and wild type PomB or PomB variants. Between 629-650 tracks per pH condition and media were analyzed. Left panel: LB medium with 171 mM NaCl, middle: LB with no added NaCl (remaining [Na^+]: 11 mM) and right panel: LB with no added NaCl but 171 mM KCl. Tracking results of individual cells were assigned to three main classes of velocities (slow, medium and fast).

The influence of site-directed mutations in PomB on the distribution of individual motilities of *V. cholerae* strains was investigated, considering the effect of pH and osmolality of the medium. The swimming speeds of *V. cholerae* Δ*pomAB* expressing plasmids encoding PomA and wild type PomB, or the PomB-S26A or PomB-S26T variants in different media are presented in Fig. B.16, the number of fast swimming cells and the percentage to the whole number of swimming cells is given in Fig. B.17.

Swimming speeds of the strain expressing wild type PomB were evenly distributed over the three classes in LB_{Na^+} medium pH 7.0 (see Fig. B.16 left panel). Rising the pH of the LB_{Na^+} medium to 8.0 or 9.0 shifted the distribution of swimming speeds slightly towards the slow and medium class of swimming speeds respectively. At pH 9.0, only few cells exhibited swimming speeds of $40\,\mu m\,s^{-1}$ or higher.

It could be confirmed, that a substitution of the critical aspartate at position 23 in PomB (which corresponds to D24 in the closely related *Vibrio alginolyticus*) (59, 65, 220) by a glutamate restored wild type phenotype concerning motility at all conditions tested (data not shown). Mutation at position 42 of PomB (D42N) resulted in a minor phenotypical variation regarding swimming speeds at high NaCl or KCl concentrations (171 mM) in media buffered to pH 8.0 (data not shown). Under these conditions, most of the *V. cholerae* cells expressing the PomB-D42N variant were clustered in the slow and medium classes of swimming speeds. Only few cells were belonging to the fast class with swimming speeds of $40\,\mu m\,s^{-1}$ or higher.

It has been shown, that motility of *V. cholerae* cells, determined by swarming assays or by analyzing tracks of cells belonging to the medium class of velocity, critically depends on osmolality and pH (65). The analysis of a large set of tracks performed here revealed an unexpected phenotype of cells carrying mutations at position S26 of PomB (Fig. B.17).

An effect of salt on the performance of the PomB-S26T stator could be observed at pH 8.0 (highlighted in red in Fig. B.16). With *V. cholerae* expressing wild type PomB, velocities of cells were distributed in all three classes (slow, medium, fast), independent of the salt content of the medium. By introducing the S26T mutation, hypermotility was lost without added salt. Replacing S26 with A, on the other hand, resulted in a loss of hypermotility in the presence of 171 mM KCl, but not without added salt (residual Na^+ concentration 11 mM). A critical role of S26 in the presumed cation channel formed by PomB was also evident for the pH dependency of hypermotility (highlighted in green in Fig. B.16). While *V. cholerae* expressing wild type PomB exhibited high motility under all conditions of pH and salt tested, the PomB-S26T variant displayed a loss of fast cells at pH 7.0 (with or without added salt). Only at pH 9.0, when the concentration

of protons was very low, did the flagellar motor carrying PomB-S26T promote fast swimming of cells, albeit still less than the wild type motor under these conditions.

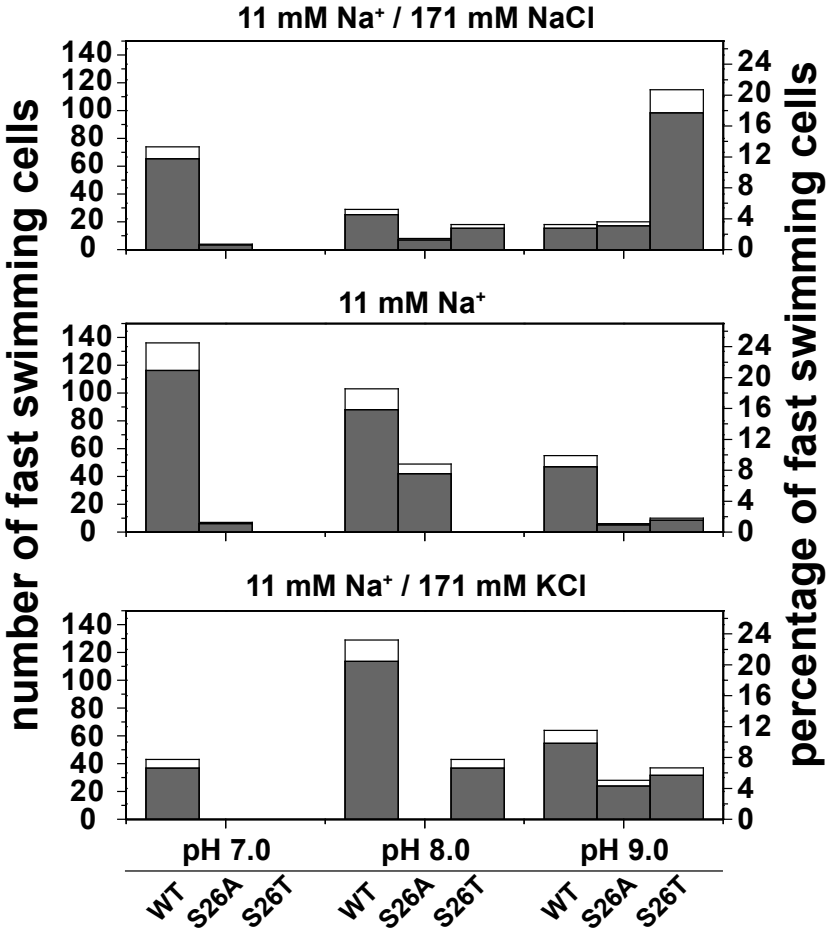

Figure B.17: Number (■) and percentage (□) of fast swimming *V. cholerae* Δ*pomAB* complemented with plasmids coding for PomA and wild type PomB or PomB variants. Total number of swimming cells for each strain and media condition (pH7/ pH8/ pH9): 11 mM Na^+ / 171 mM NaCl: WT (629/641/650), S26A (650/647/650), S26T (650/650/650); 11 mM Na^+: WT (650/650/649), S26A (650/650/649), S26T (650/677/650); 11 mM Na^+ / 171 mM KCl: WT (649/631/650), S26A (640/659/650), S26T (650/650/650).

3 Response of *Vibrio cholerae* towards the catecholamine hormones epinephrine and norepinephrine

Petra Halang, Bernadette Geissel, Birgit Flauger, Volker Stefanski, Julia Steuber

Manuscript in preparation

Stress enhances the feasibility of a mammalian host to infection by bacteria. Thus, it could be demonstrated that the stress associated mammalian hormones epinephrine and norepinephrine support growth (54, 55, 56) and motility (18, 19) of the enterobacteria *E. coli*, *S. enteric Serovar Typhimurium* and *Klebsiella pneumoniae* (20), of *Pseudomonas aeruginosa* (20, 74) and some *Vibrio* species (155) in serum-based bacteriostatic media. As epinephrine and norepinephrine share structural similarities to the bacterial catechol siderophores – a benzene ring with two adjacent hydroxyl groups – it was suggested that these stress hormones may be involved in the binding and uptake of iron by bacteria, thus promoting growth or motility (18, 19, 54, 55, 56). Recently the mechanism was elucidated by which catecholamine hormones bind to the ferrous ion inside the lactoferrin/ transferrin complex. The catecholamines are able to reduce Fe(III) to Fe(II), which results in a lower affinity for transferrin or lactoferrin to Fe(II) (174). It could be demonstrated for *E. coli* that norepinephrine works as a transcription factor, enhancing the expression of the siderophore enterobactin and as a direct consequence iron uptake (29). Structural similarities between bacterial siderophores and the catecholamine hormones and the availability of epinephrine and norepinephrine in the host gut strongly suggest that pathogenic bacteria are able to use these compounds as pseudosiderophores for the uptake of iron. Epinephrine and norepinephrine is an example of inter-kingdom communication, since bacterial gene expression pattern is influenced by host's hormones. Epinephrine and norepinephrine are sensed via the two component system QseBC, with QseC as the receptor for these catecholates and QseB as its cognate response regulator, which initiates transcription of different virulence associated genes (18, 192). *Vibrio cholerae* belongs to a group of human pathogens, which causes the severe illness cholera. During infection, *V. cholerae* colonizes the small intestine where it attaches itself to the epithelial cells (178). It secretes an enterotoxin during reproduction, which leads to an acute gastroenteritis (81). Using *V. cholerae* strain RIMD2203102, Nakano and coworkers did not observe specific response towards epinephrine or norepinephrine (155). Yet, the genome of *V. cholerae* O395-N1 (142) revealed the presence of a gene with a significant homology to *qseC* from *E. coli*. Here we present evidence that *V. cholerae* O395-N1 specifically responds to catecholate hormones, and discuss the significance of our findings with respect to stress-dependent modulation of *V. cholerae* within the host.

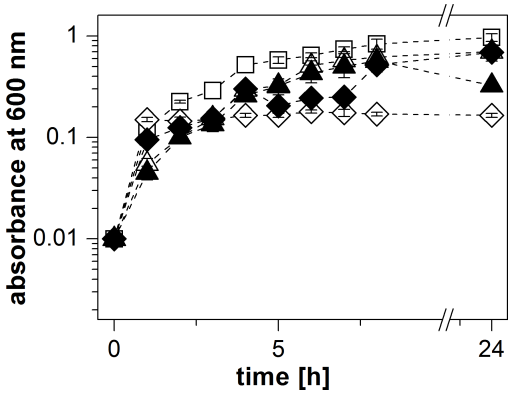

Figure B.18: The effect of different serum based SAPI media on growth of *V. cholerae*. □: heat-treated FCS-RPMI-1640, △: serum-SAPI (FCS), ▲: heat-treated serum-SAPI (FCS), ◇: serum-SAPI (ACS), ◆: heat-treated serum-SAPI (ACS). Average and standard deviation of two experiments are shown.

The subsequent chapters will focus on the effect of the catecholamine hormones epinephrine and norepinephrine on the growth and swarming behavior of the human pathogen *V. cholerae*.

3.1 Stimulation of growth of *V. cholerae* by catecholamines is dependent on cultivation medium

The effect of different cultivation media in combination with epinephrine or norepinephrine on the growth of *V. cholerae* was investigated. Growth was monitored over 24 h by measuring the optical density of the bacterial cultures at 600 nm. Each condition was tested as duplicates. The effect of growth was investigated in the following serum supplemented cultivation media: heat-treated FCS-RPMI-1640 (FCS, fetal calf serum), untreated or heat-treated serum-SAPI (FCS) and serum-SAPI (ACS, adult calf serum).

Growth curves of *V. cholerae* in the above mentioned cultivation media with no hormones added are illustrated in Fig. B.18. Best growth was found in heat-treated FCS-RPMI-1640 media. Here, *V. cholerae* reached a higher final OD_{600} after 24 h growth than in the other cultivation media. No significant differences were visible in the first 8 h of growth, when *V. cholerae* was grown in either heat-treated or untreated serum-SAPI (FCS) cultivation media. But while growth of *V. cholerae* continued in heat-treated serum-SAPI (FCS), the final OD_{600} after 24 h was lower in the untreated serum-SAPI (FCS) culture compared to the reading point after 8 h. The first reading point (after 1 h) of both serum-SAPI (FCS) cultures was significantly lower than the first reading point of all the other cultures (FCS-RPMI-1640 and serum-SAPI (ACS)).

Growth was also monitored in heat-treated or untreated serum-SAPI (ACS). While *V. cholerae* showed a more or less continuous growth in heat-treated serum-SAPI (ACS) and reached a final OD_{600} comparable to the OD_{600} achieved in serum-SAPI (FCS),

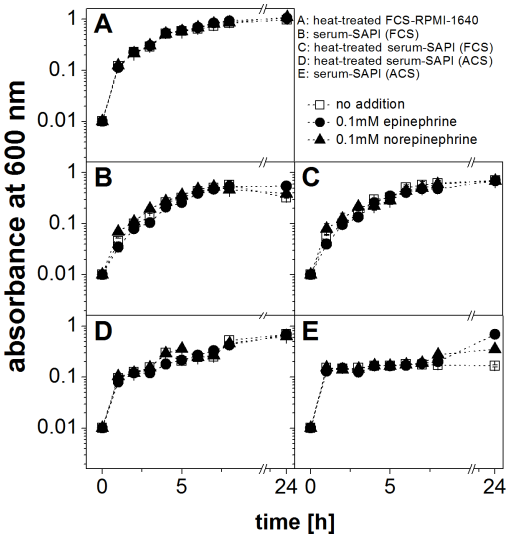

Figure B.19: The effect of catecholamines on growth of *V. cholerae* was investigated in different cultivation media. Optical density of the different cultures was measured every hour, the final OD_{600} was measured after 24 h. Average and standard deviation of two experiments are shown.

cells, grown in serum-SAPI (ACS) reached a rather high OD_{600} after 1 h compared to the other cultures, but then stopped growing and obviously had already reached its stationary phase.

The effect of 0.1 mM epinephrine or norepinephrine on growth of *V. cholerae* was also investigated in different cultivation media and is illustrated in Fig. B.19 A-E. This hormone concentration was chosen based on previous publications (20, 57, 160), and reflects the hormone levels found in mammalian target tissues (104, 114, 160). Growth of *V. cholerae* was not affected by the addition of either epinephrine or norepinephrine in heat-treated FCS-RPMI-1640 (Fig. B.19 A) and in heat-treated serum-SAPI (FCS) (Fig. B.19 C). The hormone treated cultures reached a similar OD_{600} after 24 h as the cultures without added hormones. Epinephrine and norepinephrine gave a slight advantage in growth, when *V. cholerae* was grown in serum-SAPI (FCS) Fig. B.19 B. While the final OD_{600} after 24 h of the untreated control declined compared to the reading point after 8 h, the absorbance of the hormone treated cultures remained constant or rised slightly.

Finally, the effect of epinephrine and norepinephrine was investigated in heat-treated and untreated serum-SAPI media (ACS). Growth of these strains was decelerated compared to cells which were grown in FCS based media. Epinephrine and norepinephrine did not promote growth, when *V. cholerae* was cultivated in heat inactivated serum-SAPI (ACS). Hormone-treated cells reached a similar final OD_{600} compared to the cultures without added hormones (Fig. B.19 D). An effect of the hormones was seen, when *V. cholerae* was cultivated in serum-SAPI (ACS) (Fig. B.19 E). After a huge gain of cell

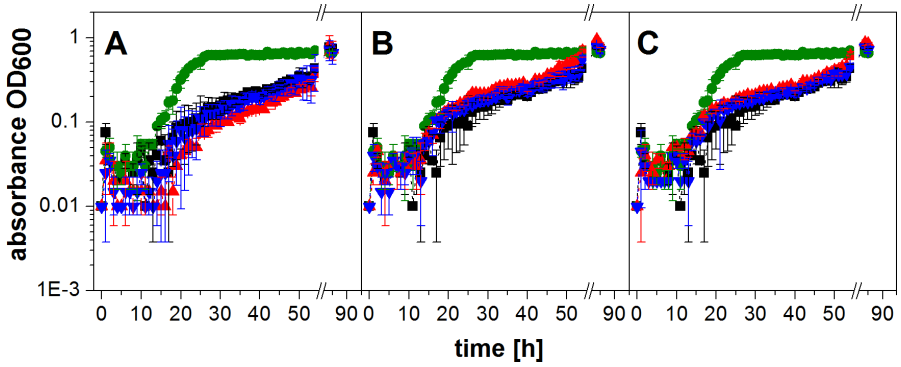

Figure B.20: Influence of low catecholamine concentrations on growth of *V. cholerae*. Serum-SAPI (ACS) medium supplemented with either 0.0001 mM (A), 0.001 mM (B) or 0.01 mM (C) epinephrine or norepinephrine. ■: untreated control, ●: 0.26 mM $FeSO_4$, ▼: norepinephrine, ▲: epinephrine. Experiments were performed as triplets and the outlier were omitted. The average and standard deviations were calculated from two experiments.

mass (reading point 1 h), the cells stopped to grow. Growth eventually continued after 8 h in the hormone treated cultures, with an advantage for the norepinephrine treated cells. After 24 h, the hormone treated cultures clearly reached higher OD values compared to the cultures without added hormones. *V. cholerae*, treated with epinephrine had at this point an advantage over the norepinephrine culture. This late effect on growth was in accordance with the literature, as it has been demonstrated that the release of iron by catecholamines takes about 24 h (127, 174).

The growth of *V. cholerae* was best stimulated by catecholamines in cultivation medium containing adult calf serum (serum-SAPI (ACS)) which had not been inactivated by heating. Cultures treated with either epinephrine or norepinephrine reached a higher OD_{600} after 24 h. For all further experiments (motility assays, RT-PCR and the detection of catecholates in bacterial supernatant via HPLC) SAPI medium supplemented with 30 % adult calf serum was used. For convenience, this medium will be referred to as serum-SAPI.

3.2 Epinephrine and norepinephrine stimulate growth of *V. cholerae*

As experiments from the above mentioned chapter revealed, effects of catecholamine hormones on growth were only visible in SAPI medium supplemented with adult bovine serum, which had not been heated. Experiments were performed with a final concentration of 0.1 mM (0.18 ng mL^{-1} epinephrine and 0.17 ng mL^{-1} norepinephrine) of each hormone. To investigate if lower concentrations of epinephrine and norepinephrine also

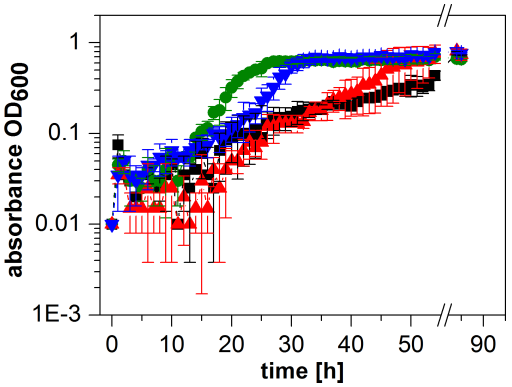

Figure B.21: Norepinephrine at a concentration of 0.1 mM **significantly enhanced growth of *V. cholerae*.** Bacterial growth was monitored for 85 h by measuring the optical density at 600 nm every hour. ■: untreated control, ●: 0.26 mM $FeSO_4$, ▼: norepinephrine, ▲: epinephrine. Experiments were performed as triplets and the outlier was omitted. The average and standard deviations were calculated from two experiments.

lead to a stimulation of growth, following concentrations were also included in growth experiments performed in serum-SAPI cultivation media: 0.0001 mM, 0.001 mM and 0.01 mM. To monitor the growing behavior of *V. cholerae* in serum-SAPI with sufficient iron supply, 0.26 mM $FeSO_4$ (final concentration) was added. Growth was monitored over a period of time of 85 h. The results are illustrated in Fig. B.20 A, B and C. The doubling rate (μ) and the generation time (t_d) of each culture was calculated (Tab. B.3).

The iron treated culture entered exponential growth phase after approximately 15 h and reached the stationary phase of growth after 26 h in which it remained until the end of the experiment. The bacterial cultures treated with 0.0001 mM, 0.001 mM and 0.01 mM catecholamine hormones entered exponential phase of growth after approximately 20 h. The doubling times of the cells was significantly higher than in the iron treated culture (see Tab. B.3). After 85 h the cultures reached the same final OD_{600} as the iron treated culture, nevertheless – at these hormone concentrations – *V. cholerae* did not exhibit an advantage in growth compared to the untreated culture (no addition of $FeSO_4$, epinephrine or norepinephrine).

The growth experiment was also performed with a concentration of 0.1 mM epinephrine or norepinephrine (Fig. B.21). In contrast to the experiments before, *V. cholerae* entered the exponential growth phase after 15 h when treated with 0.1 mM norepinephrine and entered the stationary phase of growth after 30 h. The doubling time was nonetheless decelerated compared to the iron treated culture.

At this concentration of 0.1 mM hormones, epinephrine also showed an effect on growth of *V. cholerae* compared to the experiments performed with lower concentrations. *V. cholerae* entered exponential phase of growth – later than the norepinephrine treated culture – after 20 h. The doubling time of the culture with epinephrine ($0.08\,h^{-1}$) is comparable to the doubling time of the culture without any treatment in the first 26 h of the experiments. After 40 h, the epinephrine treated culture enhanced its growth and

Growth condition	Point in time when stationary phase was reached [h]	Doubling rate [h^{-1}] (equation D.1)	Generation time [h] (equation D.2)
0.26 mM $FeSO_4$	26	0.16	4.4
0.1 mM norepinephrine	30	0.13	7.6
0.0001 mM epinephrine	85	0.05	18.4
0.001 mM epinephrine	85	0.05	18.6
0.1 mM epinephrine	85	0.05	19.0
no addition	85	0.05	19.1
0.01 mM epinephrine	85	0.05	19.1
0.0001 mM norepinephrine	85	0.05	19.2
0.001 mM norepinephrine	85	0.05	19.2
0.01 mM norepinephrine	85	0.05	19.5

Table B.3: Doubling time and generation time of *V. cholerae* under the influence of catecholamines and iron.

reached the stationary phase of growth after approximately 50 h. The doubling rate and generation times of the untreated and the epinephrine treated cultures were also calculated from date point 35 h on. At this late point in time, the epinephrine treated culture had a much higher doubling rate (0.08 h^{-1}) and a shorter generation time (12.7 h) compared to the untreated control (0.03 h^{-1} and 26.7 h).

As it can be seen from these experiments, norepinephrine had a greater influence on growth of *V. cholerae* than epinephrine, reducing the generation time from 19 h to 7.6 h.

3.3 Increased swarming of *V. cholerae* in the presence of norepinephrine.

To study the effect of the catecholamines epinephrine and norepinephrine on the swarming behavior of *V. cholerae*, swarming assays were performed on serum-SAPI soft agar as described in Chap. D, 3.3.2.

The diameters of the swarming rings were measured after 24 h. The results are illustrated in Fig. B.22. As expected, the *pomAB* deletion strain, lacking a functional flagellum (63) showed no motility, although growth was slightly stimulated in the presence of norepinephrine. After 24 h of incubation, an increase in swarming could be seen for *V. cholerae* in both the epinephrine and norepinephrine treated cells. The addition of phentolamine, a reversible, non-selective α-adrenergic antagonist (35) reduced motility in the epinephrine and norepinephrine treated culture. It is noteworthy that there was

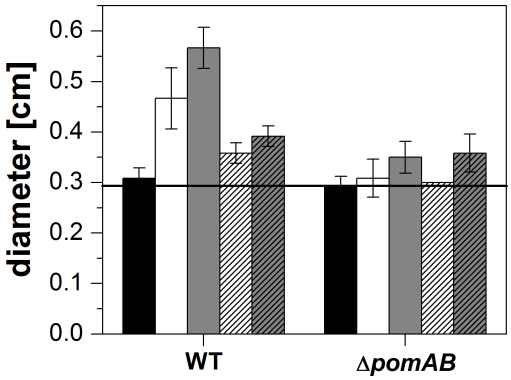

Figure B.22: Epinephrine or norepinephrine enhance swarming of *V. cholerae* on serum based SAPI softagar. Diameters of swarming rings of both *V. cholerae* and *V. cholerae* Δ*pomAB* were determined after 24 h. The average and standard deviations of six experiments are presented. ■: control without addition, □: 0.1 mM epinephrine, ■: 0.1 mM norepinephrine. Columns with hatching symbolize treatments with either 0.1 mM epinephrine or norepinephrine in the presence of 0.35 mM phentolamine. *V. cholerae* Δ*pomAB* is immotile due to the lack of the flagellar stator components PomAB and served as a indicator for colony growth in the absence of swarming ability.

some stimulation of growth (but no swarming) in the *V. cholerae* Δ*pomAB* strain with both norepinephrine and phentolamine, in accord with the observed stimulation of the Δ*pomAB* deletion strain in the presence of norepinephrine.

3.4 Detection of epinephrine and norepinephrine in bacterial supernatants using HPLC

To elucidate the fate of epinephrine and norepinephrine in bacterial supernatants, the detection of these catecholate hormones in bacterial supernatants at point in time 0 h and 48 h was tried using high-performance liquid chromatography (HPLC). Supernatant from serum-SAPI or bacterial serum-SAPI cultures were prepared as described in Chap. D, 9. The results are illustrated in Fig. B.23.

Norepinephrine and epinephrine were recovered from bacterial supernatant or serum-SAPI supernatant at the expected retention times at 4.2 min and 4.9 min at the start of the experiments. The detected amount of catecholates in these supernatants was around $2 \times 10^4\,\mathrm{ng\,mL^{-1}}$ (see Tab. B.4). After 48 h, the catecholamines were no longer detectable in serum-SAPI without bacteria.

A peak appeared in the supernatant from bacterial cultures treated with norepinephrine at point in time 48 h. The retention time was 4.48 min, which lay between the retention times of norepinephrine and epinephrine. The calculated amount of this unknown substance was $49.1 \pm 10.9\,\mathrm{pg\,mL^{-1}}$. In the bacterial cultures treated with epinephrine an additional peak appeared after 48 h at a retention time of 4.38 min. The

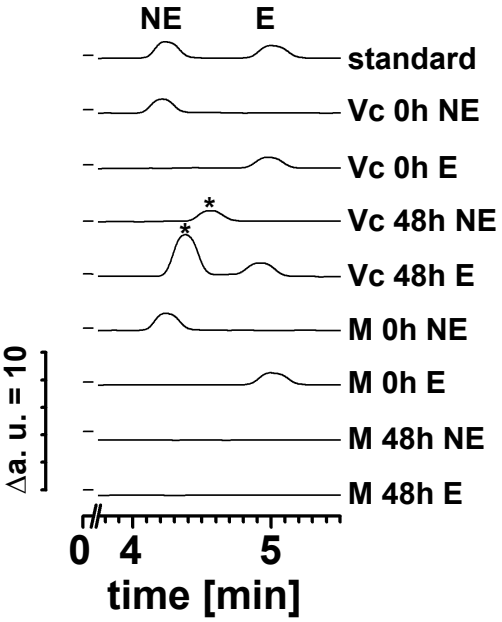

Figure B.23: Detection of norepinephrine (NE) and epinephrine (E) from serum-SAPI supernatant using HPLC. Norepinephrine and epinephrine have a distinct retention time at 4.2 min and 4.9 min. Samples were isolated at point in times 0 h and 48 h. standard: 1000 pg mL^{-1} norepinephrine and epinephrine in serum-SAPI, Vc: supernatant from *V. cholerae* grown in serum-SAPI, M: supernatant from serum-SAPI. Epinephrine or norepinephrine were added at a final concentration of 0.1 mM (18×10^3 ng mL^{-1} and 17×10^3 ng mL^{-1}) at point in time 0 h. Dilutions: Vc/M (E/NE) 0 h: 1:20.000; Vc/M (E/NE) 48 h: 1:80. Asterisks mark a peak of a yet unidentified compound.

Medium	Extraction of catecholamines after incubation [h]	Catecholamines added	Catecholamines recovered [ng mL^{-1}]	Catecholamines recovered [mM]
serum-SAPI	0	NE	2×10^4 $\pm$ 0.1×10^4	0.12 $\pm$ 0.01
	48	NE	0	0
	0	E	2×10^4 $\pm$ 0.2×10^4	0.11 $\pm$ 0.01
	48	E	662	3.7×10^{-3}
serum-SAPI with *V. cholerae*	0	NE	1.9×10^4 $\pm$ 0.6×10^4	0.11 $\pm$ 0.04
	48	NE	0	0
	0	E	2.2×10^4 $\pm$ 0.2×10^4	0.12 $\pm$ 0.01
	48	E	99 $\pm$ 5	5.5×10^{-4} $\pm$ 0.28×10^{-4}

Table B.4: Amount of epinephrine (E) and norepinephrine (NE) in serum-SAPI supernatant in the absence or presence of *V. cholerae*. Epinephrine or norepinephrine was added at point in time 0 h at a final concentration of 0.1 mM (18×10^3 ng mL^{-1} or 17×10^3 ng mL^{-1}).

Medium	Catecholamines added	Compound x [pg mL^{-1}]	Compound x [mM]
serum-SAPI	NE	0.0675	3.97×10^{-10}
	E	0.0388 ± 0.0145	2.15×10^{-7} ± 0.81×10^{-7}
serum-SAPI with *V. cholerae*	NE	49.1 ± 10.9	2.89×10^{-7} ± 0.64×10^{-7}
	E	173.98 ± 36.96	9.67×10^{-7} ± 0.21×10^{-7}

Table B.5: Estimation of the amount of a yet unidentified compound x formed in serum-SAPI in the absence or presence of *V. cholerae* after 48 h. Epinephrine (E) or norepinephrine (NE) was added at point in time 0 h at a final concentration of 0.1 mM 0.1 mM (18×10^3 ng mL^{-1} or 17×10^3 ng mL^{-1}). The retention time of these peaks were 4.48 min and 4.38 min, respectively (see Fig. B.23, asterisks).

peak for epinephrine appeared at the expected retention time of 4.92 min.

In summary, growth experiments and swarming assays indicate the presence of a receptor for epinephrine or norepinephrine in *V. cholerae*.

3.5 Search for a QseC-type protein in *V. cholerae* by sequence comparison

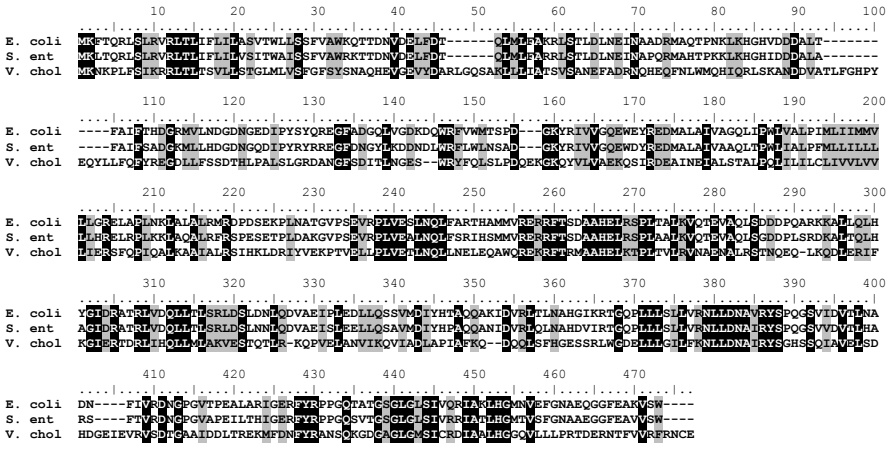

Figure B.24: Sequence alignment of QseC from *E. coli* and *S. enterica* and a sensor histidine kinase of *V. cholerae*. Identical or similar residues were identified using an identity and similarity threshold of 83 % and BLOSUM62 scoring matrix. *E. coli* QseC: gi|157156217, *S. enterica* QseC: gi|16766478 (87 % identity and 79 % similarity) and *V. cholerae* sensor histidine kinase gi|147672219. (49 % identity and 30 % similarity).

Bacteria are able to sense catecholamine hormones. Several studies have been accomplished, characterizing the two component system QseBC of *E. coli* (83) and *S. enterica* Serovar Typhimurium (18, 19). A protein-protein BLAST was performed with the aminoacid sequence from QseC (YP_001464488.1) from *E. coli*. The results are summarized in Tab. B.6 and revealed that a protein homologous to QseC is present in a variety of important human, animal or plant pathogens. A phylogenetic tree (Fig. B.25), based on the sequences from Tab. B.6 elucidated the relationship of the different QseC homologs. A sequence alignment of QseC from *E. coli*, *S. enterica* Serovar Typhimurium (87 % identity and 79 % similarity) and *V. cholerae* (49 % identity and 30 % similarity) is illustrated in Fig. B.24 and indicated the existence of a homolog of a QseC receptor within *V. cholerae*, with a putative histidine kinase domain (228) from aminoacid 254 to 319 and a HATPase_c site from aminoacid 362 to 471 as predicted by SMART ((117, 179)).

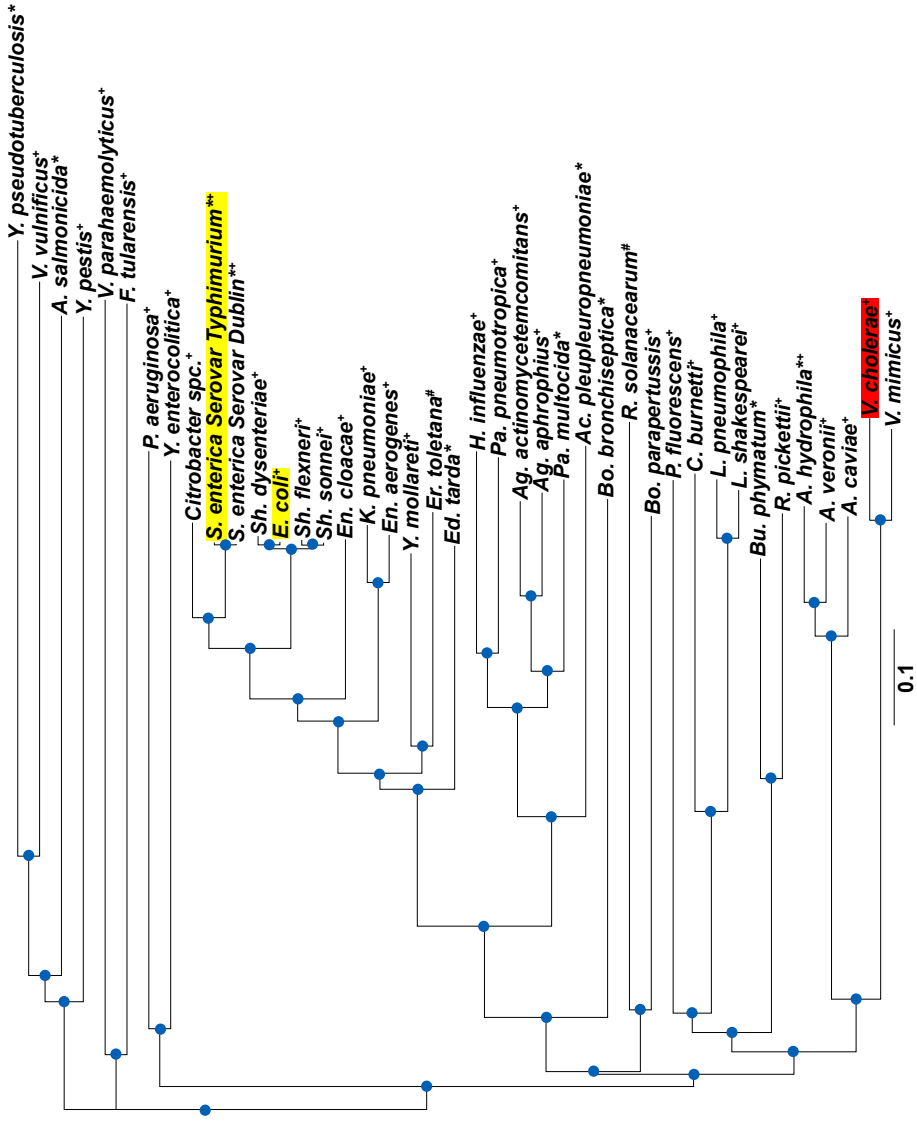

Figure B.25: Phylogenetic tree of QseC homologs based on sequences from Tab. B.6. Important plant (#), animal (*) and human (+) pathogens are grouped according to their phylogenetic relationship. The scale bar indicates the amount of genetic changes over time, blue nodes represent putative, common ancestors. Ac: *Actinobacillus*, A: *Aeromonas*, Ag: *Aggregatibacter*, Bo: *Bordetella*, Bu: *Burkholderia*, C: *Coxiella*, Ed: *Edwardsiella*, En: *Enterobacter*, Er: *Erwinia*, E: *Escherichia*, F: *Francisella*, H: *Haemophilus*, K: *Klebsiella*, L: *Legionella*, P: *Pseudomonas*, Pa: *Pasteurella*, R: *Ralstonia*, S: *Salmonella*, Sh: *Shigella*, V: *Vibrio*, Y: *Yersinia*.

Organism	Annotation	GenBank accession	Similarity	Identity	Reference
Actinobacillus pleuropneumoniae Serovar 5b str. L20	sensor protein QseC	YP_001053761.1	61 %	35 %	(118)
Aeromonas hydrophila	QseC	AEQ26013.1	51 %	30 %	(96)
Aeromonas caviae	histidine kinase	WP_010673792.1	52 %	32 %	this work
Aeromonas salmonicida	two-component system sensor histidine kinase	YP_001143700.1	47 %	28 %	this work
Aeromonas veronii B565	two-component system sensor histidine kinase	YP_004391584.1	51 %	31 %	this work
Aggregatibacter actinomycetemcomitans	sensor protein QseC	WP_005576433.1	64 %	47 %	(157)
Aggregatibacter aphrophilus NJ8700	sensor protein QseC	YP_003006953.1	64 %	47 %	this work
Bordetella bronchiseptica MO149	sensor histidine kinase QseC	YP_006899401.1	56 %	38 %	this work
Bordetella parapertussis 12822	two-component system histidine kinase	NP_884854.1	56 %	38 %	this work
Burkholderia phymatum STM815	integral membrane sensor signal transduction histidine kinase	YP_001862413.1	53 %	36 %	this work
Citrobacter sp. KTE151	sensor protein QseC	WP_016154513.1	89 %	80 %	this work
Coxiella burnetii	histidine kinase	WP_017253493.1	53 %	36 %	this work
Edwardsiella tarda ATCC 15947	QseC	ADO24152.1	73 %	58 %	(224)

Enterobacter aerogenes EA1509E	Sensory histidine kinase QseC	YP_007390817.1	82 %	68 %	this work
Enterobacter cloacae EC_38VIM1	sensor protein QseC	EPY95090.1	83 %	71 %	(160)
Erwinia toletana	sensor protein QseC	WP_017800276.1	72 %	57 %	this work
Escherichia coli E24377A	sensor protein QseC	YP_001464488.1	100 %	100 %	(192)
Francisella tularensis subsp. holarctica OSU18	sensor kinase	YP_764109.1	56 %	32 %	(48)
Haemophilus influenzae 10810	sensory histidine kinase in two-component regulatory system with QseB	YP_005179904.1	66 %	44 %	(212)
Klebsiella pneumoniae subsp. pneumoniae NTUH-K2044	sensor protein QseC	YP_002921274.1	81 %	66 %	this work
Legionella pneumophila	two component sensor kinase	YP_095321.1	58 %	35 %	this work
Legionella shakespearei	sensor histidine kinase	WP_018576931.1	52 %	31 %	this work
Pseudomonas aeruginosa	histidine kinase	WP_003149813.1	50 %	30 %	(160)
Pseudomonas fluorescens	sensor histidine kinase	WP_016979617.1	53 %	29 %	this work
Pasteurella multocida	sensor protein QseC	WP_005751165.1	65 %	47 %	this work
Pasteurella pneumotropica	hypothetical protein	WP_018355569.1	63 %	45 %	this work
Ralstonia pickettii 12J	integral membrane sensor signal transduction histidine kinase	YP_001898159.1	51 %	34 %	this work

Ralstonia solanacearum IPO1609	two-component sensor histidine kinase protein	YP_002258229.1	55 %	36 %	this work
Salmonella enterica Serovar Typhimurium	sensor protein QseC	EKT14049.1	87 %	80 %	(18, 19, 143, 151, 152)
Salmonella enterica Serovar Dublin	sensor protein QseC	YP_002217156.1	87 %	79 %	(171)
Shigella dysenteriae Sd197	sensor protein QseC	YP_404713.1	99 %	99 %	this work
Shigella flexneri 5 str. 8401	sensor protein QseC	YP_690440.1	99 %	99 %	this work
Shigella sonnei	sensor protein QseC	YP_311984.1	99 %	99 %	(160)
Vibrio cholerae O395	sensor histidine kinase	YP_001214981.1	49 %	30 %	this work
Vibrio mimicus	sensor histidine kinase	WP_000792142.1	51 %	30 %	(155)
Vibrio parahaemolyticus RIMD 2210633	phosphate regulon sensor protein	NP_796949.1	48 %	32 %	(155)
Vibrio vulnificus	histidine kinase	WP_017789708.1	47 %	29 %	this work
Yersinia enterocolitica (type O:9) str. YE56/03	two-component system sensor protein	CCV36244.1	50 %	31 %	this work
Yersinia mollaretii	sensor protein QseC	WP_004875233.1	77 %	63 %	this work
Yersinia pestis	two-component regulatory system, sensor kinase protein	YP_003567735.1	51 %	32 %	this work
Yersinia pseudotuberculosis IP 32953	two-component system sensor kinase	YP_071228.1	46 %	28 %	this work

Table B.6: Occurrence of QseC or putative QseC proteins in different pathogenic bacteria. A protein-protein BLAST was performed with the aminoacid sequence from QseC (YP_001464488.1) from *E. coli* used as reference.

3.6 Expression of *qseC* and *pomB* is enhanced in the presence of catecholamines

To demonstrate expression of the *qseC*-like gene in *V. cholerae* and to study if expression is modulated by epinephrine or norepinephrine, qRT-PCR on *qseC* was performed. In parallel, the expression of the housekeeping gene *rssA* (coding for 16S RNA) was followed as a control. In addition, we followed *pomB* expression in response to epinephrine or norepinephrine, since expression of flagellar genes is known to be stimulated upon catecholate treatment (18). 5 mL of serum-SAPI supplemented with either 0.1 mM epinephrine, norepinephrine or $FeSO_4$ was inoculated with *V. cholerae* to a final OD_{600} of 0.02. Cells were grown aerobically at 37 °C for 25 h. Total RNA of each culture were isolated as described in Chap. D, 4.5. The quality of the isolated RNA was confirmed by gel-electrophoresis. Control cells (with no added hormones) were also grown in LB media or serum-SAPI (with heat-treated adult calf serum) as the RNA yield from cells grown in serum-SAPI was not sufficient. The yields of isolated RNA of *V. cholerae* are summarized in Tab. B.7.

Medium		RNA yield [ng µL^{-1}]
LB medium		1994
inactivated serum-SAPI		675
$FeSO_4$ (0.1 mM)	in serum-SAPI	386
epinephrine (0.1 mM)		182
norepinephrine (0.1 mM)		772

Table B.7: Yield of isolated mRNA from *V. cholerae* grown in different cultivation media.

The yield of cells and hence, the yield of RNA from serum-SAPI without the additions of hormones were too low to be used in a qRT-PCR reaction. Therefore, RNA isolation was optimized, starting with cells grown in either LB medium or heat-treated serum-SAPI medium. The yield of RNA was very promising (1994 ng µL^{-1} from cells in LB medium and 675 ng µL^{-1} from cells in heat-treated serum-SAPI). But qRT-PCR revealed, that the fold expression of *qseC* was remarkably higher in heat-treated serum-SAPI (without hormones) than in serum-SAPI (with the addition of hormones) (data not shown). The same effect was seen, when cells were grown in LB medium (data not shown). These media were therefore not suited to be used as controls in qRT-PCR.

For further experiments, cells were grown in serum-SAPI with the addition of 0.1 mM $FeSO_4$ to improve growth of *V. cholerae* and RNA was isolated from these cultures (386 ng µL^{-1} RNA).

Primer pair	Efficiency [%]	R^2
rrsA	97.6 %	0.997
pomB	103.1 %	0.988
qseC	129 %	0.994

Table B.8: Calculated primer efficiencies of primer pairs rrsA, pomB and qseC. Efficiencies of primers used in the qRT-PCR were calculated using CTX Manager (Bio-Rad). qRT-PCR products are shown in Fig. B.26.

The efficiencies of primers with regard to binding to *rssA*, *pomB* and *qseC* were tested as triplets with different cDNA concentrations (0.0025 ng, 0.025 ng, 0.25 ng and 2.5 ng), as described in Chap. D, 4.2. The results of two qRT-PCR preparations (0.0025 ng, 0.025 ng) of *qseC* were dismissed as the concentrations were too low to be detected. The primer efficiencies are shown in Tab. B.8. All primer pairs had an R^2 greater than 0.988 and efficiencies greater than 97.6 %, which lay in an optimal range.

The change in gene expression of *pomB* and *qseC* under the influence of 0.1 mM epinephrine or norepinephrine was investigated using qRT-PCR. Each gene and condition was measured as triplets. The size of the qRT-PCR products were confirmed by gel-electrophoresis (see Fig. B.26).

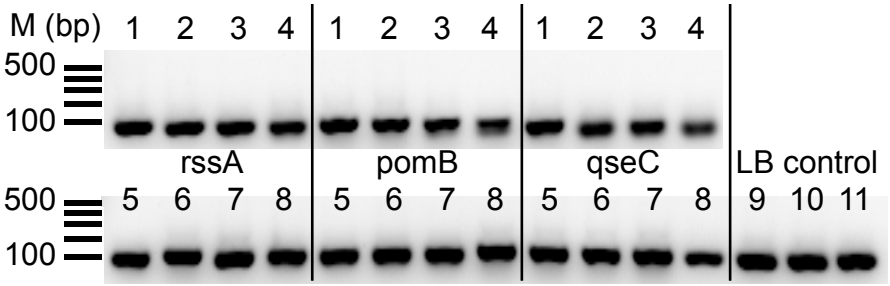

Figure B.26: The qRT-PCR products of *rssA*, *qseC* and *pomB* exhibit the expected lengths. Upper lane: cDNA preparations in combination with one of the tested primer pairs used for the primer efficiency tests, 1: 2.5 ng, 2: 0.25 ng, 3: 0.025 ng, 4: 0.0025 ng. Lower lane: cDNA obtained in the reverse transcriptase reaction from mRNA from cells grown in heat-treated serum (5), serum-SAPI with $FeSO_4$ (6), serum-SAPI with 0.1 mM epinephrine (7) and serum-SAPI with 0.1 mM norepinephrine (8). *RssA* (9), *qseC* (10) and *pomB* (11)were also amplified from LB cultures without added catecholamines (LB control).

The expression of both genes was increased by one third in the epinephrine treated cells. In the norepinephrine treated cells the expression of *pomB* and *qseC* is approximately doubled. The experiments should be repeated since in an independent study (master thesis of Bernadette Geißel), we observed increased stimulation of *qseC*-like gene expression with epinephrine rather than norepinephrine.

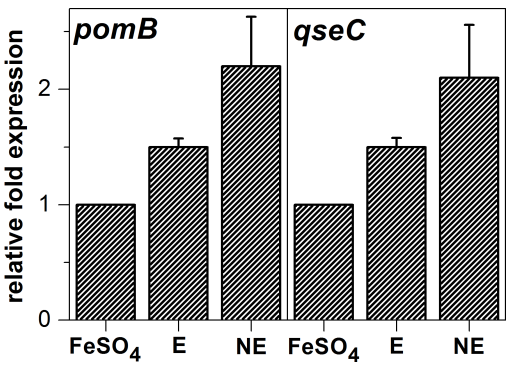

Figure B.27: Expression of *pomB* and *qseC* under the influence of epinephrine and norepinephrine. The relative fold expression of *pomB* and *qseC* was calculated using the Pfaffl-equation with the housekeeping gene *rssA* as reference. Expression of *pomB* and *qseC* from untreated cells ($FeSO_4$) was set to 1 and the expression of *pomB* and *qseC* from hormone treated cells was set in relation to that. Average and standard deviation were calculated from triples.

Chapter C

Discussion

1 Motility of *V. cholerae* is rather determined by salinity than the absolute sodium concentration of the environment

Motility of bacteria is achieved by their possession of extracellular, helical filaments, called flagella. These can be rotated counterclockwise (CCW) or clockwise (CW), either for straight swimming towards an attractant or tumbling, to change the swimming direction (23). The torque which is needed for driving the flagellum is generated by an ion gradient across the cell membrane. Important for the passage of ions across the cell membrane is the stator complex, which is embedded in the flagellar motor. The stator complex of sodium dependent motors is composed of four PomA (or MotA in proton depending motors) and two PomB (or MotB) subunits (25, 135, 201). One requirement of flagellar rotation is the binding of Na^+ to D24 in PomB from *V. alginolyticus* (59) or – as it has been shown for the closely related *V. cholerae* – to D23 (220). An exchange of this critical aspartate for asparagine resulted in an immotile phenotype, nonetheless this critical carboxylic residue does not represent the sole explanation for the cation selectivity in sodium driven flagellar motors. A comparison of observations from different experiments on flagellar motors, which are build up by subunits from sodium- and proton-depending motors led to the assumption "that there is no single determining component for ion selectivity" (188). These stands in contrast to other investigations concerning the function of the other rotational nanomachine, the Na^+-translocating F_1F_o ATPase.

1.1 The transmembrane helix III of PomA inherits structural similarities to the inner helix of the c ring from the Na^+-translocating F_1F_o ATPase

ATPases use for the synthesis of ATP an ion gradient (H^+ or Na^+) across the cell membrane to generate torque. The composition of these nano-sized rotary engines consists of two major parts, the hydrophilic F_1 complex in the cytoplasm and the hydrophobic, membrane embedded F_o complex (Fig. C.1) (218). The c ring structure of the F_o complex plays major role in the passage of Na^+. Well characterized is the hourglass-shaped c ring of *Ilyobacter tartaricus*, which consists of 11 subunits (139). Its hourglass shape is achieved by the possession of a proline residue in the transmembrane helix of the c ring (see Fig. C.2) and also helix III of PomA inherits a proline residue, which leads to a bend in the helix structure (219) (a computer model was compiled using PHYRE (95)). For comparison, the inner helix of the c ring from *B. pseudofirmus* does not inherit a proline residue and thus lacks a bend in the helix.

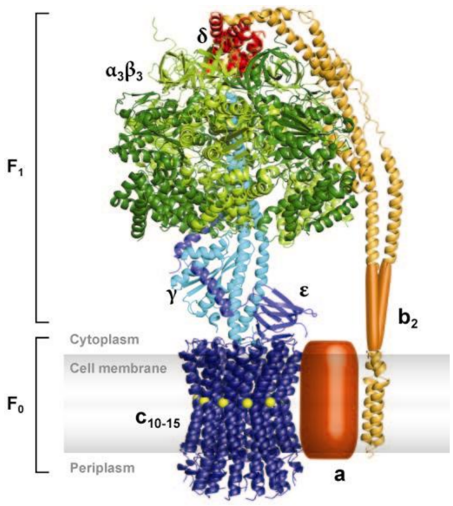

Figure C.1: Secondary structure elements and organisation of the F_1F_o ATPase subunits. Image was taken from (218).

The single monomers of the c ring possess two transmembrane helices which are connected via a hydrophilic loop in the cytoplasm. The N terminal helices form a tightly packed inner ring, due to a conserved motif build up by four glycine residues (see Fig. C.3). Glycine is the smallest aminoacid of the twenty aminoacids, which are found in proteins, for this reason the diameter in the N terminal helices is smaller at these positions (Fig. C.2). The c ring is able to bind 11 Na^+, which are located in the middle of the bilayer structure of the c ring. Four aminoacid residues play a role in the binding of Na^+: Q32 ($helix_{in}$), E65 ($helix_{out}$) on one c-subunit and V63 and S66 ($helix_{out}$) on subunit c^*. To prevent horizontal transfer of Na^+, E65 is also connected via hydrogen bonds to Q32, S66 and Y70 from the c^*-ring (underlined aminoacids in Fig. C.3). These conserved, critical aminoacid residues of the c ring determine the coupling ion specifity (H^+ or Na^+) of the rotor (106, 139). Despite structural similarities – helix III of PomA also inherits a conserved motif composed of glycines, helix IV of PomA and PomB possess

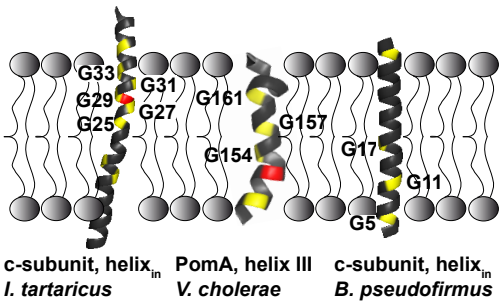

Figure C.2: Comparison of the inner transmembrane helices of the c rings of *I. tartraicus* and *B. pseudofirmus* and helix III of PomA of *V. cholerae*. Inner helices of *I. tartaricus* and *B. pseudofirmus* were drawn with Pymol using pdb files 1YCE and 2X2V. Model of helix III of PomA from *V. cholerae* was compiled using PHYRE (95). Numbered yellow residues stand for the conserved glycine motif, red residue stands for the proline.

several charged or polar residues – the selectivity for one specific ion (H^+ or Na^+) is not determined as strictly as in the Na^+-translocating F_1F_o ATPase.
In this work, the function of the conserved aminoacids D23, S26 and D42 of PomB from *V. cholerae* was investigated.

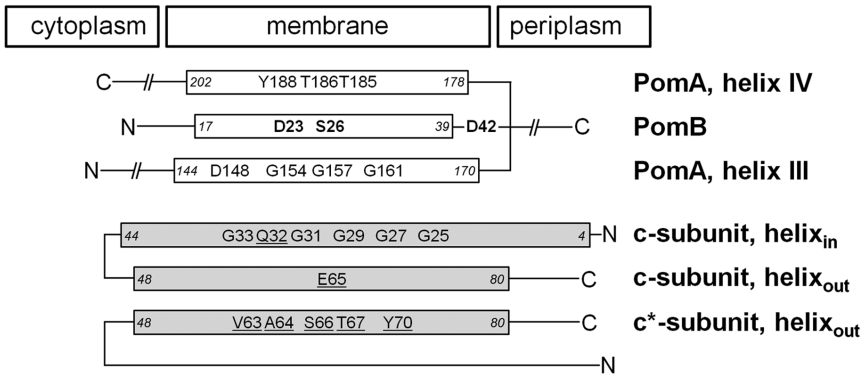

Figure C.3: Schematic illustration of the transmembrane helices III and IV of PomA and the single helix of PomB from the flagellar stator complex in comparison with helices from the c ring of the F_1F_o ATPase (65).

1.2 The aminoacid residues D23, S26 and D42 determine motility at decreased [H^+] in the environment

Previous studies revealed that D23 in *V. cholerae* (220) or D24 in the closely related *V. alginolyticus* (59) is essential for motility. While Homma and coworkers suggested that this lack of motility is due to a failure of integration into the flagellar motor (59), experiments performed in this study revealed different. Polar localization of GFP-PomB (and variants) was confirmed by fluorescence microscopy and a quantification of polar spots (see Chap. B, 1.4). SDS-PAGE and western blot analysis (see Chap. B, 4.7.2,

Fig. B.7) revealed an equal amount of GFP-PomB (and variants) in the cell membrane.

Assuming that both H^+ and Na^+ have access to the aspartate 23 in the PomAB stator complex via a channel opening towards the periplasm, a competition between these ions for binding to functional sites on PomA and/ or PomB is expected. A pH profile of flagellar activity should thus reveal an increase from pH 7.0 towards pH 9.0. Motility experiments performed with *V. cholerae* $\Delta pomAB$ transformed with plasmids encoding for PomA and PomB revealed the contrary. Highest motility was observed on rich and minimal media at pH 7.0.

Protonation of carboxylic residues in the transmembrane helices of PomA and PomB, which comprise binding sites for the coupling cation, should be prevented or diminished by the addition of Na^+. Results of ^{14}C-DCCD labeling experiments demonstrated that the presence of Na^+ did not protect the PomAB complex from labeling. These results suggest that Na^+ is not directly coordinated with carboxylic residues in the transmembrane helices of PomA and PomB. The actual binding affinity of Na^+ in the PomAB complex appears to be lower than in the Na^+-translocating F_1F_o ATPase (107, 138), nevertheless the specifity for Na^+ remains high in the PomAB stator complex, as the flagellar motor of *V. cholerae* cannot be operated with a H^+ motif force.

Another explanation, for the failure to detect a protection of ^{14}C-DCCD modification by Na^+ could be due to an inaccessibility of a Na^+ site in the PomAB stator complex. PomB possess in its periplasmic region a structure, which functions a plug for the sodium channel (119, 243). It is therefore probable that the PomAB stator complex was purified in its closed/ plugged conformation (e.g. as precomplexes (208)) before its use in ^{14}C-DCCD modification experiments.

The access of Na^+ to D24 in PomB of *V. alginolyticus* was studied by total reflectance-Fourier transform infrared (ATR-FITR) spectroscopy (198). The infrared absorbance spectra of purified PomB and PomB-D24N – reconstituted in proteoliposomes – were compared in these experiments. They rate K_d values for the binding of Na^+ to D24 to be 85 mM and 98 mM. The spectra were recorded at pH 5.5 – a non physiological environment – in which *V. cholerae* could not be studied, due to a lack of growth. At these pH conditions, nevertheless, the critical carboxylic residues, which are required for Na^+ can be labeled by ^{14}C-DCCD, despite saturating concentrations of Na^+ (106).

Motility experiments were also performed with S26 variants from PomB. Both amino-acids – D23 and S26 – are located in the transmembrane helix of PomB and are set apart by one helical turn. They are most likely located at the same side of the transmembrane helix (see Chap. B, 1.1, Fig. B.1). It has been demonstrated that a mutation in S27 from *V. alginolyticus* leads to a reduced motility compared to the wild type (206). Based

on the results of this work, it is proposed that D23 and S26 of PomB might contribute to the arrangement of water molecules or a hydrogen bond network in the stator complex, as it could be shown for the ATPase (106, 139). This hydrogen bond network might be important for a proper function in the Na^+ passage through the stator complex. These residues might also contribute to the Na^+ coordination within the stator. Under physiological ion concentrations, PomAB is still highly specific to Na^+ but the affinity for Na^+ is much lower, as motility experiments revealed. Motility of *V. cholerae* can be enhanced by the addition of chloride, which can act as a chaotrope (36). Cl^- may alter structural water molecules close to D23 and S26 and thus facilitates the access of Na^+ to the stator complex. These considerations are confirmed by motility experiments, in which the S26A/T and the D42N variants lost their motility on media with low ionic strength. Motility could be partially restored at pH 7.0 – but not at pH 9.0 – when chloride was added. It is concluded that D23 and S26 in the transmembrane helix of PomB have a functional importance, especially at decreased H^+ concentrations. D42, which is located just outside at the periplasmic side of the cell membrane, is also required for motility at alkaline conditions (pH 9.0).

2 Serine 26 is essential for proper Na^+ flux in different environmental conditions

Observing motility of bacterial cells on soft agar plate gives general information of motility within a bacterial colony but not the effect of external influences on single cells. Differences in swimming speeds can only be seen when velocities of a certain quantity of single cells are evaluated. Therefore, tracks of single *V. cholerae* cells in different liquid media were analyzed. The first thing, which struck was the observation that the swimming speed of all tested *V. cholerae* strains greatly varied, even within the same cultivation condition. The swimming speeds of cells of a given strain may vary from $4\,\mu m\,s^{-1}$ to $95\,\mu m\,s^{-1}$. Thus, presenting the average values for swimming speeds – as it has been performed in (101, 187, 206) – shows only an incomplete picture of the situation. This approach only yields representative results if the standard deviation between individual velocities is small. In the present study, the swimming speeds were grouped into three different classes, which cluster different ranges of velocities ($4\,\mu m\,s^{-1}$ to $17\,\mu m\,s^{-1}$, $18\,\mu m\,s^{-1}$ to $40\,\mu m\,s^{-1}$ and $> 40\,\mu m\,s^{-1}$). These classes were grouped into subclasses covering velocity ranges of $3\,\mu m\,s^{-1}$.

To establish the experimental setup, the distribution of the velocities of the reference

strain with the *V. cholerae pomAB* deletion strain transformed with a plasmid encoding for wild type PomA and PomB has to be compared. While the swimming speed of the *V. cholerae* reference strain ranged from $4\,\mu m\,s^{-1}$ to $49\,\mu m\,s^{-1}$, higher speeds were achieved by the transformed $\Delta pomAB$ strains. This might be due to the overexpression of plasmid encoded PomA and PomB. Most likely, more $PomA_4PomB_2$ precomplexes are located in the cell membrane and thus available for a "dynamical exchange" (208) of yet "to be used" stator complexes and precomplexes. Using this overexpression system, effects of PomB mutations on flagellar performance became apparent. This indicates that in vivo, the availability and/or insertion of the stator complex limits the maximal performance of flagellar function.

A helical wheel prediction of PomB suggests that S26 resides on the same side as the critical D23 and faces the inside of the transmembrane channel built by $PomA_4PomB_2$ (65, 97). It is thus very likely that S26 plays a role in the sodium ion transport across the cell membrane. The insertion of a threonine at position 26 of PomB led to a loss of hypermotility at pH 7.0. Hypermotility could only be restored at low external proton concentration, suggesting that threonine distorts a network of hydrogen bonds within the channel formed by PomB. Further support for this assumption comes from the observation that the S26A, but not the S26T variant, promotes hypermotility at pH 8.0 and low Na^+ concentration. We propose that serine 26 in the PomB channel is critical for coordinating water to maintain a hydrogen bond network independent of the pH, ensuring Na^+ flux through $PomA_4B_2$ in very different environments of *V. cholerae*.

3 *V. cholerae* responds to the catecholates epinephrine and norepinephrine

It has long been known that stress increases the risk of infection by pathogenic microorganisms. Studies, mainly performed on the human pathogen EHEC (83, 192) or the human and animal pathogen *S. enterica* Serovar Typhimurium (18, 19, 143, 151, 152) revealed the existence of a membrane embedded receptor (QseC) which is able to sense the catecholamine hormones epinephrine and norepinephrine or the bacterial aromatic autoinducer-3 (AI-3). The binding of one of these compounds leads to an expression of virulence genes in bacteria (83).

3.1 Epinephrine and norepinephrine enhance growth and motility of *V. cholerae*

V. cholerae is a human pathogen, which causes the severe illness cholera. It was therefore of an interest, to investigate if *V. cholerae* – like other human pathogens (e.g. EHEC or *S. enterica*) – also responds to the catecholamine hormones epinephrine and norepinephrine. In an earlier study by Nakano *et al.* (155), the effect of norepinephrine on bacterial growth was investigated with different *Vibrio* species (*V. parahaemolyticus*, *V. vulnificus*, *V. mimicus* and *V. cholerae*). The authors demonstrated that *V. cholerae* was unable to grow under iron limiting conditions and in the presence of the mammalian complement system (as it is given in serum-SAPI media). The addition of epinephrine or norepinephrine to serum-SAPI used for cultivation also showed no effect on growth of *V. cholerae*. These results stand in contrast to observations performed in this work.

Growth experiments in different cultivation media revealed that growth of *V. cholerae* was impaired in serum-SAPI (either heat-inactivated or untreated adult calf serum), but was not completely prevented. The addition of 0.1 mM of either epinephrine or norepinephrine enhanced growth of *V. cholerae*. Norepinephrine also shortened the log phase when compared to epinephrine.

Motility of *V. cholerae* was also enhanced in the presence of either epinephrine or norepinephrine. The addition of phentolamine – a reversible, non-selective α-adrenergic antagonist (35) – reduced motility of *V. cholerae*, when treated with either epinephrine or norepinephrine. But the diameters of these swarming rings were still at least double the size of untreated cultures.

These results indicate that *V. cholerae* might possess one or several membrane embedded receptors, which are able to bind epinephrine and/ or norepinephrine. The fact that phentolamine did not inhibit motility completely might be due to the low concentration of inhibitor used. It is also possible that epinephrine and norepinephrine bind with a higher affinity to its cognate receptors than phentolamine.

The stimulation of motility of *V. cholerae* by catecholamines, together with the observed growth stimulation in the presence of these hormones, strongly suggests that *V. cholerae* possess a specific apparatus for sensing of catecholamines. The immotile control strain (*V. cholerae* $\Delta pomAB$) showed bigger colonies, when exposed to epinephrine or norepinephrine (after 72 h) or phentolamine (after 48 h). Here, phentolamine might also play a role in iron sequestering, as phentolamine also possesses one hydroxyl group, which might bind to iron.

S. enterica Serovar Typhimurium inherits three outer membrane proteins – IroN,

FepA and Cir – which are needed for iron acquisition by binding of specific catecholate siderophores (enterobactin, salmochelines and 2,3-dihydroxybenzoylserine) (229). It has also been demonstrated that all three proteins are essential for the norepinephrine facilitated iron uptake from transferrin. A triple deletion mutant in *S. enterica* Serovar Typhimurium was unable to grow in serum based medium, despite the presence of norepinephrine (229). The growth effect on the immotile *V. cholerae* $\Delta pomAB$ suggests that *V. cholerae* inherits outer membrane receptors which not only bind to catecholate siderophores but also to norepinephrine-iron complexes. These systems will not only necessarily promote expression of flagellum associated genes but they will enhance proliferation. The effect of norepinephrine mediated iron uptake should therefore be studied in a deletion mutant of *V. cholerae* lacking receptors for the uptake of iron.

3.2 *V. cholerae* might stabilize epinephrine over a period of 48 h

Analysis of hormones added to serum-SAPI supernatant revealed, that epinephrine and norepinephrine incubated at 37 °C under shaking are unstable. After 48 h of incubation HPLC analyses revealed two compounds eluting at 4.38 min and 4.48 min, which appeared later than norepinephrine and epinephrine. It is not clear, if these peaks also characterize epinephrine and norepinephrine, with a decelerated retention time compared to the control. These peaks might also represent degradation products of epinephrine and norepinephrine. Both catecholates are known to degrade by oxidation into the final compound adrenochrome or noradrenochrome, respectively. This reaction is pH dependent and should be decelerated at physiological pH conditions (pH 7.4) (202). At the end of the oxidation procedure of epinephrine stands adrenochrome. This compound is formed by sequential electron loss (Fig. C.4). The first intermediate is an epinephrine quinone which changes via cyclization into leucochrome, the precursor of adrenochrome. Epinephrine tends to react with the hydroxyl radical ·OH (a reaction product of O^{2-} and H_2O_2) to form an *o*-semiquinone (4, 149). Investigations of bacterial serum-SAPI supernatant revealed that after a period of 48 h norepinephrine is completely degraded as well as a great part of epinephrine (Fig. B.23). At a retention time, which lies between the retention time of norepinephrine and epinephrine, a peak appears. This peak is remarkably bigger than in the untreated cultures. *V. cholerae* is known to produce extracellular superoxide (O^{2-}) (121). These superoxides are likely to react with either epinephrine or norepinephrine to oxidize these compounds into adrenochrome. Dhalla and coworkers were able to detect leucochrome – a precursor compound of adrenochrome – in different plasma samples but no adrenochrome. They suggested that the extraction process where

perchloric acid had been used, led to a decomposition of adrenochrome to its precursor substance leucochrome. Nevertheless they could draw conclusions on the amount of adrenochrome from the quantity of leucochrome detected (46). As the hormone treated supernatants in the present study were also extracted with 0.2 mM perchloric acid, the additional peak eluting between epinephrine and norepinephrine on HPLC might thus indicate the presence of leucochrome. In a next step, the characterization of the compound giving rise to this peak should be performed. A possible approach is described by Ochs *et al.*. They were able to detect different aminochromes (adrenochrome, noradrenochrome and dopaminochrome) in the presence of catecholates by electrochemical detection HPLC (159). In this study, analysis of epinephrine treated bacterial supernatant after incubation of 48 h revealed a small peak shortly after the expected retention time of epinephrine (4.9 min vs. 5.0 min (Fig. B.23)). One can assume that this peak results from epinephrine. It seems, that *V. cholerae* is not able to degrade or metabolize epinephrine in the same manner as norepinephrine. Another possibility might be that *V. cholerae* secretes compounds which stabilize the structure of epinephrine. Measurements should be repeated with bacterial serum-SAPI supernatant without the addition of catecholate hormones, as described by Kinney and coworkers, *E. coli* is able to produce small amounts of norepinephrine (98). It might be that *V. cholerae* is able to produce at least epinephrine, which would as well answer the question about the remaining epinephrine peak in the 48 h bacterial supernatant.

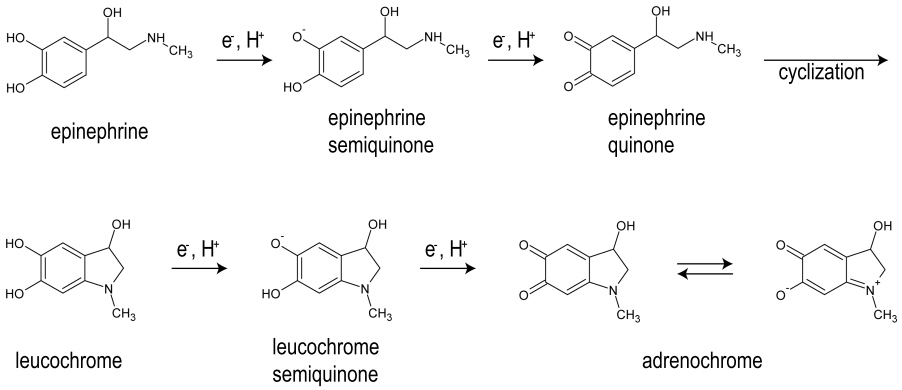

Figure C.4: Mechanism of epinephrine oxidation. Adrenochrome, the final product of the oxidation of epinephrine is achieved by the sequential loss of one electron. (159, 202).

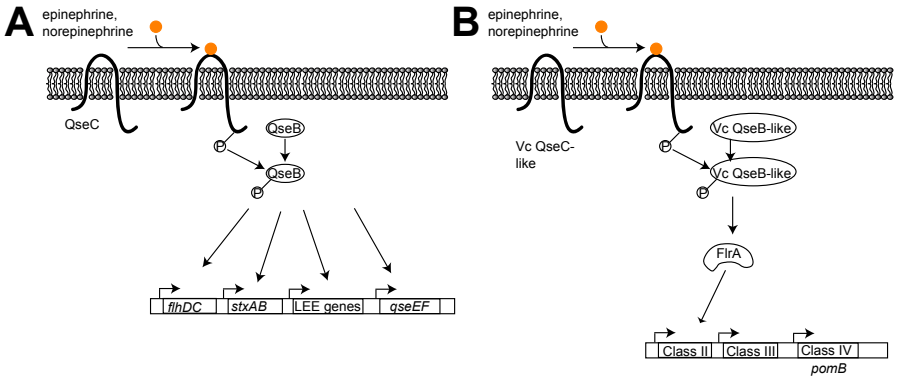

Figure C.5: Proposed model of signal transduction via QseBC in *V. cholerae*. Epinephrine and norepinephrine bind to the membrane embedded receptor QseC, which results in it autophosporylation. QseC then passes its phosphate to its cognate response regulator QseB, which eventually triggers the master regulator of the flagellar gene transcription FlrA.

3.3 The expression of *pomB* and *qseC* in *V. cholerae* is enhanced in the presence of epinephrine or norepinephrine

Protein-protein BLAST revealed a homolog protein to the well characterized QseC of *E. coli* and *S. enterica* Serovar Typhimurium, and to QseC or not yet characterized two component histidine kinases of other pathogens (Tab. B.6, Fig. B.25). *V. cholerae* also possesses a homolog response regulator protein (gi|147672339) with 44 % sequence identities and 67 % sequence similarities to the QseB from *E. coli* (gi|188490918).

Gene expression of this putative *qseC* sequence was tested in quantitative RT-PCR, together with the expression of *pomB* – a component of the flagellar stator complex. A higher expression level of *pomB* and *qseC* can be found, when *V. cholerae* was exposed to either epinephrine or norepinephrine. As a consequence, following model of signal transduction in *V. cholerae* is proposed based on models established for *S. enterica* (18) and *E. coli* (83, 156):

Epinephrine or norepinephrine bind to the membrane embedded receptor QseC of *V. cholerae*. This results in its autophosphorylation. QseC then transfers its phosphate to its cognate response regulator (the putative) QseB, which triggers the expression of flagellar genes. It may induce expression of the master regulator FlrA (39).

It would be interesting if the expression of toxin associated genes also increases upon hormone addition. Though it has been shown that hypermotile strains of *V. cholerae* are less virulent (62), the presence of epinephrine and norepinephrine might give *V. cholerae* an advantage in the colonization of the small intestine through a wider spreading within

the small intestine and a faster reaching of the epithelial cells. The results presented in this work, give first hints of the presence of andregenic receptors. But it still needs further experiments to prove this.

The next step should be the construction of a *qseC* deletion mutant in the apathogenic and as well in the pathogenic strains of *V. cholerae*. Plasmids and strains for this procedure have already been constructed. The characterization of *V. cholerae* $\Delta qseC$ should include swarming assays an motility agar plates containing catecholamine hormones. It should be expected that motility will be decreased. A different pattern in gene expression (especially in the expression of flagellum associated genes) can also be expected. qRT-PCR experiments should also include the detection of virulence associated genes in the pathogenic strain of *V. cholerae*.

Chapter D

Materials & methods

1 Bacterial strains, oligo-nucleotides and plasmids

1.1 Bacterial strains

Strain	Genotype	Reference
E. coli		
DH5α	*supE44 ΔlacU169 (ϕ80lacZ ΔM15) hsdR17 recA1 endA1 gyrA96 thi-1 relA1*	(69)
XL10 Gold	*endA1 glnV44 recA1 thi-1 gyrA96 relA1 lac Hte Δ(mcrA)183 Δ(mcrCB-hsdSMR-mrr)173 tet^R* F'[*proAB lacIqZΔM15 Tn10(Tet^R Amy Cm^R)*]	Stratagene
TOP10	*F$^-$ mcrA Δ(mrr-hsdRMS-mcrBC) φ80lacZ ΔM15 ΔlacX74 nupG recA1 araD139 Δ(ara-leu)7697 galE15 galK16 rpsL(Str^R) endA1λ^-*	Invitrogen
C43 (DE3)	F$^-$ *ompT gal dcm hsdSB(rB$^-$ mB$^-$)*(DE3)	(148)
π3813	B462 Δ*thyA::(erm-pir-116) (Erm^R)*	(112)
β2155	*thrB1004 pro thi strA hsdS lacZ ΔM15 (F' lacΔM15 laqIq traD36 proA$^+$ proB$^+$) ΔdapA::erm (Erm^R) recA::RPA-2-tet (Tc^R)::Mu-km (Km^R) λ pir*	(44)
β3914	β2163 *gyrA462 zei-298::Tn10 (Km^R Em^R Tc^R)*	(112)
MFD*pir*	MG1655 RP4-2-Tc::[ΔMu1::*aac(3)IV*-Δ*aphA*-Δ*nic35*-Δ*Mu2::zeo*] Δ*dapA::(erm-pir)* Δ*recA*	(51)

V. cholerae		
O395 N1	Δ*ctxA* Sm^R	(142)
O395 N1 Δ*pomAB*	Δ*ctxA* Δ*pomAB* Sm^R	(63, 142)
O395 N1 Δ*fliG*	Δ*ctxA* Δ*fliG* Sm^R	(63)
O395 N1 Δ*nqr*	Δ*ctxA* Δ*nqr* Sm^R	(16)

Table D.1: Bacterial strains used in this study.

1.2 Oligo-nucleotides

Name	Sequence
Vcb50R-S26T	GCACATCAGCAGTGTCATCAAGTCCGCAAAGGT ACCCAGCC
VCb50R-S26A	GCACATCAGCAGTGCCATCAAGTCCGCAAAGGT ACCCAGCC
pomB-D42N fwd (*AclI*)	CGGAGATG*AACGTT*CTGAAATTTAAGCAGATCG CTGGC
pomB-D42N rev (*AclI*)	GCCAGCGATCTGCTTAAATTTCAG*AACGTT*CAT CTCCG
VCb82V-D23N (*KpnI*)	GGCTG*GGTACC*TTTGCGAACTTGATGTCACTGC
VCb49R-D23N (*KpnI*)	GCAGTGACATCAAGTTCGCAAA*GGTACC*CAGCC
VCb82V-D23E (*KpnI*)	GGCTG*GGTACC*TTTGCGGAATTGATGTCACTGC
VCb49R-D23E (*KpnI*)	GCAGTGACATCAATTCCGCAAA*GGTACC*CAGCC
VCb90V-S26A (*KpnI*)	GGCTG*GGTACC*TTTGCGGACTTGATGGCACTGC TGATGTGC
VCb50R-S26A (*KpnI*)	GCACATCAGCAGTGCCATCAAGTCCGCAAA*GG TACC*CAGGG
VCb90V-S26T (*KpnI*)	GGCTG*GGTACC*TTTGCGGACTTGATGACACTGC TGATGTGC
VCb50R-S26T (*KpnI*)	GCACATCAGCAGTGTCATCAAGTCCGCAAA*GGT AC*CCAGGG
VCmotAV III (*NdeI*)	GCCGCGCGGCAGC*CATATG*GATTTAGCAAC
VCmotAV IV	GAAAGATCACACCGCCGTGGAAGAG
VCmotBR III (*XhoI*)	GGTGGCTCCA*CTCGAG*TTGTTGTCCACCGC
VcmotBR IV	ACATTTCCCCGAAAAGTGCCACCTG
WS-013-GFPend-f	CCCAACGAAAAGCGTGACCACATGGTC
rssA fwd	ACCGGAGGAAGGTGGGGACG

rssA rev	CTCGCGGTATCGCTGCCCTC
qseC fwd	TACTGGGGCCGCGATTGACG
qseC rev	TCGACATGCCAAGCCCTGCG
pomB fwd	CGCAGTTTCGGTGGCGCAAG
pomB rev	TGCCCGTTGCGCTTCGGTAT

Table D.2: Oligo-nucleotides used in this study. Italic parts in the sequence confer to an introduced restriction site.

1.3 Vectors

Vector	Size	Characteristics	Reference
pEC422		Confers His6-tag to the N-terminus of a target protein, Amp^R	(180)
pISC-2		p_{ara}BAD, *ara*, Amp^R	(9)
pJET1.2	2974 bp	$P_tlacUV5$, *eco47IR*, Amp^R	Thermo Scientific

Table D.3: Vectors used in this study.

1.4 Plasmids

Plasmid	Resistance	Characteristics	Reference
pISC-H	Amp^R	MCS of pISC-2 inserted into pEC422	(220)
pAB	Amp^R	p_{ara}BAD, codes for His6-PomA and PomB-Strep	(220)
pAB-D23N	Amp^R	p_{ara}BAD, codes for His6-PomA and D23N variant of PomB-Strep	(220)
pAB-D23E	Amp^R	p_{ara}BAD, codes for His6-PomA and D23E variant of PomB-Strep	(220)
pAB-S26A	Amp^R	p_{ara}BAD, codes for His6-PomA and S26A variant of PomB-Strep	this work
pAB-S26T	Amp^R	p_{ara}BAD, codes for His6-PomA and S26T variant of PomB-Strep	this work
pAB-D42N	Amp^R	p_{ara}BAD, codes for His6-PomA and D42N variant of PomB-Strep	this work

pAB *NheI* *AgeI*	Amp^R	p_{ara}BAD, codes for His6-PomA and PomB-Strep, *NheI* and *AgeI* restriction sites upstream of *pomB*	Vorburger (unpublished)
pAB_{GFP}	Amp^R	p_{ara}BAD, codes for His6-PomA and GFP-PomB-Strep	Thomas Vorburger
pAB_{GFP}-D23N	Amp^R	p_{ara}BAD, codes for His6-PomA and D23N variant of GFP-PomB-Strep	this work
pAB_{GFP}-D23E	Amp^R	p_{ara}BAD, codes for His6-PomA and D23E variant of GFP-PomB-Strep	this work
pAB_{GFP}-S26A	Amp^R	p_{ara}BAD, codes for His6-PomA and S26A variant of GFP-PomB-Strep	this work
pAB_{GFP}-S26T	Amp^R	p_{ara}BAD, codes for His6-PomA and S26T variant of GFP-PomB-Strep	this work
pAB_{GFP}-D42N	Amp^R	p_{ara}BAD, codes for His6-PomA and D42N variant of GFP-PomB-Strep	this work

Table D.4: Plasmids used in this study.

2 Media & Antibiotics

2.1 Lysogenic broth (LB) medium

LB medium [1 % tryptone (w/v), 0.5 % yeast extract (w/v), 1 % NaCl (w/v)] was used for cultivation of *E. coli* and *V. cholerae*. For growth on solid medium 1.5 % bactoagar (w/v) was added before autoclaving. 0.25 % bactoagar (w/v) was added for the use as motility agar plates. In the case of sodium free media for motility assays, NaCl was replaced by 1 % KCl (w/v) or no chloride salt was added.

2.2 YT medium

YT medium [1.6 % tryptone (w/v), 1 % yeast extract (w/v), 0.5 % NaCl (w/v)] was used as culture medium in the production of competent *V. cholerae*.

2.3 Sodium free M9 minimal medium

The sodium free M9 minimal medium is based on a recipe by Sambrook and Russel (173), sodium salts were replaced with the corresponding potassium salts (1.03 % K_2HPO_4 x 3 H_2O (w/v), 0.3 % KH_2PO_4 (w/v), 0.1 % NH_4Cl (w/v), 2 mM $MgCl_2$,

0.1 mM $CaCl_2$),the residual Na^+ concentration was 16 µM. As carbon source, 0.2 M glucose was added (final concentration).

2.4 Serum based SAPI medium

Serum based SAPI medium was used for growth experiments and motility assays in the presence of catecholamine hormones. SAPI is a salt based medium, containing 0.05 % NH_4NO_3 (w/v), 0.025 % KH_2PO_4 (w/v), 0.025 % KCl (w/v), which were dissolved in 680 mL deionized H_2O. The pH was adjusted to 7.2 - 7.5 with 5M HCl.

After autoclaving, 0.1 % of sterile 1 M $MgSO_4$ (v/v), 0.277 % of sterile 1 M glucose (v/v) and 1 % of sterile 1 M HEPES (v/v) pH7.5 was added. Prior to experiments 30 % (v/v) untreated serum from fetal (Seromed) or adult *Bos taurus* (Sigma) was added. 0.25 % of bactoagar (w/v) was added prior to autoclaving if medium was used for motility experiments.

To inactivate the bacteriostatic compounds, the serum was heated to 60 °C and incubated at this temperature for 30 min (heat-treated serum). This treatment inactivates heat-sensitive viruses and mycoplasms and reduces the amount of heat-sensitive components in the serum, e.g. vitamins, growth factors and the mammalian complement system.

2.5 Serum based RPMI-1640 medium (Biochrom, FG 1385)

RPMI-1640 is generally used as a cultivation medium for eukaryotic cell cultures (122). It contains salts (NaCl and KCl), aminoacids, vitamins and glucose as a carbon source and 20 mM HEPES as a buffer substance. Phenolred was added as a pH indicator. 30 % (w/v) of inactivated fetal calf serum was added prior to experiments.

2.6 Antibiotics

Antibiotics were steeped in $H_2O_{millipore}$ as 1000x concentrated stock solution, sterilized, using a 0.2 µm filter and stored at -20°C. Working concentrations of antibiotics used in this work were 200 µg mL^{-1} for ampicilline and 50 µg mL^{-1} for streptomycin.

3 Methods in Microbiology

3.1 Conservation of bacterial strains

1.1 mL of an overnight culture was pipetted into an glass tube containing 400 µL of 50 % glycerine to achieve a final concentration of 10 % to 15 % glycine. Glycerol stocks were stored at -80°C and used for long-term storage of bacterial strains.

3.2 Monitoring growth of bacteria

Bacterial growth experiments were accomplished in 5 mL liquid serum-SAPI media in sterile test tubes under aerobic conditions. 1 mL of a *V. cholerae* overnight culture was centrifuged at 11.000 rpm for 1 min. The bacterial pellet was resuspended in an equal amount of SAPI medium. This culture was used to inoculate 5 mL of serum-SAPI medium to a final OD_{600} of 0.01. Growth was monitored by measuring the optical density at 600 nm at specific points in time. The doubling rate (μ) and the generation time (t_d) of each culture was calculated using formulas D.1 and D.2.

$$\mu = \frac{ln(x_{t26}) - ln(x_{t0})}{t_x - t_0} \tag{D.1}$$

$$t_d = \frac{0.693}{\mu} \tag{D.2}$$

3.3 Observation of bacterial motility

Swimming of bacteria were monitored either on motility plates or measured quantitatively by video sequence analysis.

3.3.1 Motility assay on LB based softagar

Single colonies of an overnight culture were stabbed on motility plates using a round-tipped toothpick. Plates were incubated at 30 °C or 37 °C for indicated times.

3.3.2 Motility assay on serum-SAPI softagar

In sterile 50 mL reaction tubes, 14 mL SAPI softagar and 6 mL adult calf serum was propounded and supplemented with 20 µg µL^{-1} streptomycin and either 0.1 mM epinephrine or norepinephrine. To investigate the effect of phentolamine swarming plates were prepared containing 0.1 mM epinephrine or norepinephrine combined with 0.35 mM phentolamine. All components were briefly vortexed and poured into sterile petridishes. These

plates were kept close over night at room temperature and dried with partially opened lid under a sterile bench for about 1 h prior to handling.

5 mL of LB medium supplemented with streptomycin, was inoculated with a single colony of either *V. cholerae* or the *V. cholerae* deletion mutant Δ*pomAB* and grown overnight at 37 °C. Fresh LB medium was inoculated with the over night cultures to a final OD_{600} of 0.01 and incubated aerobically until an OD_{600} of 0.5 was reached. Cells were briefly centrifuged and resuspended in the equal amount of SAPI medium. 1.25 µL of the bacterial cultures were spotted on the soft agar plates - overall, for each conditions six spots. The soft agar plates were incubated at 37 °C.

3.3.3 Determination of swimming speed by microscopy.

Fresh LB medium (1 % tryptone, 0.5 % yeast extract) buffered with 10 mM Tris-HCl pH 7.0, 8.0 or 9.0, supplemented with 50 µg mL^{-1} streptomycin and 200 µg mL^{-1} ampicillin, was inoculated with an overnight culture of a given *V. cholerae* strain to an OD_{600} of 0.01. The residual Na^+ concentration in the medium was 11 mM as determined by atomic absorption spectroscopy (65). Arabinose at a final concentration of 10 mM was added immediately after inoculation. After incubation at 30 °C, 180 rpm for 3 h, cultures were diluted 1:100 in LB medium buffered with 10 mM Tris, and the pH was adjusted with 5 M KOH or 5 M HCl. If indicated, 171 mM NaCl (LB_{Na+}) or KCl (LB_{K+}) were added. The media contained 50 µg mL^{-1} streptomycin, 200 µg mL^{-1} ampicillin and 50 mM L-serine to enhance straight swimming of the bacteria (238). Tracking by light microscopy requires cells with a distinct contrast to their background. Therefore two different fluorescent dyes (MitoTracker®, invitrogen™ and SYBR Green® I, Molecular Probe) were tested but with minor success (data not shown). The dyes attached to the bacterial cell and produced clear images of single cells but they could not be used due to the following reasons. In case of the MitoTracker®, cells which were immotile produced a far too strong fluorescent signal, which overlay the fluorescent signal of the swimming cells. The fluorescent signal produced by SYBR Green® I was too unstable, therefore the obtained video sequences were too short for analysis. It was also of concern that the fluorescent dyes might affect the swimming speed and motility of the bacteria, motility was therefore determined of unstained cells. 30 µL were pipetted into one channel of a flat μ-Slide VI (ibidi, Germany) and cells were immediately observed under 200 magnification using a fluorescence microscope (Zeiss Imager M1, Zeiss, Germany) in its differential interference contrast (DIC) mode. After determination of adequate settings for the light exposure using the Auto-Exposure function of AxioVision and manual focusing in the

z-axis to the middle between the base and the top of the channel, about 30 series of time sequences were taken. The typical exposure time was 20 ms, and the constant interval between two consecutive images was 50 ms. The total length of a typical sequence of images was 12 s (= 250 individual images in one tracking experiment). At least 305 tracks per condition and strain were recorded and analyzed by software, developed by Wimasis, GmbH (Germany). All bacteria showing a minimum speed of 4 µm s^{-1} were included in the analysis. Bacterial cells were divided into three main classes according to their measured swimming speeds, namely class I: between 4 µm s^{-1} to 17 µm s^{-1}(slow), class II: between 18 µm s^{-1} to 40 µm s^{-1} (medium) and class III, faster than > 40 µm s^{-1} (fast). Results are presented as histograms created with the help of the software Origin (release 8.0), with sub-classes of velocities starting at the lowest value considered in our analysis. Each sub-class covers a range of 3 µm s^{-1}.

3.4 Yield of competent cells

3.4.1 Production of competent *E. coli* ($CaCl_2$-method)

200 mL of fresh, sterile LB-medium (see Chap. 2.1) was inoculated with 2 mL of an *E. coli* overnight culture and grown aerobically at 37 °C until an OD_{600}=0.3. The bacterial culture was split into four sterile 50 mL reaction tubes (Sarstedt, Nuembrecht) and incubated for 10 min in an ice bath under occasional agitation. The culture was centrifuged for 5 min at 6000 rpm and 4 °C. The bacterial pellet was resuspended in 20 mL of cold 100 mM $CaCl_2$ solution. The bacterial suspensions were incubated for further 10 min to 15 min in an ice bath. The content of two tubes were joined and centrifuged for 5 min at 6000 rpm and 4 °C. The pellets were resuspended in 2 mL of cold 100 mM $CaCl_2$ solution with 15 % gylcerin (v/v) added and incubated for further 15 min in an ice bath. The solutions were aliquoted à 200 µL in 1.5 mL reaction tubes and stored at −80 °C.

3.4.2 Production of competent *V. cholerae*

50 mL of fresh, sterile YT-medium (see Chap. 2.2) was inoculated with a single colony of *V. cholerae* and incubated aerobically at 37°C until an OD_{600}=0.6. The culture was centrifuged at 4000 rpm and 4°C for 10 min, the pellet was resuspended in 4 mL of cold, sterile sucrose-HEPES solution (137 mM sucrose and 1 mM HEPES). Cells were centrifuged again for 10 min at 4000 rpm and 4°C. The cell pellet was resuspended in 4 mL sucrose-HEPES solution (137 mM sucrose and 1 mM HEPES) with 12 % glycerine

(v/v) added. The solution was aliquoted à 100 µL in 1.5 mL reaction tubes and stored at -80°C.

3.5 Transformation of competent *E. coli* and *V. cholerae*

3.5.1 Transformation of *E. coli* using Heat Shock

Competent *E. coli* cells were thawn on ice. After addition of 1 µL to 10 µL plasmid-DNA, cells were incubated for 30 min on ice followed by a heat shock step at 42 °C for 2 min. After incubation on ice for 1 min, 800 µL of sterile LB-medium (see Chap. 2.1) was added. Cells were incubated at 37 °C for one hour. 100 µL of the cell suspension and the concentrated rest (after centrifugation) were spread on LB agar plates containing appropriate antibiotics.

3.5.2 Transformation of *V. cholerae* using electroporation

An aliquot of electro-competent *V. cholerae* cells was thawn on ice. Immediately prior to transfer of these cells to a 0.2 cm electorporarion cuvette, 1 µL to 5 µL salt-free plasmid-DNA was added. For transformation program Ec1 (1.8 kV) was used. After applying the current pulse, 500 µL of sterile LB-medium (see Chap. 2.1) was added to the cells, mixed and transferred back to a 1.5 mL reaction tube. Cells were incubated for one hour at 37 °C. 100 µL of the cell suspension and the concentrated rest were spread on LB agar plates containing appropriate antibiotica (163).

4 Enzymatic reactions with nucleic acid

4.1 Polymerase Chain Reaction (PCR)

Mutations in gene sequences were performed following a two step PCR protocol using Phusion™ High-Fidelity DNA Polymerase (FINNZYMES) according to the manufacturer's protocol. Amplification of fragments for chromosomal gene deletions were performed following a two step PCR protocol using One Taq™ DNA Polymerase and Q5™ High-Fidelity DNA Polymerase (NEB), according to manufacturer's protocol. Colony-PCR was performed with MyTaq™ HS DNA Polymerase (Bioline) in a volume of 10 µL according to manufacturer's protocol.

4.2 Quantitative Real Time-PCR

SensiFAST™ SYBR & Fluorescein Kit (bioline) was used, to determine the expression level of specific target genes in a quantitative Real Time PCR reaction. The reaction mix was prepared according to manufacturer's protocol with 1 pM of each primer (final concentration) Tab. D.2 and 2.5 nM cDNA (final concentration). The qRT-PCR reaction was accomplished in a CFX96 cycler (BioRad) after a 2-step cycling protocol with a melt-profile analysis at the end of the reaction. qRT-PCR transcripts were amplified in triplicates with the following thermal cycling parameters: 95 °C for 2 min (polymerase activation), 40 cycles at 95 °C for 10 s (denaturation), 60 °C for 20 s (annealing), 95 °C for 10 s (final extension), finishing the PCR reaction with a melt curve analysis (65 °C to 95 °C increasing the temperature in 0.5 °C steps). The analysis of the qRT-PCR run and the calculation of primer efficiencies were performed with CFX Manager (BioRad). The C_t values of *pomB* and *qseC* were normalized using *rssA*, a housekeeping gene coding for the 16S rRNA. The values of *pomB* and *qseC* were then standardized with the values obtained from the iron treated sample (*V. cholerae* cultivated in serum-SAPI with the addition of 0.1 mM $FeSO_4$) using the 'Pfaffl-equation' (formula D.3) (168) with E_{target}: RT-PCR efficiency of target gene transcript, $E_{reference}$: RT-PCR efficiency of a reference gene transcript, CP: crossing point (point at which the fluorescence rises above the background fluorescence), ΔCP_{target}: CP deviation of control minus sample of the target gene transcript and $\Delta CP_{reference}$: CP deviation of control minus sample of reference gene transcript.

$$ratio = \frac{(E_{target})^{\Delta CP_{target}(control-sample)}}{(E_{reference})^{\Delta CP_{reference}(control-sample)}} \tag{D.3}$$

4.3 Enzymatic digest of DNA by restriction endonucleases

Restriction of DNA was done according to manufacturer's protocol using restriction enzymes of NEB. Calf intestinal phosphatase (CIP) was added to the restriction preparation of vectors, to inhibit self ligation of vectors in adjacent ligation approach.

4.4 Ligation of DNA fragments

Ligation of DNA fragments in vectors was performed according to manufacturer's protocol using T4 DNA ligase of NEB. For construction of pJET1.2 based plasmids following kit and protocol was used: CloneJet™ PCR Cloning Kit (Fermentas).

Enzyme	Restriction site
AclI	AA/CGTT
AgeI	A/CCGGT
KpnI	GGTAC/C
NdeI	CA/TATG
XhoI	C/TCGAG

Table D.5: Restriction enzymes used in this work were purchased from NEB. Backslash in the nucleotide sequence marks the position of restriction.

4.5 Isolation of total RNA from of *V. cholerae*

5 mL of fresh LB medium supplemented with 50 µg mL^{-1} streptomycin was inoculated with a single colony of *V. cholerae* and grown aerobically over night at 37 °C. 1 mL of the bacterial culture was centrifuged the next day and the bacteria pellet was resuspended in the equal volume of SAPI media. 5 mL of serum-SAPI media (30 % adult calf serum (v/v)) supplemented with either 0.1 mM epinephrine, norepinephrine or $FeSO_4$ was inoculated with the overnight culture to a final OD_{600} of 0.02. The cells were grown aerobically (180 rpm) at 37 °C for 25 h.

Cells were harvested (centrifugation at 4000 rpm for 10 min), the pellet was resuspended in RNA*later* RNA stabilization reagent (QIAGEN) and centrifuged for further 10 min at 4000 rpm. The pellet was resupended in 500 µL TE-buffer containing 5 mg mL^{-1} lysozyme, 1 mM $MgCl_2$, 1 mM $CaCl_2$ and few crystals of DNaseI and incubated at 30 °C for 20 min. ProteinaseK was added to the preparation to a final concentration of 1 mg mL^{-1} and incubated for further 15 min.
Total mRNA was isolated from these cell lysate using the RNeasy Mini Kit of Qiagen, according to manufacturer's protocol. The quality of the isolated mRNA was assessed by gel-electrophoresis (1x TAE buffer supplemented with 0.75 % LE GP Agarose (Biozym), 20 µL 37 % formaldehyde and 1x GelRed™ (10.000x concentrated stock solution, Biotium)). RiboRuler™ High Range RNA Ladder (Thermo Scientific) was used as molecular standard.

4.6 Synthesis of cDNA

For the synthesis of cDNA, the SuperScript™ III First-Strand Synthesis System for RT-PCR kit (invitrogen™) was used according to manufacturer's protocol. The random hexamer primers, supplied by the manufacturer, were used in the synthesis reaction.

4.7 Isolation and purification of nucleic acid

4.7.1 Preparation of plasmid DNA out of *E. coli*

E. coli DH5α, XL10 Gold or TOP10 served as hosts for plasmids. Isolation and purification of plasmids were done according to manufacturer's protocol, using following kit, NucleoSpin® Plasmid of Macherey-Nagel.

4.7.2 Purification of PCR products

PCR products and DNA fragments (after enzymatic digest) were separated by gel-electrophoresis using 1 % agarose gels [75 mL 1x TAE buffer, 1 % agarose (w/v) and 3.8 µL GelRed (10.000x concentrated)], [1x TAE buffer: Dissolve 4.84 g Tris in 10 mL H_2O. After adding 2 mL 0.5 M Na_2EDTA (pH 8.0) and 1.142 mL glacial acetic acid, adjust the volume to 1 L and store solution at room temperature]. Samples were mixed with 6x DNA loading dye [25 mg bromphenol blue, 4 g sucrose, 3 mL glycerol (99 %) in 10 mL $H_2O_{millipore}$] and loaded onto the gel. After gel-electrophoresis, the DNA band was excised and purified according to manufacturer's protocol (NucleoSpin® Gel and PCR Clean-up, Macherey-Nagel). As molecular standard following DNA ladders were used: Trackit™ 100 bp DNA ladder (Invitrogen) and Gene Ruler™ 1kb (Fermentas).

5 Production of the flagellar stator components PomA and PomB in *V. cholerae* O395 N1 Δ*pomAB*

V. cholerae Δ*pomAB* containing plasmids encoding PomA and PomB were grown in LB medium (see Chap. 2.1) buffered with 50 mM KPi (pH 8.0) and supplemented with 200 µg mL^{-1} ampicillin and 50 µg mL^{-1} streptomycin. Single colonies were used to inoculate 10 mL medium. After 16 h at 37 °C, the cultures were transferred to 1 L fresh medium in 5 L Erlenmeyer flasks, and aerobic growth was continued at 37 °C, 160 rpm until an OD_{600} of 0.6 - 0.7 was reached. Protein expression was induced by adding 10 mM arabinose (final concentration) and growth was continued for 3 h at 30 °C. Cells (4 g to 6 g wet weight) were harvested by centrifugation (6000 rpm, 30 min, 4 °C) and washed with buffer ZW [50 mM Tris-HCl pH 8.0, 100 mM NaCl]. Pellets were stored at −80 °C.

6 Purification of *V. cholerae* membranes

Pellets were resuspended in buffer A [50 mM Tris-HCl pH 8.0, 300 mM KCl, 10 % glycerol (v/v), 5 mL buffer per g of cells]. After addition of a few crystals DNaseI, 0.5 mM $MgCl_2$ and 0.2 mM DFP, cells were broken by passages through an EMULSIFLEX Cell Disruptor at 20.000 psi. Unbroken cells were removed by low-speed centrifugation (10.000 g, 30 min, 4°C). Membranes were collected by ultracentrifugation of the supernatant at 55.000 rpm for 1 h at 4°C. The sedimented membranes were resuspended in buffer A (1 mL per g of cells). Aliquots of 200 µL were taken for SDS-PAGE and protein determination. Gradient centrifugation of membranes was performed with 30 % to 60 % sucrose gradients in buffer A in polycarbonate ultracentrifugation tubes (25 x 89 mm, Beckman) to remove inclusion bodies with aggregated proteins. Centrifugation was performed for 2 h in a Ti70 rotor (Beckman) at 50.000 rpm and 4°C in an ultracentrifuge L7 (Beckman). After centrifugation, a distinct brown fraction, containing purified membranes, was visible, which was used for further analysis.

7 Localization of GFP tagged PomB in *V. cholerae*

Overnight cultures of *V. cholerae* Δ*pomAB* transformed with plasmids pAB_{GFP} encoding for His-PomA and PomB variants fused to GFP were added to 5 mL LB medium supplemented with 50 µg mL^{-1} streptomycin, 200 µg mL^{-1} ampicillin and 0.4 mM, 1 mM or 10 mM arabinose to give an OD_{600} of 0.01. After aerobic growth for 5 h at 39 °C (180 rpm), 20 µL of the culture were spotted on a poly-L-lysine coated glass slide (Sigma-Aldrich Chemie GmbH, Germany). *V. cholerae* Δ*fliG*, transformed with plasmids coding for PomA and GFP-PomB wild type or variants, served as negative controls. Cells were visualized using a fluorescence microscope (Zeiss Imager M1, Zeiss, Germany) equipped with the 38 HE filter set. Wavelengths were 470 nm for excitation (bandpass: 40 nm) and 525 nm for emission (bandpass: 50 nm). Pictures were analyzed with the help of the software AxioVision (Zeiss, Germany).

8 Transmission electron microscopy (TEM)

Cells were grown at 30 °C for 30 h in salt based minimal medium (see Chap. 2.3) buffered with 10 mM Tris-HCl (pH7 or pH8). The final pH of the medium was adjusted with 5 M KOH. Production of PomAB was induced by the addition of 10 mM arabinose. 10 µL of the bacterial solution was adsorbed on pioloform coated copper grids (Plano, Germany).

The suspensions were allowed to adsorb for 2 min and unbound material was removed using filter paper (Whatman, GE Healthcare, Germany) prior to two washing steps with a drop of distilled water for 1 min. The excess water was removed with filter paper. 5 µL of 2 % uranyl acetate was then applied onto the grid and after incubating for 1 min, the excess stain was removed with filter paper. The grid was dried at room temperature and examined using a Transmission Electron Microscope (LEO 912AB, Zeiss, Germany) at 80 kV.

9 Preparation of supernatants from bacterial cultures for analysis of catecholates

V. cholerae was grown in 30 mL serum-SAPI (30 % adult calf serum) with the addition of 50 µg mL^{-1} streptomycin and either 0.1 mM epinephrine or norepinephrine. The OD_{600} at the beginning of the experiments were adjusted to 0.01 with an liquid overnight culture of *V. cholerae*. For this purpose, the OD_{600} of the overnight culture was determined and 1 mL of the culture was centrifuged for 1 minute at 10.000 rpm. The supernatant was discarded and the bacterial pellet was resuspended in an equal amount of SAPI medium. As controls, serum-SAPI media with either 0.1 mM epinephrine or norepinephrine but without the addition of *V. cholerae* were included.

At point in time 0 h, an aliquot of each sample was taken and centrifuged. The supernatant was filtered through a 0.2 µm filter device and shock frozen in liquid nitrogen. Samples were then stored at −80 °C. Aerobic cultivation was continued under shaking at 180 rpm at 37 °C for 48 h. Aliquots were then taken and treated as mentioned before.

For the detection of epinephrine and norepinephrine in supernatant, samples were thaw on ice. The extraction of epinephrine and norepinephrine was performed as described in Chap. 10.5. The setup of the HPLC and conditions during measurement are also described in Chap. 10.5.

10 Analytical methods

10.1 Atomic absorption spectroscopy (AAS)

The concentration of sodium ions in liquid media was determined with a Shimadzu AAS-6300 atomic absorption spectrophotometer equipped with a sodium lamp. NaCl solutions with concentrations of 0 µM, 5 µM, 10 µM, 25 µM and 50 µM were used as standards.

10.2 Quantification of proteins using BCA

Protein concentration was determined by the BCA method (186) using reagents from Pierce Biotechnology (USA). Bovine serum albumin solution with concentrations of $0\,\mu g\,\mu L^{-1}$, $20\,\mu g\,\mu L^{-1}$, $40\,\mu g\,\mu L^{-1}$, $60\,\mu g\,\mu L^{-1}$ and $80\,\mu g\,\mu L^{-1}$ served as standard.

10.3 SDS-PAGE

Proteins were separated on SDS-PAGE (177) containing 10 % acrylamide/bisacrylamide (37.5:1.0) using a BioRad Mini-PROTEAN Tetra System. 200 µg of protein were loaded, samples were mixed previously with 5x loading buffer containing DTT [77.1 mg DTT, 750 µL 5x loading buffer, fill up to 1 mL $H_2O_{millipore}$; 5x loading dye: 5 mL Tris-HCl (1 M, pH 6.8), 2 g SDS, 11.5 mL 87 % glycerine, one tip of a scoop bromphenol blue, fill up to 20 mL $H_2O_{millipore}$]. Precision Plus Protein Western C (BioRad) or Prestained Protein Marker Broad Range (7 kDa to 175 kDa) (NEB, P7708) were used as protein standards.

10.3.1 Staining of proteins on SDS-PAGEs

Staining of SDS-PAGEs using Coomassie Blue Silver. SDS-PAGEs were incubated over night in Coomassie Blue Silver stain [To 100 mL $H_2O_{millipore}$ add 50 mL ortho-phosporic acid. Dissolve 50 mg $(NH_4)_2SO_4$ and 0.6 g Coomassi G250. Fill up to 400 mL with $H_2O_{millipore}$ and add 100 mL MetOH]. Gels were discolored by washing in H_2O.

Silver staining. Proteins were retained by incubating the SDS-PAGE in 50 % MetOH for 30 min, followed by incubating in 75 % MetOH until the SDS-PAGE turned completely white. After wards they were washed two times in 50 % MetOH. For impregnation, SDS-PAGEs were soaked in 50 mL impregnation solution [10.5 mL 0.36 % NaOH, 0.7 mL MetOH, 2 mL 19.4 % $AgNO_3$, fill up to 50 mL H_2O] for 15 min. SDS-PAGEs were rinsed two times in H_2O for 15 min and soaked in 50 mL developer [250 µL citric acid, 25 µL formaldehyde in 50 mL H_2O] until brownish bands appear. To stop the reaction, SDS-PAGEs were soaked in 20 mL stop solution [10 % AcOH (v/v), 45 % MetOH (v/v), 45 % H_2O (v/v)].

10.3.2 In-gel flurescence

The fluorescence of the GFP tagged PomB wt and variants on SDS-PAGEs was detected using a Typhoon Trio laser scanner (GE Healthcare) with excitation at 488 nm and 526 nm emission filter. As a molecular standard the Precision Plus Protein WesternC Standards (BioRad) were used.

10.4 Protein transfer and immunostaining

Western Blots were performed using a Mini Trans-Blot Cell (BioRad) following a wet blot procedure. Proteins were blotted on nitrocellulose membrane (Whatman optitron BA-S85, 0.45 µm) for 1 h under constant volt (100 V) in cold transfer buffer [15.1 g Tris, 72.1 g glycine, 750 mL MetOH fill up to 5000 mL with $H_2O_{millipore}$]. Nitrocellulose membrane was incubated with Strep-Tactin®-HRP conjugate (iba) according to manufacturer's protocol. Proteins labelled with a Strep-tag were made visible by a chromogenic reaction [3 % 4-chloro-1-naphtol (w/v) in MetOH, 30 % H_2O_2] or via chemiluminescence via a ECL detection kit (Roti®-Lumin (Roth).

10.5 High-performance liquid chromatography (HPLC)

The detection of epinephrine and norepinephrine from bacterial supernatants was performed on a UHPLC- system (UltiMate 3000) (Thermo Fischer Scientific GmbH) with following configurations: Pump ISO-3100BM, Solvent-Rack SRD-3200, Sampler WPS-3000TBSL, electro-chemical detector Coulochem III.

On the day before measurement, recipe columns were prepared by weighting in 20 mg Al_2O_3 into the columns. The Al_2O_3 was activated over night with 600 µL 2 mM TRIS/EDTA buffer (pH 8.7).

1 mL of sample media was pipetted onto the recipe columns, 50 µL of the internal standard solution (3,4 Dihydroxybenzylamin) was pipetted directly into the sample media. The samples were thoroughly mixed in an overhead shaker for 10 min. The columns were opened at the bottom, placed into glass test tubes and centrifuged for 1 min (1000 g, 4 °C). The flow through was discarded, the columns closed and filled with 1 mL wash buffer (16.5 mM TRIS/EDTA). Open columns were centrifuged again for 1 min (1000 g, 4 °C). The washing procedure was repeated two times.

Prior to the elution step, the recipe columns were closed with elution vials and placed into clean glass test tubes. Catecholates were eluted by adding 120 µL 0.2 M $HClO_4$. Columns were vortexed for 30 s and centrifuged for 1 min (1000 g, 4 °C).

The eluate was loaded onto a microcentrifuge filter (placed in a micro reaction tube) and centrifuged for 2 min at 1000 rpm. For subsequent autosampling, the eluate was filled into a glass-μ-inset and placed into a glass vial.

For the detection of catecholates, 30 µL of the eluate (cooled to 4 °C) was injected. The conditions of the HPLC during the run were: Flow 1 mL min^{-1}, flux material Cat A-Phase II Mobile Phase (Thermo Scientific), conditioning cell 200 mV, electrode I 50 mV, electrode II −250 mV, oven room temperature. The column HR-80 (C18 4.6 x 80 mM, 3 µm, 120 A) from ESA was used for separation.

11 Bioinformatical tools

11.1 Sequence alignments and phylogenetic tree modeling

Aminoacid sequences of QseC homologs were obtained from NCBI BLAST®, algorithm blastp (protein-protein BLAST) with query sequence YP_001464488.1 QseC from *E. coli*. A multiple sequence alignments of 40 sequences for QseC were performed using the ClustalW algorithm (207) implemented in the BioEdit Sequence Alignment Editor (Version 7.0.5.3), (66) with default settings. Identical and similar residues were identified with BioEdit using an identity and similarity threshold of 83 % and BLOSUM62 (76) scoring matrix.

A neighbor-joining tree of QseC homologs was build using the Jukes-Cantor genetic distance model and BLOSUM62 (cost matrix) (with no defined outgroups) implemented in Geneious Pro 5.4.6 created by Biomatters.

11.2 Sequence analysis

Sequence analysis, drawing of plasmid charts and design of oligonucleotides were performed using Geneious Pro 5.4.6 created by Biomatters.

Chapter E

Appendix

1 Physiological characterization of *V. cholerae* Δ*nqr*

The Na^+-translocating NADH-quinone reductase is commonly found in marine, moderately halophilic and pathogenic bacteria where it contributes to the supply of electrons into the aerobic respiratory chain. The Na^+-NQR generates a sodium motif force across the cell membrane by translocating one sodium per electron from the cytoplasm into the periplasm. This membrane potential can be used for different metabolic work within the cell.

1.1 *V. cholerae* Δ*nqr* shows an impaired motility compared to the wild type *V. cholerae* strain

Motility assays were performed as described in Chap. D, 3.3.1 on either LB softagar or sodium reduced LB softagar but without the addition of arabinose or ampicilline. Plates were incubated at 37 °C for 16 h.

Swarming of *V. cholerae* Δ*nqr* was diminished on soft agar plates containing NaCl at pH 6.0 to pH 8.0 (see Fig. E.1). At high alkaline conditions (pH 9.0) motility reached wild type level.

Motility of both strains (*V. cholerae* and *V. cholerae* Δ*nqr*) was reduced at each pH conditions tested on LB softagar without the addition of NaCl (see Fig. E.1 B). The remaining Na^+ was 11 mM as determined with AAS (65). The loss of Na^+-Nqr did not impair motility at low pH (pH 6.0 and pH 7.0) compared to the wild type. At alkalic conditions (pH 8.0 and 9.0) swarming of the *nqr* deletion mutant was reduced compared to the wild type.

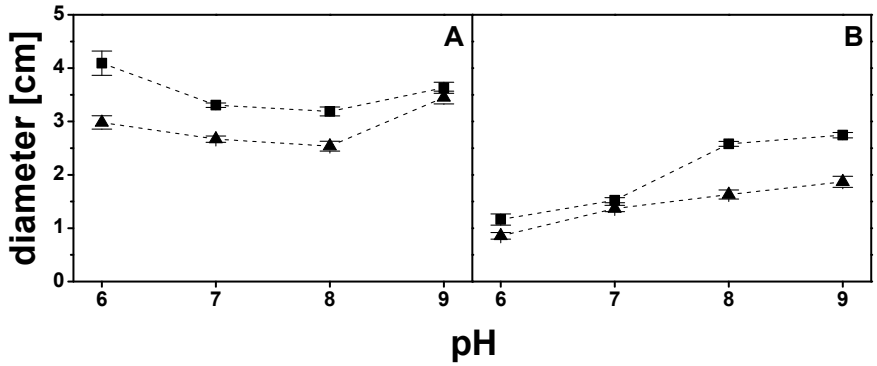

Figure E.1: Comparison of motility of *V. cholerae* and *V. cholerae* Δ*nqr* on different media. Motility of *V. cholerae* (■) and *V. cholerae* Δ*nqr* (▲) was investigated on LB softagar (A) and on sodium reduced LB softagar (B) at pH 6.0, 7.0, 8.0 or 9.0. Plates were incubated at 37 °C for 16 h. Average and standard deviations were calculated from eight experiments.

1.2 Nqr is important for fast swimming under alkaline and Na^+ limited conditions

Cells were prepared for tracking as described previously (Chap. D, 3.3.3) but without the use of arabinose or ampicilline. Between 218 and 343 video sequences for each strain and each condition were recorded and analyzed with the help of the software WimTaxis (Wimasis, Germany). Cells were grouped in three classes with swimming speeds ranging from 4 µm s^{-1} to 17 µm s^{-1}, 18 µm s^{-1} to 40 µm s^{-1} and greater than 40 µm s^{-1} and presented as histograms (see Fig. E.2).

A deletion of *nqr* improved the swimming ability of *V. cholerae* at high Na^+ concentrations and alkaline pH. Under low Na^+ concentrations (11 mM Na^+) and alkalic conditions, hypermotility was lost in the *nqr* deletion strain. The addition of chloride salt (KCl) did not rescue the ability for fast swimming.

These results indicate, that the Na^+-translocating NADH-quinone reductase is important for motility in *V. cholerae* at certain environmental conditions.

1.3 Lactate inhibits motility of both *V. cholerae* wild type and Δ*nqr*

It has been shown that the addition of lactate to the cultivation medium (LB) enhances growth of *V. cholerae* Δ*nqr* (personal communication with Yusuke Minato, University of Minnesota). It was thus of an interest, if lactate also enhances motility of the Δ*nqr* strain.

Motility assays were performed on LB based softagar plates with 100 mM NaCl and

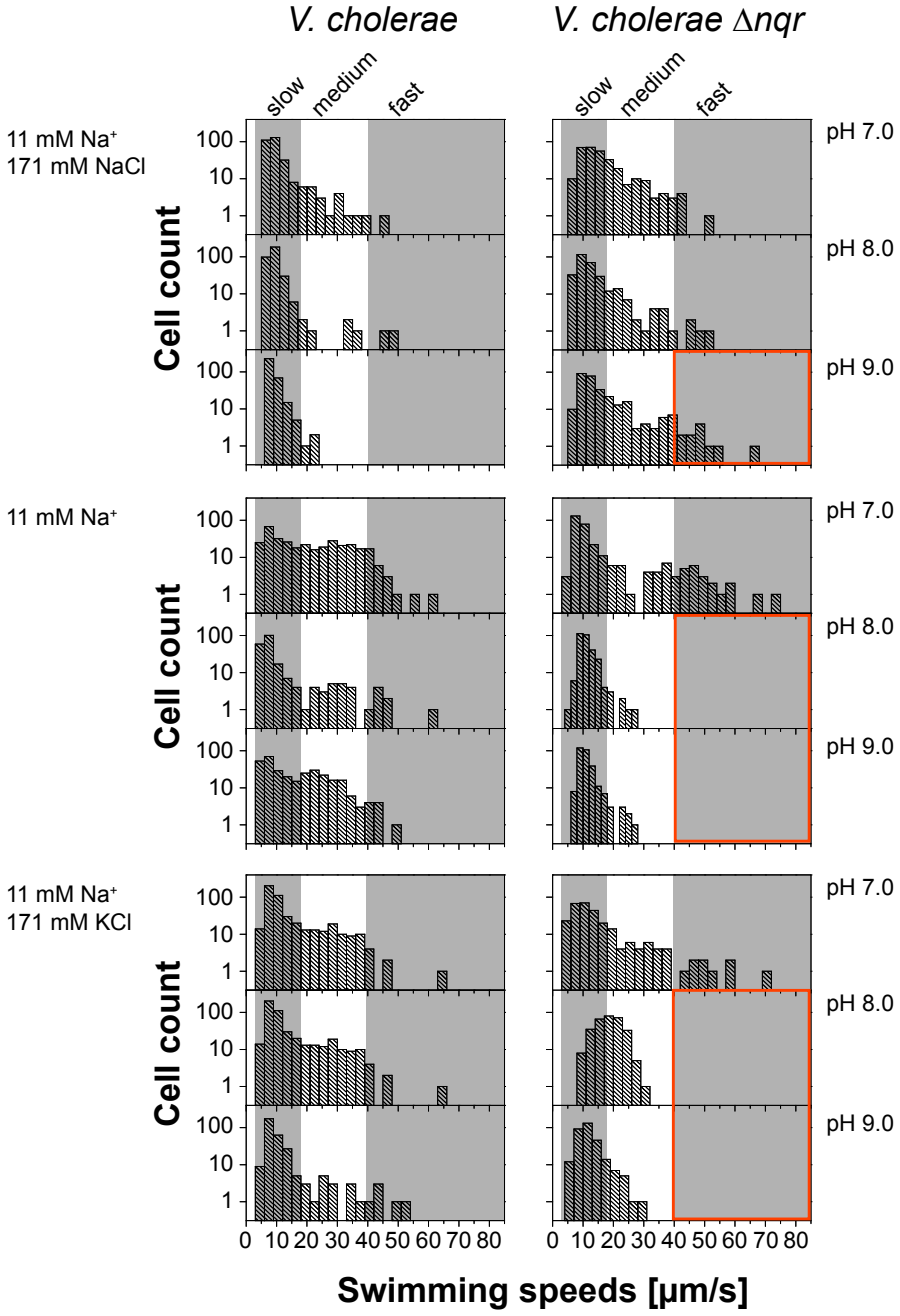

Figure E.2: Swimming speeds of single cells were determined for different media composition and pH. Cells were grown aerobically in LB medium containing either 171 mM NaCl, 0 mM NaCl or 171 mM KCl at 37 °C.

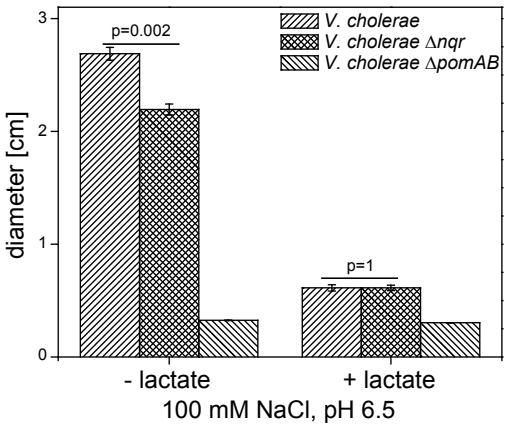

Figure E.3: Swarming behavior of *V. cholerae* Δ*nqr* was investigated in the presence of lactate. The mean value and standard error were calculated of 16 experiments. P values were obtained using Student's t test. *V. cholerae* Δ*pomAB* is immotile due to the lack of the flagellar stator components PomAB and served as a indicator for colony growth in the absence of swarming ability (147).

at low pH (pH6.5), as described in Chap. D, 3.3.1. The medium was buffered with 100 mM Bis/Tris. An over night culture of *V. cholerae* wt, Δnqr, ΔpomAB was diluted in fresh LB medium to an OD_{600} of 0.01 and incubated to an OD_{600} of 0.5-0.6. Cells were washed and diluted to an OD_{600} of 0.5. 1.5 µL of culture was spotted on dried softagar plates. The plates were incubated at 37 °C for 16 h.

Without the addition of lactate, the wild type reaches diameters of about 2.7 cm, while the *nqr* deletion mutant is impaired in motility (size of diameters around 2.1 cm) (Fig. E.3 A). This is in accordance with the results from Fig. E.1. The mutant strain *V. cholerae* Δ*pomAB*, lacking essential parts of the flagellar complex served as control and was used as an indicator for normal colony growth in the absence of swarming.

Upon addition of 30 mM D-L lactate, swarming of both strains (wild type and Δ*nqr*) is greatly diminished (Fig. E.3 B). The swarming ring just reaches diameters of around 0.75 cm, while the colony sizes of *V. cholerae* Δ*pomAB* are of comparable sizes.

It is assumed that lactate act as repellent. *V. cholerae* is inhibited in swimming towards other attractants (e.g. aminoacids) and might thus metabolize lactate in its close proximity. This effect could be already demonstrated in *E. coli* and *S. enterica* Serovar Typhimurium (244). Motility is strongly influenced by the existence of attractants or repellents in the environment which bacteria sense via their chemotactic system.

1.4 Construction of a Δ*nqrB* mutant in a *V. cholerae* Δ*pomAB* background

NqrB is one of six subunits of the Na^+-NQR and plays a role in the translocation of Na^+ from the cytoplasma into the periplasma (182). Observations revealed that *V. cholerae* Δ*nqr*, which was complemented with a plasmid encoding for the subunits A to F exhibited slightly diminished *in vivo* Na^+ extrusion rates (determined by Na^+-NMR

spectroscopy) than the wild type strain (Heiko Möller, University of Potsdam, personal communication). It was therefore concluded that overexpression of the whole complex decelerates the doubling time of *V. cholerae* Δ*nqr* transformed with plasmid encoding *nqr*A-F. It would be of interest to construct a strain lacking only the gene coding for the NqrB subunit to compare this strain with the wild type without disturbances due to overexpression. The construction of a *V. cholerae* strain lacking *nqrB* was performed as described (112), modified as follows.

1.4.1 Construction of plasmid pSW-nqrB and donor strain *E. coli* β3914 pSW-nqrB

The fragment nqrAC was amplified in a two-step PCR reaction. In a first step the up and down fragments were amplified using plasmid pNQR as template. Following primer pairs were used: up-fragment:nqrBup fwd BamHI and nqrBup rev, down-fragment: nqrBdo fwd and nqrBdo rev. In a second step, the up and down fragments were joined using primer pair nqrBup fwd BamHI and nqrBdo rev (see Tab. E.1). For both reactions Phusion™ High-Fidelity DNA Polymerase was used according to manufacturer's protocol. After purification, the 2.115 bp fragment was ligated into pJET1.2 using the CloneJET™ kit by Fermentas and transformed into chemically competent *E. coli* TOP10.

The plasmid pJET-Δ*nqrB* was isolated from *E. coli* TOP10 and restricted using enzymes BamHI and XbaI according to manufacturer's protocol and ligated into the linearized suicide plasmid pSW7848 and transformed into *E. coli* β3914.

1.4.2 Construction of a chromosomal deletion mutant in *nqrB* of *V. cholerae*

E. coli β3914 pSW-nqrB was used as donor strain and *V. cholerae* as recipient strain. Fresh LB medium (without antibiotics) was inoculated with an over night culture (1 % (v/v)) of either *V. cholerae* or *E. coli* β3914 pSW-nqrB (supplemented with 0.3 mM DAP) and grown aerobically at 37 °C to a final OD_{600} of 0.3.

Bacterial cultures were mixed in following ratio 1:1, 1:10 and 1:100 (donor:recipient strain) and 50 µL of these cultures were pipetted onto sterile filter plates (pore size 2 µm) placed on LB agar supplemented with 0.3 mM diaminopimelic acid (DAP). Plates were incubated at room temperature over night.

1. Selection of chloramphenicol resistant *V. cholerae*: Cells were harvested with 2 mL LB medium. Dilutions up to 1:1000 were prepared and 100 µL of each dilution was pipetted onto LB agarplates supplemented with streptomycine (50 µg mL^{-1}) and chloramphenicol (25 µg mL^{-1}). Plates were incubated at room temperature until small

Name	Sequence
nqrBup fwd BamHI	AAGGATCCAATGAGCCAGGCGGCAAACACG
nqrBup rev	TACAACGCTGGCGGCCAAGC
nqrBdo fwd	GGTTCGGGCGCATTATTGGCGGCGTG
nqrBdo rev	ATCCGTGTTGTGAACCCGGC
nqrA1 fwd	AGCCAACCTTGTTGCTTCGT
VM16	GCTCAATCATTGTATCGGC
pJET1.2 fwd	CGACTCACTATAGGGAGAGCGGC
pJET1.2 rev	AAGAACATCGATTTTCCATGGCAG

Table E.1: Oligo-nucleotides used in this study.

colonies appear (up to three days). These colonies should be *V. cholerae*, which inherit the suicide plasmid pSW-nqrB (also codes for chloramphenicol resistance).

2. Screening for arabinose resistant *V. cholerae*: Single colonies of *V. cholerae* were picked and streaked onto LB agarplates containing 0.2 % arabinose and 50 µg mL^{-1} streptomycine. Arabinose triggers the expression of the plasmid encoded *ccdB*, a gyrase poison (42). Thus, strains, which still inherit the plasmid pSW-nqrB are not viable in media containing arabinose. Plates were incubated at room temperature.

Positive colonies were tested in a colony PCR, using MyTaq (bioline) as described in manufacturer's protocol with primers nqrA1 fwd colony and VM16. A positive clone should show a PCR product of 260 bp. So far, this method did not lead to a strain lacking *nqrB* and should be further improved.

2 Sequence alignments of PomA and PomB

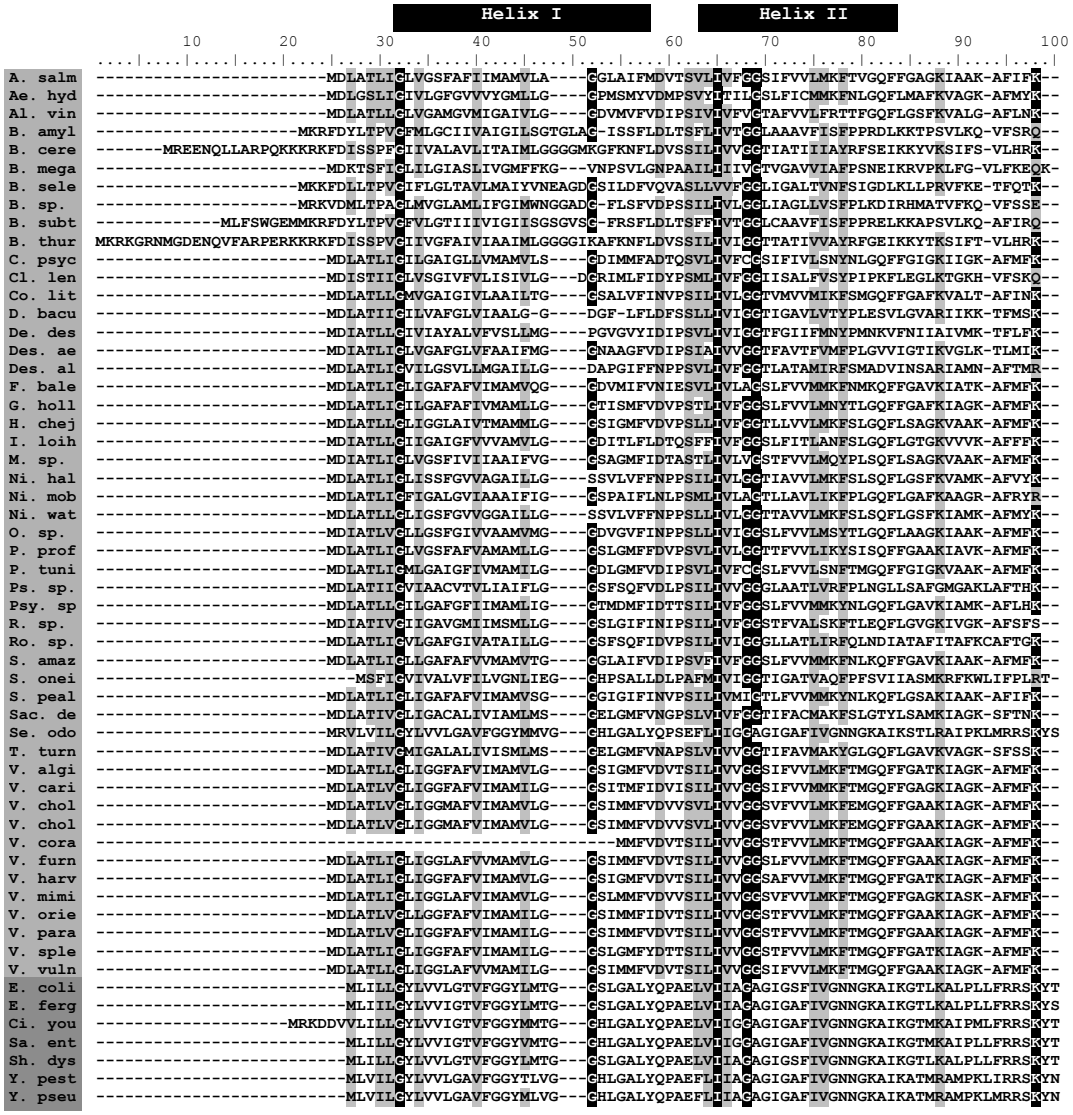

E. APPENDIX

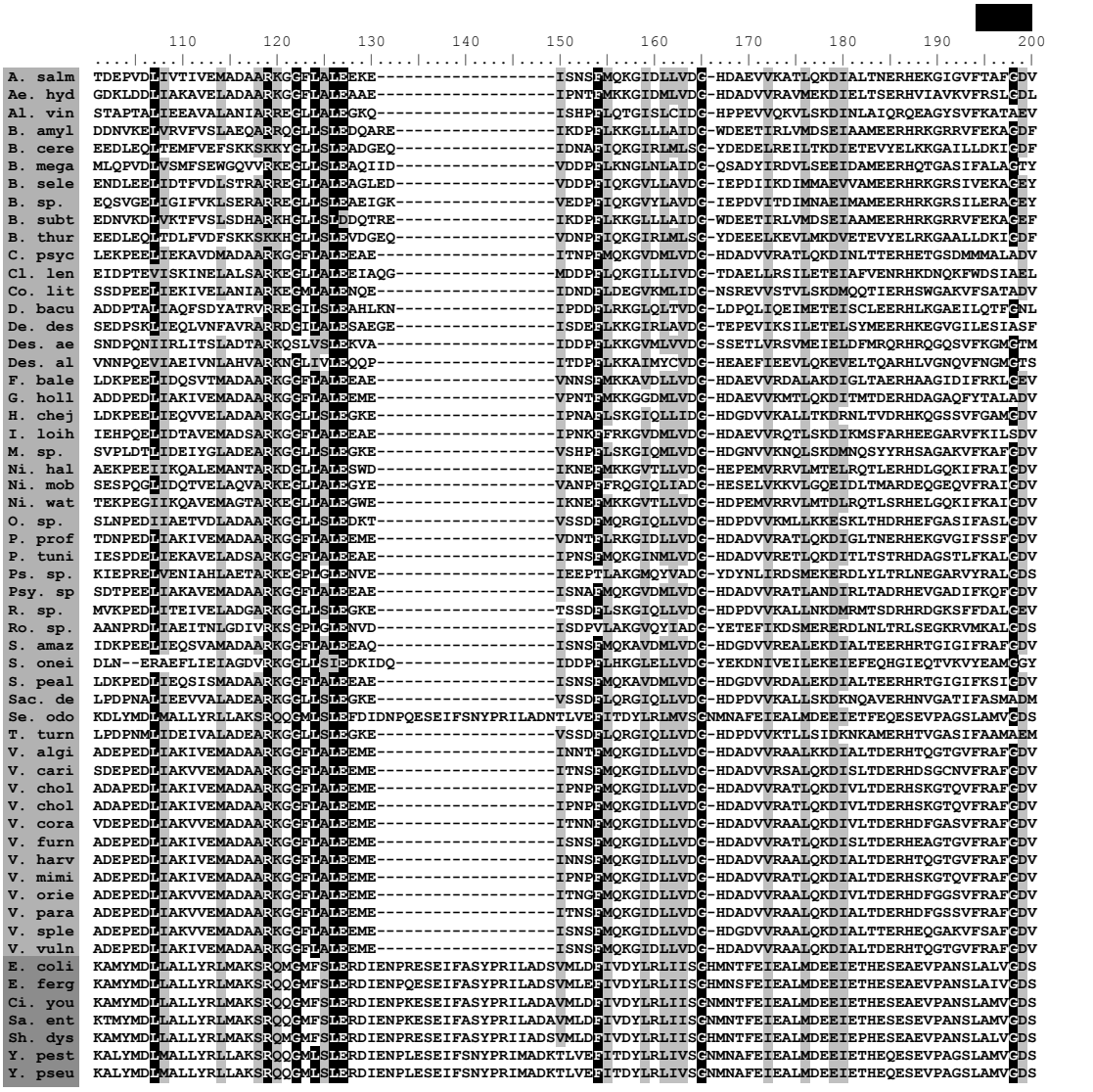
110
120
130
140
150
160
170
180
190
200
A. salm
Ae. hyd
Al. vin
B. amyl
B. cere
B. mega
B. sele
B. sp.
B. subt
B. thur
C. psyc
Cl. len
Co. lit
D. bacu
De. des
Des. ae
Des. al
F. bale
G. holl
H. chej
I. loih
M. sp.
Ni. hal
Ni. mob
Ni. wat
O. sp.
P. prof
P. tuni
Ps. sp.
Psy. sp
R. sp.
Ro. sp.
S. amaz
S. onei
S. peal
Sac. de
Se. odo
T. turn
V. algi
V. cari
V. chol
V. chol
V. cora
V. furn
V. harv
V. mimi
V. orie
V. para
V. sple
V. vuln
E. coli
E. ferg
Ci. you
Sa. ent
Sh. dys
Y. pest
Y. pseu

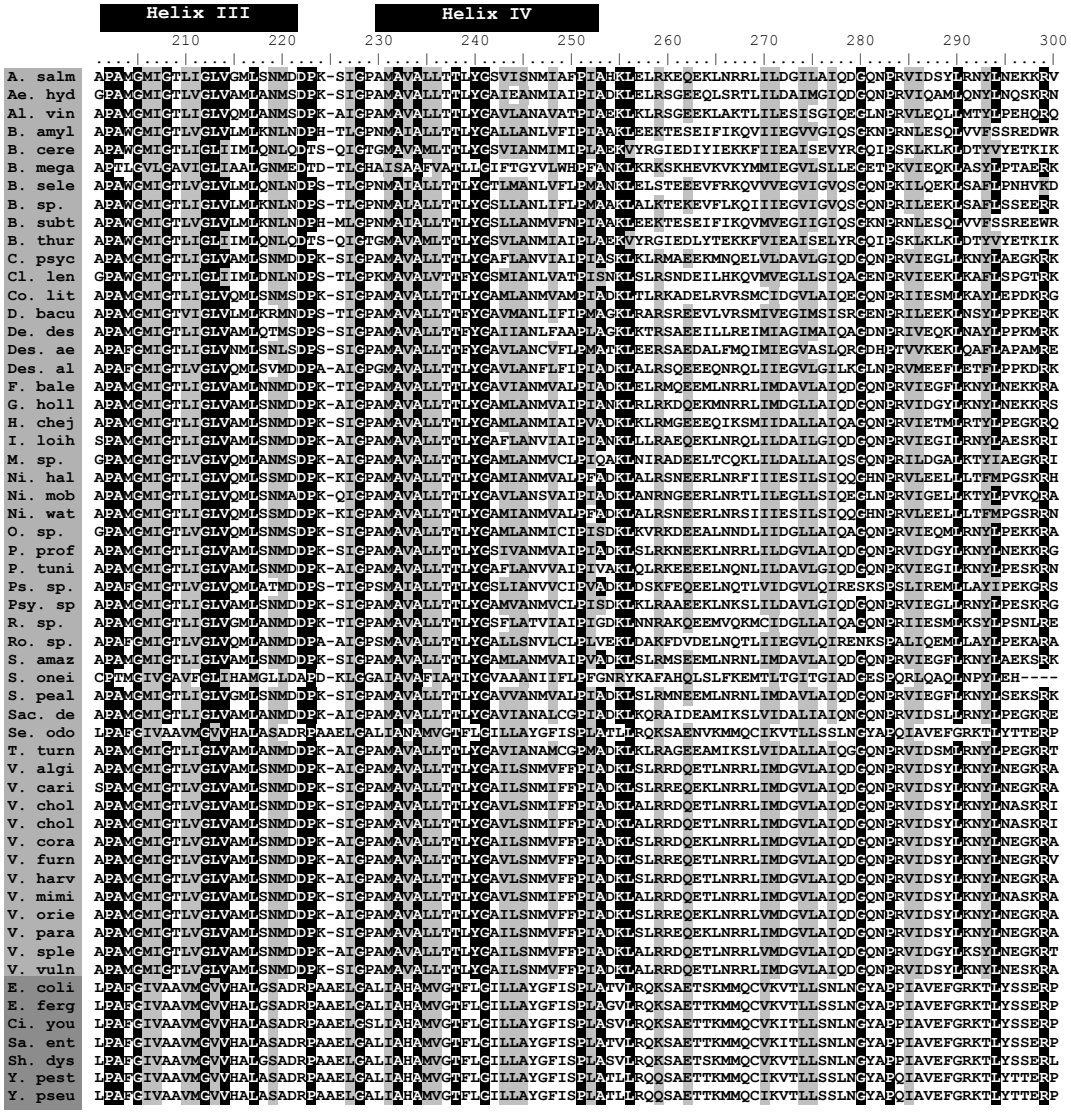
Helix III
Helix IV
210
220
230
240
250
260
270
280
290
300
A. salm
Ae. hyd
Al. vin
B. amyl
B. cere
B. mega
B. sele
B. sp.
B. subt
B. thur
C. psyc
Cl. len
Co. lit
D. bacu
De. des
Des. ae
Des. al
F. bale
G. holl
H. chej
I. loih
M. sp.
Ni. hal
Ni. mob
Ni. wat
O. sp.
P. prof
P. tuni
Ps. sp.
Psy. sp
R. sp.
Ro. sp.
S. amaz
S. onei
S. peal
Sac. de
Se. odo
T. turn
V. algi
V. cari
V. chol
V. chol
V. cora
V. furn
V. harv
V. mimi
V. orie
V. para
V. sple
V. vuln
E. coli
E. ferg
Ci. you
Sa. ent
Sh. dys
Y. pest
Y. pseu

```
                 310       320
            ....|....|....|....|....|
A. salm     V--------DTGEE-----------
Ae. hyd     N--------GTE-------------
Al. vin     S--------SKD-------------
B. amyl     KGQPS--NKKKGAVHEA--------
B. cere     K--------EKRAA-----------
B. mega     KLLQESEVGINE-------------
B. sele     K-KDEEP--EETEENE---------
B. sp.      D-LDKAVNEEEALDNEA--------
B. subt     K-QPNQVKTKKGSVHEA--------
B. thur     K--------VKRAA-----------
C. psyc     V--------DTTDE-----------
Cl. len     V-------FDVKNKDE---------
Co. lit     G--------DDG-------------
D. bacu     V--------RS--------------
De. des     S--------QFE-------------
Des. ae     Q--------A---------------
Des. al     N--------SMANR-----------
F. bale     I--------DTTED-----------
G. holl     V--------DVDG------------
H. chej     T--------EEA-------------
I. loih     G--------NEDEDE----------
M. sp.      E--------RE--------------
Ni. hal     N--------NNGEK-----------
Ni. mob     P--------AEEAA-----------
Ni. wat     N--------GYGEKGR---------
O. sp.      A--------AEG-------------
P. prof     V--------DVDG------------
P. tuni     V--------DTEG------------
Ps. sp.     D--------MIEAAA----------
Psy. sp     G--------GSTEDGAA--------
R. sp.      G--------A---------------
Ro. sp.     E--------FAEAA-----------
S. amaz     I--------DTTDGE----------
S. onei     ------------------------
S. peal     I--------DTLEGA----------
Sac. de     V--------ADAD------------
Se. odo     SFVELEEHVRRVKAPAQQATEEEQA
T. turn     V--------EAAE------------
V. algi     L--------EIDE------------
V. cari     L--------DVDNE-----------
V. chol     L--------DVDKE-----------
V. chol     L--------DVDKE-----------
V. cora     L--------DVDNE-----------
V. furn     L--------DVDNE-----------
V. harv     L--------EIDE------------
V. mimi     L--------DVDKE-----------
V. orie     L--------DVDNE-----------
V. para     L--------DVDNE-----------
V. sple     I--------DGEPA-----------
V. vuln     L--------DIND------------
E. coli     SFIELEEHVRAVKNPQQQTTTEEA-
E. ferg     SFVELEEHVRAVKNPNQQATTEEV-
Ci. you     SFIELEEHVRAVRNPAAQQTTEDA-
Sa. ent     SFIELEEHVRAVRNPNQQQTTEEA-
Sh. dys     SFIELEEHVRAVKNPQQQTTTEEA-
Y. pest     SFIELEEHVRRVKAPASQATEEDA-
Y. pseu     SFIELEEHVRRVKAPASQATEEDA-
```

Figure E.4: Sequence alignment of PomA.

Fig. E.4: A. salm: *Aliivibrio salmonicida* (gi|209694504), Ae. hyd: *Aeromonas hydrophila* (gi|117620588), Al. vin: *Allochromatium vinosum* (gi|288942519), B. amyl: *Bacillus amyloiquefaciens* (gi|308174664), B. cere: *Bacillus cereus* (gi|152975139), B. mega: *Bacillus megaterium* (gi|294498804), B. sele: *Bacillus selenitrireducens* (gi|297583 573), B. sp.: *Bacillus sp.* (gi|319651876), B. subt: *Bacillus subtilis* (gi|296332049), B. thur: *Bacillus thuringiensis* (gi|118477163), C. psyc: *Colwellia psychrerythraea* (gi|71279 500), Cl. len: *Clostridium lentocellum* (gi|296440180), Co. lit: *Congregibacter litoralis* (gi|88704265), D. bacu: *Desulfomicrobium baculatum* (gi|256830502), De. des: *Deferribacter desulfuricans* (gi|291280095), Des. ae: *Desulfovibrio aespoeensis* (gi|317153384), Des. al: *Desulfurivibrio alkaliphilus* (gi|297569176), F. bale: *Ferrimonas balearica* (gi|308 048594), G. holl: *Grimontia hollisae* (gi|262274768), H. chej: *Hahella chejuensis* (gi|8364 8503), I. loih: *Idiomarina loihiensis* (gi|56461235), M. sp.: *Marinomonas sp.* (gi|1529951 77), Ni. hal: *Nitrosococcus halophilus* (gi|292492680), Ni. mob: *Nitrococcus mobilis* (gi|88812419), Ni. wat: *Nitrosococcus watsoni* (gi|300114850), O. sp.: *Oceanospirillum sp.* (gi|89093475), P. prof: *Photobacterium profundum* (gi|90410907), P. tuni: *Pseudoalteromonas tunicata* (gi|88859187), Ps. sp.: *Pseudovibrio sp.* (gi|254473242), Psy. sp.: *Psychromonas sp.* (gi|90408166), R. sp.: *Reinekea sp.* (gi|88799580), Ro. sp.: *Roseibium sp.* (gi|307944456), S. amaz: *Shewanella amazonensis* (gi|119775567), S. onei: *Shewanella oneidensis* (gi|24375769), S. peal: *Shewanella pealeana* (gi|157962806), Sac. de: *Saccharophagus degradans* (gi|90022861), Se. odo: *Serratia odorifera* gi|270262420, T. turn: *Teredinibacter turnerae* (gi|254787124), V. algi: *Vibrio alginolyticus* (gi|91225059), V. cari: *Vibrio caribbenthicus* (gi|312884944), V. chol: *Vibrio cholerae* (gi|51241595), V. chol: *Vibrio cholerae O1 biovar El Tor str. N16961* (gi|15640908), V. cora: *Vibrio coralliilyticus* (gi|260776527), V. furn: *Vibrio furnissii* (gi|260767265), V. harv: *Vibrio harveyi* (gi|153835782), V. mimi: *Vibrio mimicus* (gi|258621631), V. orie: *Vibrio orientalis* (gi|261252276), V. para: *parahaemolyticus* (gi|254509022), V. sple: *Vibrio splendidus* (gi|84394352), V. vuln: *Vibrio vulnificus* (gi|27363787), E. coli: *Escherichia coli* (gi|89108730), E. ferg: *Escherichia fergusonii* (gi|218548502), Ci. you: *Citrobacter youngae* (gi|291085222), Sa. ent: *Salmonella enterica* (gi|161502955), Sh. dys: *Shigella dysenteriae* (gi|82776485), Y. pest: *Yersinia pestis* (gi|145599065), Y. pseu: *Yersinia pseudotuberculosis* (gi|51596730).

E. APPENDIX

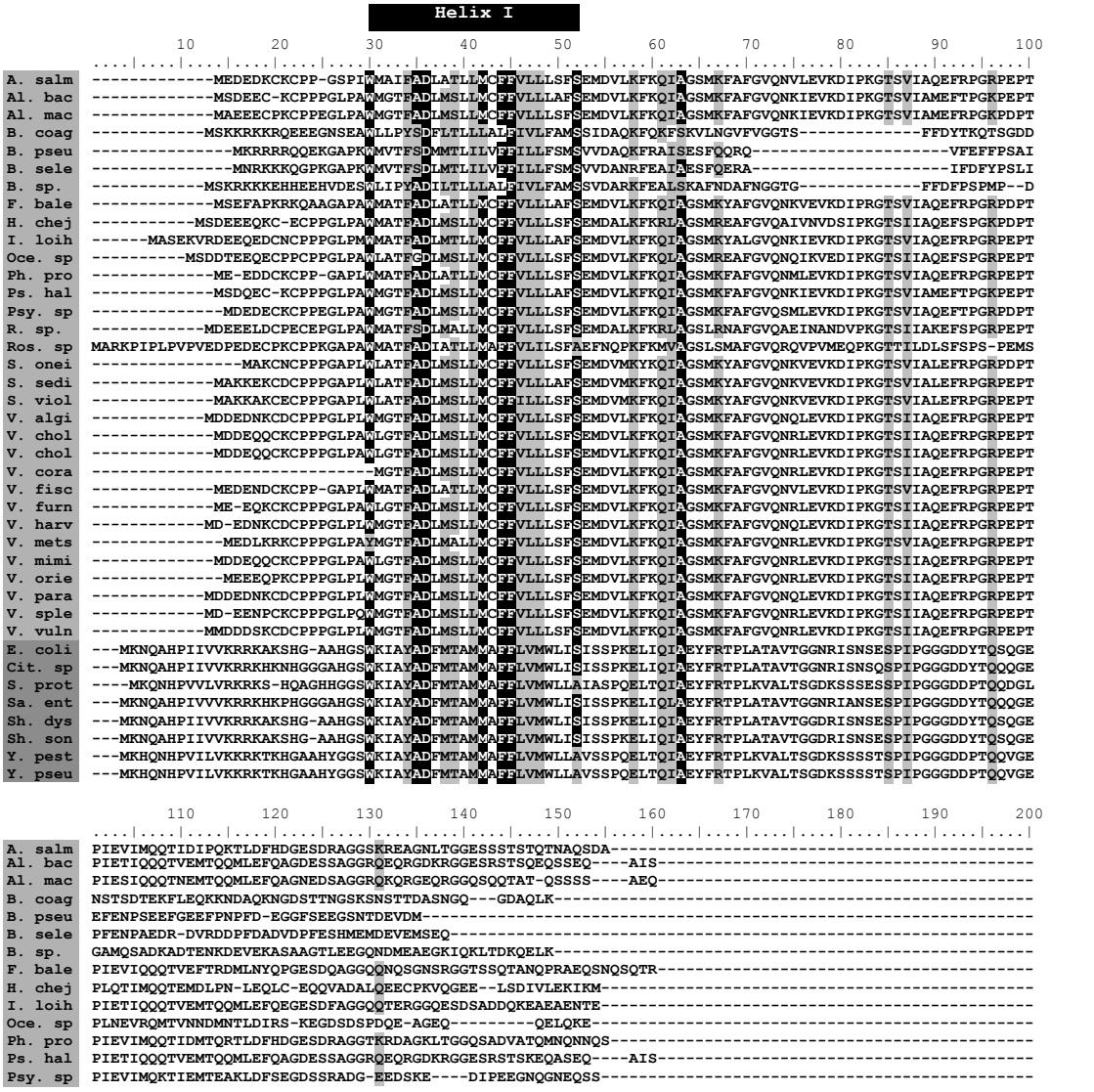
Helix I
10 20 30 40 50 60 70 80 90 100
A. salm ----------MEDEDKCKCPP-GSPIWMAIFADLATLLMCFFVLLLSFSEMDVLKFKQIAGSMKFAFGVQNVLEVKDIPKGTSVIAQEFRPGRPEPT
Al. bac ----------MSDEEC-KCPPPGLPAWMGTFADLMSLLMCFFVLLLAFSEMDVLKFKQIAGSMKFAFGVQNKIEVKDIPKGTSVIAMEFTPGKPEPT
Al. mac ----------MAEEECPKCPPEGLPAWMGTFADLMSLLMCFFVLLLSFSEMDVLKFKQIAGSMKFAFGVQNKIEVKDIPKGTSVIAMEFRPGKPDPT
B. coag ----------MSKKRKKRQEEEGNSEAWLLPYSDFLTLLLALFIVLFAMSSIDAQKFQKFSKVLNGVFVGGTS----------FFDYTKQTSGDD
B. pseu ----------MKRRRRQQEKGAPKWMVTFSDMMTLILVFFILLFSMSVVDAQKFRAISESFQQRQ----------VFEFFPSAI
B. sele ----------MNRKKKQGPKGAPKWMVTFSDLMTLILVFFILLFSMSVVDANRFEAIAESFQERA----------IFDFYPSLI
B. sp. ----------MSKRKKKEHHEEHVDESWLIPYADILTLLLALFIVLFAMSSVDARKFEALSKAFNDAFNGGTG----------FFDFPSPMP--D
F. bale ----------MSEFAPKRKQAAGAPAWMATFADLATLLMCFFVLLLAFSEMDVLKFKQIAGSMKYAFGVQNKVEVKDIPKGTSVIAQEFRPGRPDPT
H. chej ----------MSDEEEQKC-ECPPGLPAWMATFADLMSLLMCFFVLLLSFSEMDALKFKRLAGSMREAFGVQAIVNVDSIPKGTSIIAQEFSPGKPDPT
I. loih ------MASEKVRDEEQEDCNCPPPGLPMWMATFADLMTLLMCFFVLLLAFSEMDVLKFKQIAGSMKYALGVQNKIEVKDIPKGTSVIAQEFRPGRPEPT
Oce. sp ----------MSDDTEEQECPPCPPGLPAWLATFGDLMSLLMCFFVLLLSFSEMDVLKFKQLAGSMREAFGVQNQIKVEDIPKGTSIIAQEFSPGRPEPT
Ph. pro ----------ME-EDDCKCPP-GAPLWMATFADLATLLMCFFVLLLSFSEMDVLKFKQIAGSMKFAFGVQNMLEVKDIPKGTSVIAQEFRPGRPEPT
Ps. hal ----------MSDQEC-KCPPPGLPAWMGTFADLMSLLMCFFVLLLAFSEMDVLKFKQIAGSMKFAFGVQNKIEVKDIPKGTSVIAMEFTPGKPEPT
Psy. sp ----------MDEDECKCPPEGLPAWMGTFADLMSLLMCFFVLLLSFSEMDVLKFKQIAGSMKFAFGVQSMLEVKDIPKGTSVIAQEFTPGRPDPT
R. sp. ----------MDEEELDCPECEPGLPAWMATFSDLMALLMCFFVLLLSFSEMDALKFKRLAGSLRNAFGVQAEINANDVPKGTSIIAKEFSPGRPEPT
Ros. sp MARKPIPLPVPVEDPEDECPKCPPKGAPAWMATFADIATLLMAFFVLILSFAEFNQPKFKMVAGSLSMAFGVQRQVPVMEQPKGTTILDLSFSPS-PEMS
S. onei ----------MAKCNCPPPGAPLWLATFADLMSLLMCFFVLLLSFSEMDVMKYKQIAGSMKYAFGVQNKVEVKDIPKGTSVIALEFRPGRPDPT
S. sedi ----------MAKKEKCDCPPPGAPLWLATFADLMSLLMCFFVLLLAFSEMDVMKFKQIAGSMKYAFGVQNKVEVKDIPKGTSVIALEFRPGRPEPT
S. viol ----------MAKKAKCECPPPGAPLWLATFADLMSLLMCFFILLLSFSEMDVMKFKQIAGSMKYAFGVQNKVEVKDIPKGTSVIALEFRPGRPEPT
V. algi ----------MDDEDNKCDCPPPGLPLWMGTFADLMSLLMCFFVLLLSFSEMDVLKFKQIAGSMKFAFGVQNQLEVKDIPKGTSIIAQEFRPGRPEPT
V. chol ----------MDDEQQCKCPPPGLPAWLGTFADLMSLLMCFFVLLLSFSEMDVLKFKQIAGSMKFAFGVQNRLEVKDIPKGTSIIAQEFRPGRPEPT
V. chol ----------MDDEQQCKCPPPGLPAWLGTFADLMSLLMCFFVLLLSFSEMDVLKFKQIAGSMKFAFGVQNRLEVKDIPKGTSIIAQEFRPGRPEPT
V. cora ----------MGTFADLMSLLMCFFVLLLSFSEMDVLKFKQIAGSMKFAFGVQNRLEVKDIPKGTSIIAQEFRPGRPEPT
V. fisc ----------MEDENDCKCPP-GAPLWMATFADLATLLMCFFVLLLSFSEMDVLKFKQIAGSMKFAFGVQNVLEVKDIPKGTSVIAQEFRPGRPEPT
V. furn ----------ME-EQKCKCPPPGLPAWLGTFADLMSLLMCFFVLLLSFSEMDVLKFKQIAGSMKFAFGVQNRLEVKDIPKGTSIIAQEFRPGRPEPT
V. harv ----------MD-EDNKCDCPPPGLPLWMGTFADLMSLLMCFFVLLLSFSEMDVLKFKQIAGSMKFAFGVQNQLEVKDIPKGTSIIAQEFRPGRPEPT
V. mets ----------MEDLKRKCPPPGLPAYMGTFADLMALLMCFFVLLLSFSEMDVLKFKQIAGSMKFAFGVQNRLEVKDIPKGTSVIAQEFRPGRPEPT
V. mimi ----------MDDEQQCKCPPPGLPAWLGTFADLMSLLMCFFVLLLSFSEMDVLKFKQIAGSMKFAFGVQNRLEVKDIPKGTSIIAQEFRPGRPEPT
V. orie ----------MEEEQPKCPPPGLPLWMGTFADLMSLLMCFFVLLLSFSEMDVLKFKQIAGSMKFAFGVQNRLEVKDIPKGTSIIAQEFRPGRPEPT
V. para ----------MDDEDNKCDCPPPGLPLWMGTFADLMSLLMCFFVLLLSFSEMDVLKFKQIAGSMKFAFGVQNQLEVKDIPKGTSIIAQEFRPGRPEPT
V. sple ----------MD-EENPCKCPPPGLPQWMGTFADLMSLLMCFFVLLLSFSEMDVLKFKQIAGSMKFAFGVQNRLEVKDIPKGTSIIAQEFRPGRPEPT
V. vuln ----------MMDDDSKCDCPPPGLPLWMGTFADLMSLLMCFFVLLLSFSEMDVLKFKQIAGSMKFAFGVQNRLEVKDIPKGTSIIAQEFRPGRPEPT
E. coli ---MKNQAHPIIVVKRRKAKSHG-AAHGSWKIAYADFMTAMMAFFLVMWLISISSPKELIQIAEYFRTPLATAVTGGNRISNSESPIPGGGDDYTQSQGE
Cit. sp ---MKNQAHPIIVVKRRKHKNHGGGAHGSWKIAYADFMTAMMAFFLVMWLISISSPKELIQIAEYFRTPLATAVTGGNRISNSQSPIPGGGDDYTQQQGE
S. prot ----MKQNHPVVLVRKRKS-HQAGHHGGSWKIAYADFMTAMMAFFLVMWLLAIASPQELTQIAEYFRTPLKVALTSGDKSSSESSPIPGGGDDPTQQDGL
Sa. ent ---MKNQAHPIVVVKRRKHKPHGGGAHGSWKIAYADFMTAMMAFFLVMWLISISSPKELIQIAEYFRTPLATAVTGGNRIANSESPIPGGGDDYTQQQGE
Sh. dys ---MKNQAHPIIVVKRRKAKSHG-AAHGSWKIAYADFMTAMMAFFLVMWLISISSPKELIQIAEYFRTPLATAVTGGDRISNSESPIPGGGDDYTQSQGE
Sh. son ---MKNQAHPIIVVKRRKAKSHG-AAHGSWKIAYADFMTAMMAFFLVMWLISISSPKELIQIAEYFRTPLATAVTGGDRISNSESPIPGGGDDYTQSQGE
Y. pest ---MKHQNHPVILVKKRKTKHGAAHYGGSWKIAYADFMTAMMAFFLVMWLLAVSSPQELTQIAEYFRTPLKVALTSGDKSSSSTSPIPGGGDDPTQQVGE
Y. pseu ---MKHQNHPVILVKKRKTKHGAAHYGGSWKIAYADFMTAMMAFFLVMWLLAVSSPQELTQIAEYFRTPLKVALTSGDKSSSSTSPIPGGGDDPTQQVGE
110 120 130 140 150 160 170 180 190 200
A. salm PIEVIMQQTIDIPQKTLDFHDGESDRAGGSKREAGNLTGGESSSTSTQTNAQSDA----------
Al. bac PIETIQQQTVEMTQQMLEFQAGDESSAGGRQEQRGDKRGGESRSTSQEQSSEQ----AIS----------
Al. mac PIESIQQQTNEMTQQMLEFQAGNEDSAGGRQKQRGEQRGGQSQQTAT-QSSSS----AEQ----------
B. coag NSTSDTEKFLEQKNDAQKNGDSTTNGSKSNSTTDASNGQ---GDAQLK----------
B. pseu EFENPSEEFGEEFPNPFD-EGGFSEEGSNTDEVDM----------
B. sele PFENPAEDR-DVRDDPFDADVDPFESHMEMDEVEMSEQ----------
B. sp. GAMQSADKADTENKDEVEKASAAGTLEEGQNDMEAEGKIQKLTDKQELK----------
F. bale PIEVIQQQTVEFTRDMLNYQPGESDQAGGQQNQSGNSRGGTSSQTANQPRAEQSNQSQTR----------
H. chej PLQTIMQQTEMDLPN-LEQLC-EQQVADALQEECPKVQGEE--LSDIVLEKIKM----------
I. loih PIETIQQQTVEMTQQMLEFQEGESDFAGGQQTERGGQESDSADDQKEAEAENTE----------
Oce. sp PLNEVRQMTVNNDMNTLDIRS-KEGDSDSPDQE-AGEQ---------QELQKE----------
Ph. pro PIEVIMQQTIDMTQRTLDFHDGESDRAGGTKRDAGKLTGGQSADVATQMNQNNQS----------
Ps. hal PIETIQQQTVEMTQQMLEFQAGDESSAGGRQEQRGDKRGGESRSTSKEQASEQ----AIS----------
Psy. sp PIEVIMQKTIEMTEAKLDFSEGDSSRADG-EEDSKE----DIPEEGNQGNEQSS----------

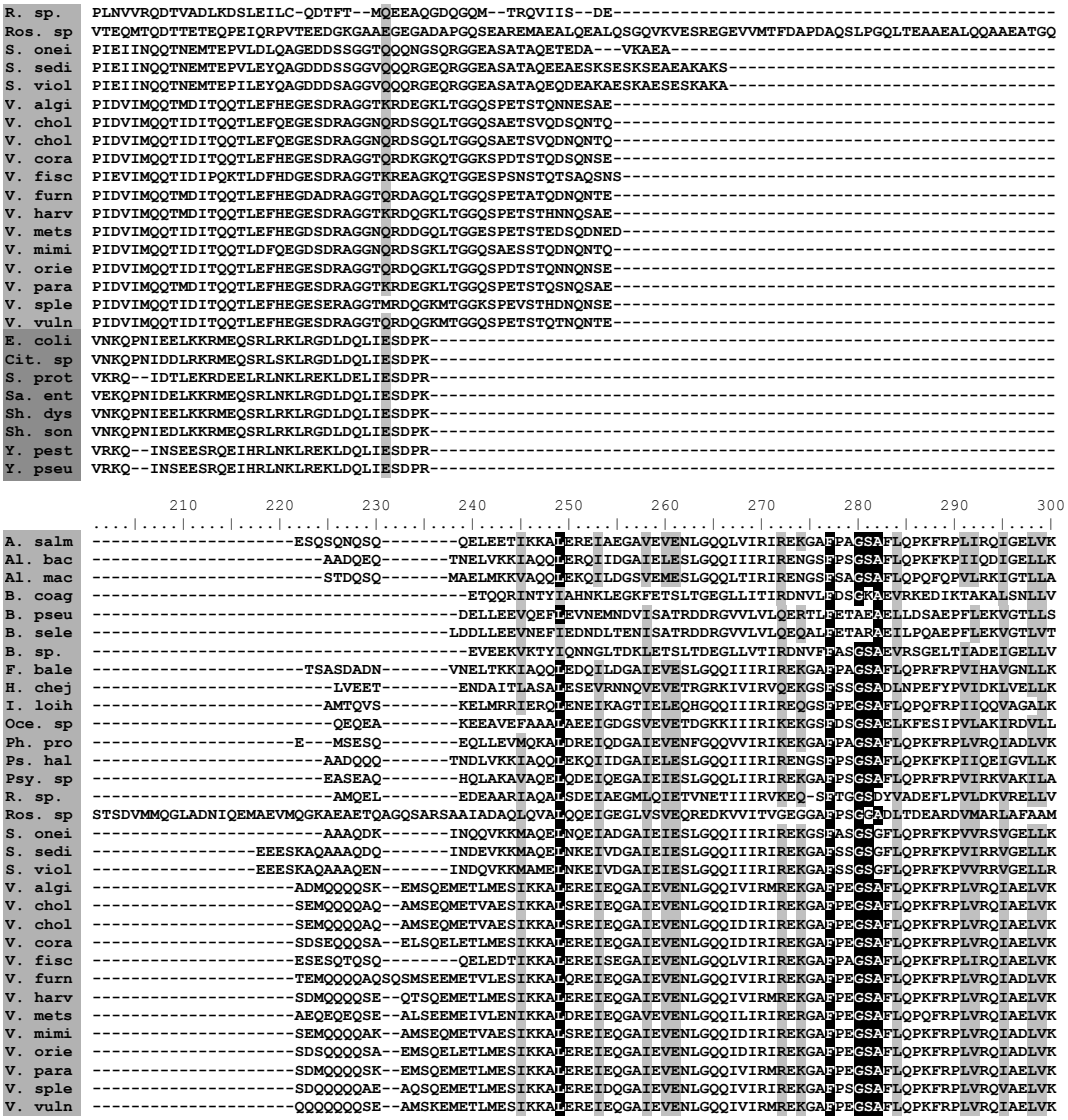
R. sp.
Ros. sp
S. onei
S. sedi
S. viol
V. algi
V. chol
V. chol
V. cora
V. fisc
V. furn
V. harv
V. mets
V. mimi
V. orie
V. para
V. sple
V. vuln
E. coli
Cit. sp
S. prot
Sa. ent
Sh. dys
Sh. son
Y. pest
Y. pseu
210
220
230
240
250
260
270
280
290
300
A. salm
Al. bac
Al. mac
B. coag
B. pseu
B. sele
B. sp.
F. bale
H. chej
I. loih
Oce. sp
Ph. pro
Ps. hal
Psy. sp
R. sp.
Ros. sp
S. onei
S. sedi
S. viol
V. algi
V. chol
V. chol
V. cora
V. fisc
V. furn
V. harv
V. mets
V. mimi
V. orie
V. para
V. sple
V. vuln

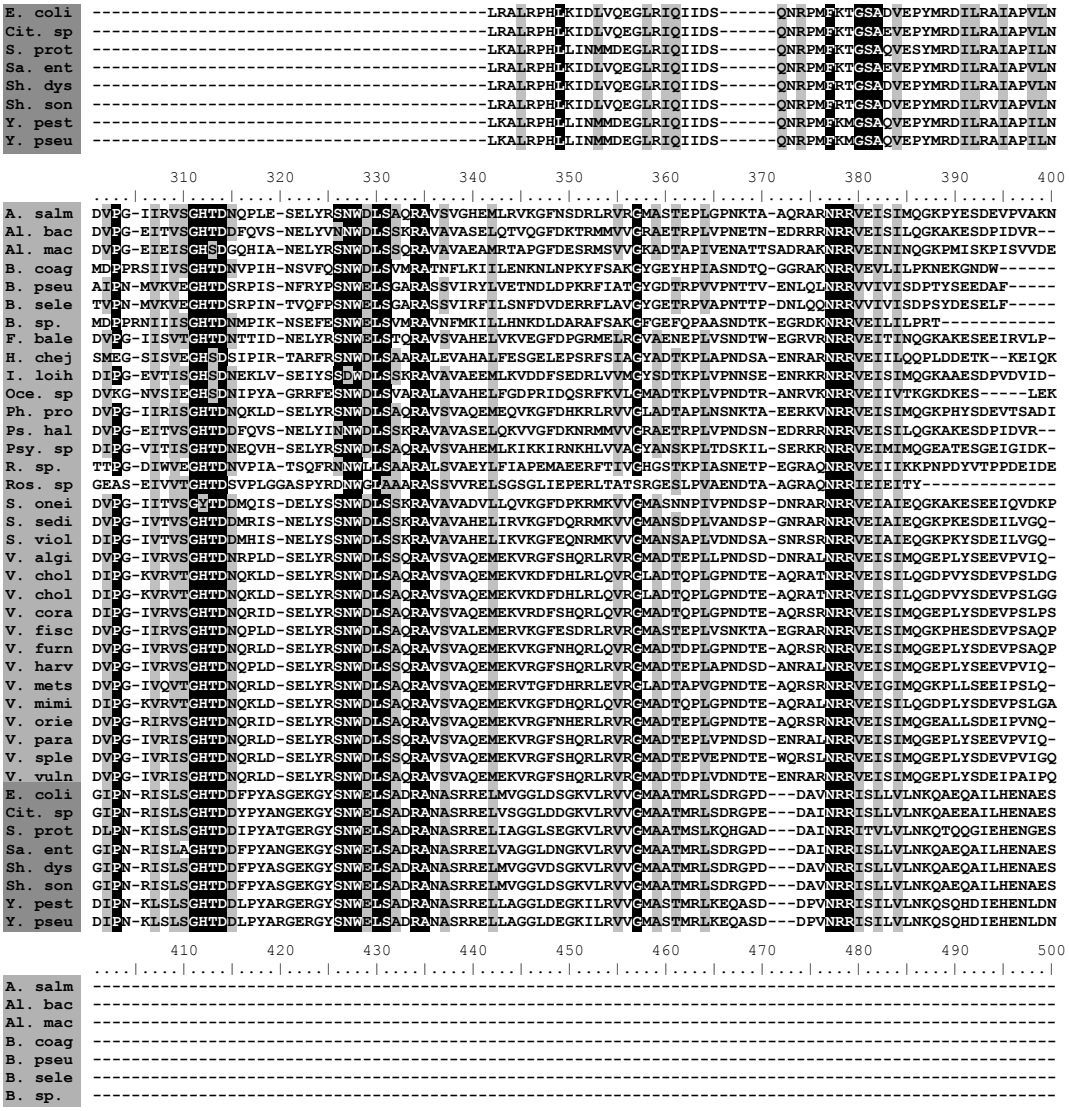
E. coli
Cit. sp
S. prot
Sa. ent
Sh. dys
Sh. son
Y. pest
Y. pseu
A. salm
Al. bac
Al. mac
B. coag
B. pseu
B. sele
B. sp.
F. bale
H. chej
I. loih
Oce. sp
Ph. pro
Ps. hal
Psy. sp
R. sp.
Ros. sp
S. onei
S. sedi
S. viol
V. algi
V. chol
V. chol
V. cora
V. fisc
V. furn
V. harv
V. mets
V. mimi
V. orie
V. para
V. sple
V. vuln
E. coli
Cit. sp
S. prot
Sa. ent
Sh. dys
Sh. son
Y. pest
Y. pseu
A. salm
Al. bac
Al. mac
B. coag
B. pseu
B. sele
B. sp.

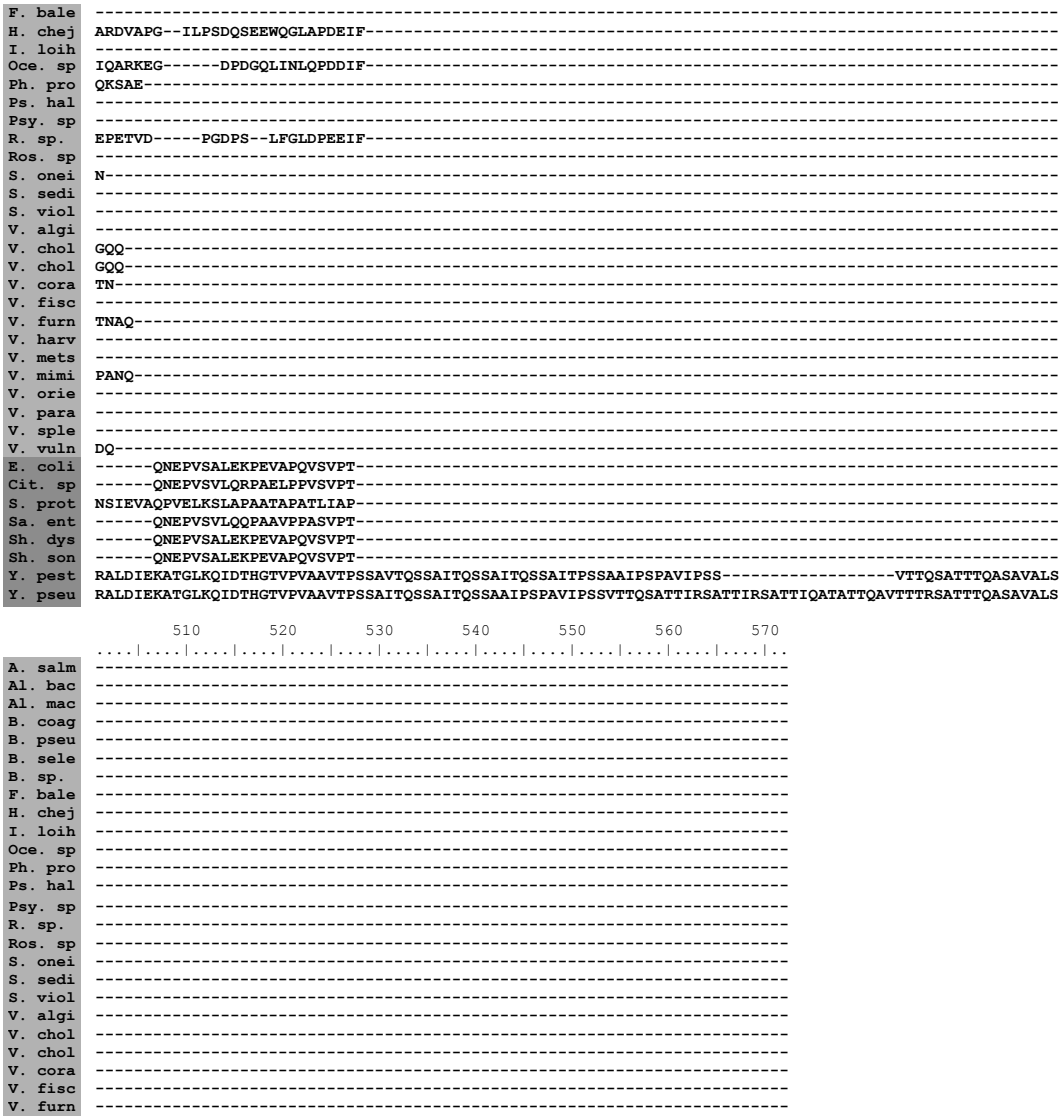
F. bale
H. chej
I. loih
Oce. sp
Ph. pro
Ps. hal
Psy. sp
R. sp.
Ros. sp
S. onei
S. sedi
S. viol
V. algi
V. chol
V. chol
V. cora
V. fisc
V. furn
V. harv
V. mets
V. mimi
V. orie
V. para
V. sple
V. vuln
E. coli
Cit. sp
S. prot
Sa. ent
Sh. dys
Sh. son
Y. pest
Y. pseu
510
520
530
540
550
560
570
A. salm
Al. bac
Al. mac
B. coag
B. pseu
B. sele
B. sp.
F. bale
H. chej
I. loih
Oce. sp
Ph. pro
Ps. hal
Psy. sp
R. sp.
Ros. sp
S. onei
S. sedi
S. viol
V. algi
V. chol
V. chol
V. cora
V. fisc
V. furn

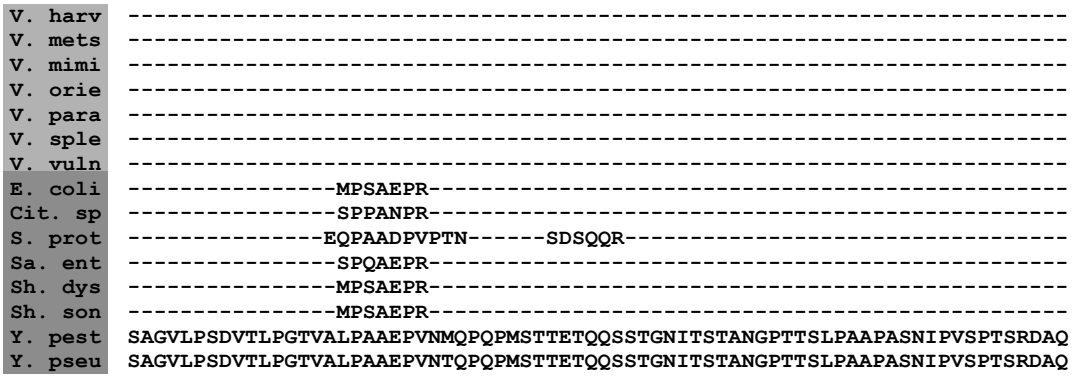

Figure E.5: Sequence alignment of PomB. A. salm: *Aliivibrio salmonicida* (gi|209694505), Al. bac: *Alteromonadales bacterium* (gi|119472095), Al. mac: *Alteromonas macleodii* (gi|196156245), B. coag: *Bacillus coagulans* (gi|229543005), B. pseu: *Bacillus pseudofirmus* (gi|288553786), B. sele: *Bacillus selenitrireducens* (gi|297583574), B. sp: *Bacillus sp.* (gi|89100891), F. bale: *Ferrimonas balearica* (gi|308048595), H. chej: *Hahella chejuensis* (gi|83648502), I. loih: *Idiomarina loihiensis* (gi|56461234), Oce. sp: *Oceanospirillum sp.* (gi|89093474), Ph. pro: *Photobacterium profundum* (gi|90410908), Ps. hal: *Pseudoalteromonas haloplanktis* (gi|77361278), Psy. sp.: *Psychromonas sp.* (gi|90408165), R. sp.: *Reinekea sp.* (gi|88799579), Ros. sp.: *Roseovarius sp.* (gi|149201621), S. onei: *Shewanella oneidensis* (gi|24347292), S. sedi: *Shewanella sediminis* (gi|157376457), S. viol: *Shewanella violacea* (gi|294139895), V. algi: *Vibrio alginolyticus* (gi|269965067), V. chol: *Vibrio cholerae V51* (gi|254225118), V. chol: *Vibrio cholerae* (gi|51241597), V. cora: *Vibrio coralliilyticus* (gi|260776526), V. fisc: *Vibrio fischeri* (gi|59711322), V. furn: *Vibrio furnissii* (gi|260767264), V. harv: *Vibrio harveyi* (gi|156973487), V. mets: *Vibrio metschnikovii* (gi|260773298), V. mimi: *Vibrio mimicus* (gi|258624381), V. orie: *Vibrio orientalis* (gi|261252277), V. para: *Vibrio parahaemolyticus* (gi|4322001), V. sple: *Vibrio splendidus* (gi|84394351), V. vuln: *Vibrio vulnificus* (gi|37679056), E. coli: *Escherichia coli* (gi|293415204), Cit. sp.: *Citrobacter spc.* (gi|237731926), S. prot: *Serratia proteamaculans* (gi|157371226), Sa. ent: *Salmonella enterica* (gi|161502956), Sh. dys: *Shigella dysenteriae* (gi|194434087), Sh. son: *Shigella sonnei* (gi|74311761), Y. pest: *Yersinia pestis* (gi|45441604), Y. pseu: *Yersinia pseudotuberculosis* (gi|170023989).

3 Construction of a *V. cholerae* Δ*qseC* mutant

The work described in Chap. B strongly indicates the presence of a QseC homolog in *V. cholerae*. The effect of catecholates should thus also be investigated in a *qseC* deletion mutant of *V. cholerae*.

3.1 Construction of plasmid pSW-qseC and donor strain *E. coli* β3914 pSW-qseC

The upstream and downstream regions of *qseC* were amplified from genomic DNA of *V. cholerae* using primer pairs QseC up fwd BamHI and QseC up rev (upstream fragment) and QseC do fwd and QseC do rev (downstream fragment). In a second step, the up and down fragments were joined using primers QseC up fwd BamHI and QseC do rev (see Tab. E.2). For both reactions Phusion™ High-Fidelity DNA Polymerase was used according to manufacturer's protocol. After purification, the 244 bp fragment was ligated into pJET1.2 using the CloneJET™ kit by Fermentas and transformed into chemically competent *E. coli* TOP10.

The plasmid pJET-Δ*qseC* was isolated from *E. coli* TOP10 and restricted using enzymes BamHI and XbaI according to manufacturer's protocol, ligated into the linearized suicide plasmid pSW7848 and transformed into *E. coli* β3914.

3.2 Procedure of homolog recombination in *V. cholerae*

E. coli β3914 pSW-qseC was used as donor strain and *V. cholerae* as recipient strain. Fresh LB medium (without antibiotics) was inoculated with an over night culture (1 % (v/v)) of either *V. cholerae* or *E. coli* β3914 pSW-qseC (supplemented with 0.3 mM DAP) and grown aerobically at 37 °C to a final OD_{600} of 0.3.

Bacterial cultures were mixed in following ratio 1:1, 1:10 and 1:100 (donor:recipient strain) and 50 µL of these cultures were pipetted onto sterile filter plates (pore size 2 µm) placed on LB agar supplemented with 0.3 mM DAP. Plates were incubated at room temperature over night.

1. Selection of chloramphenicol resistant *V. cholerae*: Cells were harvested with 2 mL LB medium. Dilutions up to 1:1000 were prepared and 100 µL of each dilution was pipetted onto LB agarplates supplemented with streptomycine (50 µg mL^{-1}) and chloramphenicol (25 µg mL^{-1}). Plates were incubated at room temperature until small colonies appear (up to three days). These colonies should be *V. cholerae*, which inherit the suicide plasmid pSW-qseC, which also codes for chloramphenicol resistance.

Name	Sequence
qseCup fwd BamHI	AAGGATCCAACGCCGACTTACCCTGACTTCTGT
qseCup rev	TTGGCGGACTGCCCAAGACG
qseCdo fwd	AAGACGTCGGATACTGGGGCCGCGAT
qseCdo rev	TCGACATGCCAAGCCCTGCG
pJET1.2 fwd	CGACTCACTATAGGGAGAGCGGC
pJET1.2 rev	AAGAACATCGATTTTCCATGGCAG

Table E.2: Oligo-nucleotides used in this study.

2. Selection of arabinose resistant *V. cholerae*: Single colonies of *V. cholerae* were picked and streaked onto LB agarplates containing 0.2 % arabinose and 50 µg mL^{-1} streptomycine. Arabinose triggers the expression of the plasmid encoded *ccdB*, a gyrase poison (42). Thus, strains, which still inherit the plasmid pSW-qseC are not viable in the presence of arabinose. Plates were incubated at room temperature.

Positive colonies were tested in a colony PCR, using MyTaq (bioline) as described in manufacturer's protocol with primers QseC up fwd BamHI and QseC do rev. A positive clone should show a PCR product of 240 bp. So far, this method did not lead to a strain lacking *qseC* and should be further improved.

4 Statistical analysis of swimming speeds of *V. cholerae* Δ*pomAB* expressing *pomA* and *pomB* wild type or variants

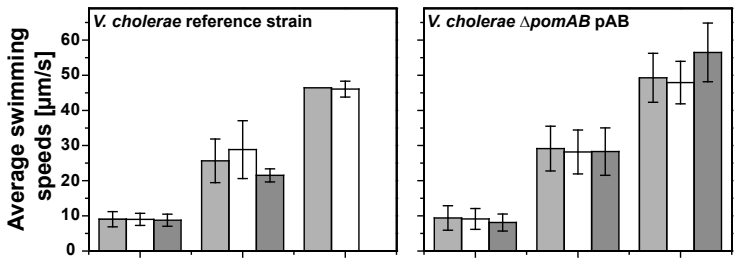

	V. cholerae reference strain									V. cholerae ΔpomAB pAB								
	slow			medium			fast			slow			medium			fast		
pH	7.0	8.0	9.0	7.0	8.0	9.0	7.0	8.0	9.0	7.0	8.0	9.0	7.0	8.0	9.0	7.0	8.0	9.0
n (cells)	284	319	317	20	5	3	1	2	-	132	215	264	163	90	41	28	11	17
Average [µm/s]	9.04	9	8.75	25.64	28.84	21.53	46.44	46.06	-	9.41	9.12	8.11	29.14	28.17	28.29	49.27	47.92	56.49
Standard deviation [µm/s]	2.15	1.72	1.72	6.2	8.24	1.86	-	2.26	-	3.49	2.95	2.41	6.37	6.25	6.74	6.96	6.04	8.33
Minimum [µm/s]	6.23	6.43	6.56	18.3	19.05	19.37	-	44.46	-	5.36	5.45	4.86	18.16	18.29	18.07	42.16	41.68	42.49
Median [µm/s]	8.41	8.59	8.29	23.11	33.02	21.37	-	46.06	-	7.93	7.98	7.17	28.76	26.91	27.98	47.77	47.52	56.11
Maximum [µm/s]	17.81	17.69	17.77	40.09	37.29	23.46	-	47.66	-	17.74	17.67	17.47	40.83	40.32	40.02	74.32	61.06	73.16

Figure E.6: Statistical analysis of tracks from *V. cholerae* reference strain and *V. cholerae* Δ*pomAB* pAB. Tracks were recorded in $LB_{Na}{}^{+}$ buffered to pH 7.0, pH8.0 and pH9.0. Number of tracks for *V. cholerae* reference strain are (305/326/320) and for *V. cholerae* Δ*pomAB* expressing PomA and wild type PomB are (323/316/322).

	WT									S26A									S26T								
	slow			medium			fast			slow			medium			fast			slow			medium			fast		
pH	7.0	8.0	9.0	7.0	8.0	9.0	7.0	8.0	9.0	7.0	8.0	9.0	7.0	8.0	9.0	7.0	8.0	9.0	7.0	8.0	9.0	7.0	8.0	9.0	7.0	8.0	9.0
n (cells)	211	385	576	344	227	56	74	29	18	384	444	510	262	195	120	4	8	20	382	308	260	268	324	275	-	18	115
Average [µm/s]	10.09	9.34	9.15	29.2	27.59	27.32	49.10	50.54	55.73	12.87	11.44	9.68	24.52	25.91	25.23	43.56	45.12	48.04	13.29	11.33	11.16	22.80	27.19	28.52	-	45.45	48.92
Standard deviation [µm/s]	3.58	3.2	2.56	6.37	6.15	6.59	6.4	9.4	8.71	2.94	3.02	3.21	5	6.29	5.86	1.24	4	8.08	3.07	3.5	3.43	3.74	5.96	6.47	-	4.5	6.06
Minimum [µm/s]	5.36	5.36	4.86	18.14	18	18.07	41.27	41.45	42.49	6.96	5.22	4.94	18.01	18.02	18.06	42.15	42.18	41.23	6.24	5.58	5.18	18.03	18.03	18.03	-	41.21	41.11
Median [µm/s]	8.73	8.16	8.66	28.54	26.54	25.6	47.07	47.52	55.75	12.75	11.02	8.71	23.64	24.84	23.11	43.45	43.31	45.29	13.73	10.88	10.77	22.03	26.68	28.37	-	44.1	47.78
Maximum [µm/s]	17.74	17.86	17.91	40.96	40.97	40.02	74.31	82.27	73.16	17.99	17.97	17.82	40.49	40.54	40.17	45.16	52.09	65.45	17.99	17.99	17.93	37.42	40.97	40.94	-	60.78	75.81

Figure E.7: Statistical analysis of tracks from *V. cholerae* Δ*pomAB* expressing either PomA and wild type PomB, PomA and PomB-S26A or PomA and PomB-S26T. Tracks were recorded in $LB_{Na}{}^{+}$ buffered to pH 7.0, pH8.0 and pH9.0. Number of tracks for WT are (629/641/650), for S26A (650/647/650) and for S26T (650/650/650).

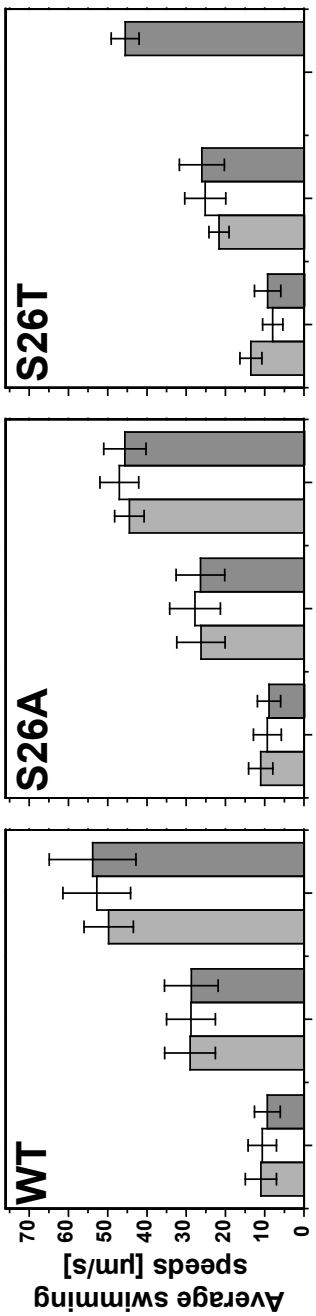

	WT						S26A						S26T					
pH	7.0	8.0	9.0	7.0	8.0	9.0	7.0	8.0	9.0	7.0	8.0	9.0	7.0	8.0	9.0	7.0	8.0	9.0
n (cells)	231	324	412	283	223	182	136	103	55	459	363	565	184	238	78	7	49	6	375	601	503	275	76	137	-	-	10
Average [µm/s]	10.97	10.61	9.33	29.01	28.78	28.69	49.75	52.78	53.83	11.02	9.33	8.9	26.25	27.77	26.38	44.48	40.03	45.63	13.52	7.96	9.26	21.63	25.16	26	-	-	45.56
Standard deviation [µm/s]	3.98	3.62	3.28	6.46	6.22	6.82	6.28	8.61	11.04	3.1	3.55	2.96	6.14	6.46	6.17	3.75	4.94	5.38	2.81	2.58	3.34	2.55	5.22	5.72	-	-	3.54
Minimum [µm/s]	4.13	4.72	4.77	18.13	18.03	18.24	41.12	41.08	41.04	5.89	4.99	4.97	18.01	18.16	18.07	41.57	41	42.17	7.51	4.38	4.33	18.03	18.1	18.05	-	-	41.01
Median [µm/s]	10.67	9.89	8.15	28.88	28.5	28.51	49.16	52.79	50.51	10.26	7.79	7.95	25.11	27.08	24.07	42.52	46.27	43.49	13.81	7.01	8.26	21.31	25.11	25.44	-	-	44.84
Maximum [µm/s]	17.89	17.92	17.93	40.78	40.59	40.51	71.23	83.41	85.73	17.95	17.81	17.87	40.21	40.99	40.32	51.78	60.92	56.17	17.97	17.92	17.93	29.56	36.62	39.25	-	-	51.53

Figure E.8: Statistical analysis of tracks from *V. cholerae* Δ*pomAB* expressing either PomA and wild type PomB, PomA and PomB-S26A or PomA and PomB-S26T. Tracks were recorded in LB medium without added salts and buffered to pH 7.0, pH8.0 and pH9.0. Number of tracks for WT are (650/650/649), for S26A (650/650/649) and for S26T (650/677/650).

	WT									S26A									S26T								
pH	**7.0**	**8.0**	**9.0**	**7.0**	**8.0**	**9.0**	**7.0**	**8.0**	**9.0**	**7.0**	**8.0**	**9.0**	**7.0**	**8.0**	**9.0**	**7.0**	**8.0**	**9.0**	**7.0**	**8.0**	**9.0**	**7.0**	**8.0**	**9.0**	**7.0**	**8.0**	**9.0**
n (cells)	289	275	488	317	227	98	43	129	64	491	485	460	149	174	162	-	-	28	519	472	239	131	135	374	-	43	37
Average [µm/s]	10.85	8.73	8.23	27.78	29.18	27.83	46.6	60.55	53.64	8.73	11.98	10.03	24.94	23.13	26.41	-	-	49.04	12.01	9.34	11.59	21.41	29.57	27.77	-	48.02	45.43
Standard deviation [µm/s]	3.59	3.34	2.7	6.32	6.47	6.37	5.31	10.82	9.19	2.94	3	3.07	4.89	4.33	5.79	-	-	9.47	3.14	2.91	3.17	3.29	7.14	5.76	-	4.58	3.52
Minimum [µm/s]	4.8	4.94	4.63	18.01	18.06	18.04	41.08	41.85	41.41	5.5	5.22	5.57	18.11	18.05	18.04	-	-	41.11	6.03	4.9	6.18	18.02	18.04	18.18	-	41.17	41.04
Median [µm/s]	9.87	7.31	7.22	27.29	28.93	27.68	45.62	58.85	51.23	7.52	11.89	8.88	24.05	22.19	25.41	-	-	44.11	11.75	8.49	11.16	20.29	31.32	27.47	-	47.44	44.83
Maximum [µm/s]	17.98	17.94	17.86	40.95	40.79	40.91	61.05	93.55	83.73	17.89	17.92	17.95	39.7	37.64	40.51	-	-	71.24	17.99	17.93	17.74	34.08	40.93	40.75	-	62.03	56.08

Figure E.9: Statistical analysis of tracks from *V. cholerae* Δ*pomAB* expressing either PomA and wild type PomB, PomA and PomB-S26A or PomA and PomB-S26T. Tracks were recorded in LB_K^+ buffered to pH 7.0, pH8.0 and pH9.0. Number of tracks for WT are (649/631/650), for S26A (640/659/650) and for S26T (650/650/650).

5 Chemicals, utilities and laboratory equipment

5.1 Chemicals used in this study

Chemicals	Distributor
A	
Acetone	Sigma-Aldrich
Acrylamide-Bis, solution (37.5:1), 30 % (w/v)	Serva
Agar	AppliChem
Agarose	invitrogen™
LE GP Agarose	Biozym
Albumin, Bovine (Fraction V, pH 7.0)	AppliChem
Aluminium oxide 90 acid	Carl Roth
L-Amino Acids	Sigma-Aldrich
Ammonia solution	Sigma-Aldrich
Ammonium chloride	Fluka
Ammonium nitrate	Merck
Ammonium sulfate	Fluka
Ampicillin, sodium salt	Carl Roth GmbH
L(+)-Arabinose	Fluka
B	
Biotin	Sigma-Aldrich
Bis(2-hydroxyethyl)amino-tris(hydroxymethyl)methan	AppliChem
Bromphenol blue	Fluka
C	
Calciumchloride anhydrous	Fluka
Chloramphenicol	Carl Roth GmbH
4-Chloro-1-naphthol	Thermo Fisher Scientific
Citric acid anhydrous	Fluka
Coomassie Brilliant blue G250	Fluka
Copper(II) sulfate x 5 H_2O	Merck
D	
2,6-Diaminopimelic acid	Sigma-Aldrich
Di-Isopropyl fluorophosphate (DFP)	Fluka
Di-Potassium hydrogen phosphate trihydrate	Merck

Di-Sodium hydrogen phosphate anhydrous	Fluka
Di-Thiothreitol (DTT)	Eurobio
E	
(-)-Epinephrine (+)-bitartate	Sigma-Aldrich
Ethanol ($\geq$ 99.8 %)	Carl Roth GmbH
Ethylenediaminetetraacetic acid (EDTA)	Fluka
F	
Formaldehyde 36.5 %	AppliChem
G	
D-(+)-Glucose anhydrous	Fluka
Glycerol, 99.5 %	Carl Roth GmbH
Glycine	Biosolve,
H	
Hydrogen peroxide 30 %	Fluka
4-(2-hydroxyethyl)-1-piperazineethanesulfonic acid (HEPES)	AppliChem
Hypoxanthine	Sigma-Aldrich
I	
Iron(III) sulfate hydrate	Honeywell Riedel-de Haën®
L	
(D-L) Lactic acid	Sigma Aldrich
Lysozyme (from hen egg white)	Fluka
M	
Magnesium chloride hexahydrate	Merck
β-Mercaptoethanol	AppliChem
Methanol	
N	
β-Nicotinamide adenine dinucleotide, reduced dipotassium salt	Sigma-Aldrich
($\pm$)-Norepinephrine (+)-bitartate salt	Sigma-Aldrich
P	
Perchloric acid 70 %	Merck
Phentolamine hydrochloride	Sigma-Aldrich
(ortho)-Phosphoric acid	Merck
Pierce BCA Protein Assay Reagent A	Thermo Fisher Scientific
Potassium chloride	Fluka

Potassium dihydrogen phosphate	Merck
Potassium hydroxide	Merck
R	
Riboflavin 5'-monophosphate sodium salt hydrate	Fluka
S	
Silver nitrate	Fluka
Sodium chloride	AppliChem
Sodium dodecy sulfate (SDS)	Acros
Streptomycin sulfate	AppliChem
D(+)-Sucrose	Fluka
SYBR Green I	invitrogen™
T	
N,N,N',N'-Tetramethylethylene-diamine (TEMED)	Serva
Tetracycline hydrochloride	Fluka
Thiamin x 2 HCl	Merck
Tris(hydroxymethyl)aminomethane	AppliChem
Tryptone	AppliChem
U	
Uracil	Fluka
Y	
Yeast extract	AppliChem
Z	
Zeocin™	invitrogen™

Table E.3: Chemicals used in this study.

5.2 Enzymes used in this study

enzymes	buffer	distributor
AclI	10x NEBuffer 4	NEB
AgeI	10x NEBuffer 1	NEB
CIP	10x NEBuffer 3	NEB
DNaseI (from bovine pancreas)		AppliChem
KpnI	10x NEBuffer 1	NEB

MyTaq™ HS DNA Polymerase	5x MyTaq reaction buffer	BIOLINE
NdeI	10x NEBuffer 4	NEB
One Taq™ DNA Polymerase	5x One Taq standard reaction buffer	NEB
Phusion™ High-Fidelity DNA Polymerase	5x Phusion HF buffer	FINNZYMES
Q5™ High-Fidelity DNA Polymerase	5x Q5 reaction buffer	NEB
Strep-Tactin®-HPR conjugate	iba	
T4 DNA ligase	5x T4 ligase buffer	NEB

Table E.4: Enzymes used in this study.

5.3 Utilities

Utilities	Specifications	Distributor
CryoPure tubes (1.6 mL)	non-cytotoxic, non-pyrogenic	Sarstedt, Nümbrecht (D)
Cultivation tubes (13 mL)	100 mm x 16 mm, non-pyrogenic	Sarstedt
test tubes	100 mm x 16 mm (⌀)	Assistent
Examination gloves	latex, powder free	vwr
Microscope slides		
μ-Slide VI flat	uncoated, sterile	ibidi®
glass slides	poly-L-lysine coated	Sigma Aldrich
Microscope cover glasses	24 x 50 mm	vwr
petri dishes	92 mm x 16 mm [⌀ x high]	Sarstedt
pipette tips (10 µL, 200 µL and 1000 µL; 5 mL)	without filter	Sarstedt
Tubes		
15 mL	120 mm x 17 mm, non-pyrogenic	Sarstedt
50 mL	115 mm x 28 mm, non-pyrogenic	Sarstedt

Ultracentrifuge tubes	25 mm x 89 mm, polycarbonate	Beckmann
Safe seal tubes (0.5 µL, 1.5 µL and 2 µL)		Sarstedt
Serological pipettes (15 mL, 25 mL and 50 mL)	single-use, non-pyrogenic	Sarstedt
Syrenges		
10 mL and 20 mL	single-use	Braun
60 mL	single-use	Carl Roth GmbH

Table E.5: Utilities.

5.4 Kits

kits	distributor
CloneJET™	Fermentas
Dionex Standard Kit	ESA
NucleoSpin® Plasmid	Macherey-Nagel
NucleoSpin® Gel and PCR Clean-up	Macherey-Nagel
Roti®-Lumin	Carl Roth GmbH
SensiFAST™ SYBR & Fluorescein Kit	BIOLINE
SuperScript™ III First-Strand Synthesis System for RT-PCR	invitrogen™

Table E.6: Kits.

5.5 Equipment used in this study

equipment	distributor
AccuBlock™ digital dry bath	Labnet International
AAS-6300 atomic absorption spectrophotometer	Shimadzu Europe
Autoclave, Systec VX	Systec GmbH
Centrifuges	
Avanti™ J-25 Centrifuge Centrifuge5418	Eppendorf AG
Diode Array Spectrophotometer	Hawlett Packard
Electrophoresis Power Supply	BioRad
Fluorescence microscope, Zeiss Imager M1	Zeiss

Gene Pulser/MicroPulser Cuvettes 0.2 cm gap	BioRad
HABAEUS Multifuge3SR+	Thermo Electron LED GmbH
Ultracentrifuge Beckmann L7	Beckmann
Centrifuge rotors	
JLA 10.500	Beckmann
JA 20.000	Beckmann
TI 70	Beckmann
Certomat® BS-1	Sartorius Stesim Bioteck GmbH
Emulsiflex C3	Avestin
MicroPulser Electroporator	BioRad
Mini PROTEAN® Tetra Cell	BioRad
Mini Trans-Blot® Cell	BioRad
pioloform coated copper grids	Plano
Pipetman (P2, P20, P100, P200, P1000)	Gilson
Power Source 250 V	vwr
Thermomixer Comfort	Vaudaux-Eppendorf
Transmission Electron Microscope (LEO 912AB)	Zeiss
Typhoon Trio laser scanner	GE Healthcare
UHPLC- system (UltiMate 3000)	Thermo Fischer Scientific

Table E.7: Equipment used in this study.

6 Contributions by collaborating persons

Chapter A:
Electron micrographs of *V. cholerae* were taken by Dr. Sebastian Leptihn (Fig. A.1, A.4, A.5 and B.11).
Fig. B.12 was generated by Dr. Thomas Vorburger.
Chapter C:
The data depicted in Fig. B.23 was generated with the help of Dr. Birgit Flauger and Bernadette Geißel.

7 Financial Disclosure

The work featured in Chapter A & B was supported by a grant from the Velux Foundation. The Life Science Center of the University of Hohenheim financed the work of Chapter C.

List of Figures

List of Tables

Literature

[1] Alam, M., Hasan, N. A., Sadique, A., Bhuiyan, N. A., Ahmed, K. U., Nusrin, S., Nair, G. B., Siddique, A. K., Sack, R. B., Sack, D. A., Huq, A., and Colwell, R. R. **Seasonal cholera caused by *Vibrio cholerae* serogroups O1 and O139 in the coastal aquatic environment of Bangladesh**. *Applied and Environmental Microbiology*, **72**(6):4096–4104, June 2006.

[2] Alam, M., Sultana, M., Nair, G. B., Sack, R. B., Sack, D. A., Siddique, A. K., Ali, A., Huq, A., and Colwell, R. R. **Toxigenic *Vibrio cholerae* in the aquatic environment of Mathbaria, Bangladesh**. *Applied and Environmental Microbiology*, **72**(4):2849–2855, April 2006.

[3] Alam, M., Sultana, M., Nair, G. B., Siddique, A. K., Hasan, N. A., Sack, R. B., Sack, D. A., Ahmed, K. U., Sadique, A., Watanabe, H., Grim, C. J., Huq, A., and Colwell, R. R. **Viable but non-culturable *Vibrio cholerae* O1 in biofilms in the aquatic environment and their role in cholera transmission**. *Proceedings of the National Academy of Sciences*, **104**(45):17801–17806, November 2007.

[4] Alhasan, R. and Njus, D. **The epinephrine assay for superoxide: Why dopamine does not work**. *Analytical Biochemistry*, **381**(1):142–147, October 2008.

[5] Alverdy, J., Holbrook, C., Rocha, F., Seiden, L., Licheng, R., Wu, Musch, M., Chang, E., Ohman, D., and Suh, S. **Gut-derived sepsis occurs when the right pathogen with the right virulence genes meets the right host: evidence for *in vivo* virulence expression in *Pseudomonas aeruginosa***. *Annals of Surgery*, **232**(4):480–489, 2000.

[6] Archibald, F. ***Lactobacillus plantarum*, an organism not requiring iron.** *FEMS Microbiology Letters*, **19**(1):29–32, June 1983.

[7] Armitage, J. P. **Bacterial tactic responses**. In Poole, R., editor, *Advances in Microbial Physiology*, **Volume 41**, pages 229–289. Academic Press, 1999.

[8] Armstrong, D. and Zidovetzki, R. **Id: wheel.pl,v 1.4 2009-10-20 21:23:36 don Exp**.

[9] Arslan, E., Schulz, H., Zufferey, R., Künzler, P., and Thöny-Meyer, L. **Overproduction of the *Bradyrhizobium japonicum* c-type cytochrome subunits of the *cbb3* oxidase in *Escherichia coli***. *Biochemical and Biophysical Research Communications*, **251**(3):744–747, October 1998.

[10] Asai, Y., Kawagishi, I., Sockett, R. E., and Homma, M. **Hybrid motor with H^+- and Na^+-driven components can rotate *Vibrio* polar flagella by using sodium ions**. *Journal of Bacteriology*, **181**(20):6332–6338, October 1999.

[11] Asai, Y., Shoji, T., Kawagishi, I., and Homma, M. **Cysteine-scanning mutagenesis of the periplasmic loop regions of PomA, a putative channel component of the sodium-driven flagellar motor in *Vibrio alginolyticus***. *Journal of Bacteriology*, **182**(4):1001–1007, February 2000.

[12] Asai, Y., Yakushi, T., Kawagishi, I., and Homma, M. **Ion-coupling determinants of Na^+-driven and H^+-driven flagellar motors**. *Journal of Molecular Biology*, **327**(2):453–463, March 2003.

[13] Bakeeva, L. E., Chumakov, K. M., Drachev, A. L., Metlina, A. L., and Skulachev, V. P. **The sodium cycle. III. *Vibrio alginolyticus* resembles *Vibrio cholerae* and some other vibriones by flagellar motor and ribosomal 5S-RNA structures.** *Biochimica et Biophysica Acta*, **850**(3):466–472, July 1986.

[14] Baker, M. D., Wolanin, P. M., and Stock, J. B. **Signal transduction in bacterial chemotaxis.** *Bioessays*, **28**(1):9–22, January 2006.

[15] Barik, S. **Site-directed mutagenesis by double polymerase chain reaction : megaprimer method.** *Methods in Molecular Biology*, **15**:277–286, February 1993.

[16] Barquera, B., Hellwig, P., Zhou, W., Morgan, J. E., Häse, C. C., Gosink, K. K., Nilges, M., Bruesehoff, P. J., Roth, A., Lancaster, C. R. D., and Gennis, R. B. **Purification and characterization of the recombinant Na^+-translocating NADH:quinone oxidoreductase from *Vibrio cholerae*.** *Biochemistry*, **41**(11):3781–3789, February 2002.

[17] Bartolomucci, A. **Social stress, immune functions and disease in rodents.** *Frontiers in Neuroendocrinology*, **28**(1):28–49, April 2007.

[18] Bearson, B. L. and Bearson, S. M. D. **The role of the QseC quorum-sensing sensor kinase in colonization and norepinephrine-enhanced motility of *Salmonella enterica* Serovar Typhimurium.** *Microbial Pathogenesis*, **44**(4):271–278, April 2008.

[19] Bearson, B. L., Bearson, S. M. D., Lee, I. S., and Brunelle, B. W. **The *Salmonella enterica* Serovar Typhimurium QseB response regulator negatively regulates bacterial motility and swine colonization in the absence of the QseC sensor kinase.** *Microbial Pathogenesis*, **48**(6):214–219, June 2010.

[20] Belay, T. and Sonnenfeld, G. **Differential effects of catecholamines on *in vitro* growth of pathogenic bacteria.** *Life Sciences*, **71**(4):447–456, June 2002.

[21] Bentivoglio, M. and Pacini, P. **Filippo Pacini: A determined observer**. *Brain Research Bulletin*, **38**(2):161–165, 1995.

[22] Berg, H. C. **Dynamic properties of bacterial flagellar motors.** *Nature*, **249**(452):77–79, May 1974.

[23] Berg, H. C. **The rotary motor of bacterial flagella.** *Annual Review of Biochemistry*, **72**(1):19–54, June 2003.

[24] Berg, H. C. **Swarming motility: It better be wet.** *Current Biology*, **15**(15):599–600, August 2005.

[25] Blair, D. F. and Berg, H. C. **The MotA protein of *Escherichia coli* is a proton-conducting component of the flagellar motor.** *Cell*, **60**(3):439–449, February 1990.

[26] Braun, T. F., Al-Mawsawi, L. Q., Kojima, S., and Blair, D. F. **Arrangement of core membrane segments in the MotA/MotB proton-channel complex of *Escherichia coli*.** *Biochemistry*, **43**(1):35–45, December 2003.

[27] Braun, T. F. and Blair, D. F. **Targeted disulfide cross-linking of the MotB protein of *Escherichia coli*: Evidence for two H^+ channels in the stator complex.** *Biochemistry*, **40**(43):13051–13059, October 2001.

[28] Burnette, W. N. **AB5 ADP-ribosylating toxins: comparative anatomy and physiology.** *Structure*, **2**(3):151–158, March 1994.

[29] Burton, C. L., Chhabra, S. R., Swift, S., Baldwin, T. J., Withers, H., Hill, S. J., and Williams, P. **The growth response of *Escherichia coli* to neurotransmitters and related catecholamine drugs requires a functional enterobactin biosynthesis and uptake system**. *Infection and Immunity*, **70**(11):5913–5923, November 2002.

[30] Butler, S. M. and Camilli, A. **Going against the grain: chemotaxis and infection in *Vibrio cholerae*.** *Nature Reviews. Microbiology*, **3**(8):611–620, August 2005.

[31] bvl. **Stellungnahme der ZKBS zur Risikobewertung von *Vibrio cholerae* O395-N1 als Spender- oder Empfängerorganismus bei gentechnischen Arbeiten gemäß§Absatz 1 GenTSV.**, Februar 2010.

[32] Cameron, D. E., Urbach, J. M., and Mekalanos, J. J. **A defined transposon mutant library and its use in identifying motility genes in *Vibrio cholerae*.** *Proceedings of the National Academy of Sciences*, **105**(25):8736–8741, June 2008.

[33] Casper-Lindley, C. and Yildiz, F. H. **VpsT is a transcriptional regulator required for expression of *vps* biosynthesis genes and the development of rugose colonial morphology in *Vibrio cholerae* O1 El Tor.** *Journal of Bacteriology*, **186**(5):1574–1578, March 2004.

[34] Chiavelli, D. A., Marsh, J. W., and Taylor, R. K. **The mannose-sensitive hemagglutinin of *Vibrio cholerae* promotes adherence to zooplankton.** *Applied and Environmental Microbiology*, **67**(7):3220–3225, July 2001.

[35] Clarke, M. B., Hughes, D. T., Zhu, C., Boedeker, E. C., and Sperandio, V. **The QseC sensor kinase: A bacterial adrenergic receptor**. *Proceedings of the National Academy of Sciences*, **103**(27):10420–10425, July 2006.

[36] Collins, K. D. **Ions from the Hofmeister series and osmolytes: effects on proteins in solution and in the crystallization process**. *Methods*, **34**(3):300–311, November 2004.

[37] Colwell, R. R. **Global climate and infectious disease: The cholera paradigm.** *Science*, **274**(5295):2025–2031, December 1996.

[38] Colwell, R. R., Brayton, P. R., Grimes, D. J., Roszak, D. B., Huq, S. A., and Palmer, L. M. **Viable but non-culturable *Vibrio cholerae* and related pathogens in the environment: Implications for release of genetically engineered microorganisms**. *Nature Biotechnology*, **3**(9):817–820, September 1985.

[39] Correa, N. E., Peng, F., and Klose, K. E. **Roles of the regulatory proteins FlhF and FlhG in the *Vibrio cholerae* flagellar transcription hierarchy.** *Journal of Bacteriology*, **187**(18):6324–6332, September 2005.

[40] Costerton, J. W., Cheng, K. J., Geesey, G. G., Ladd, T. I., Nickel, J. C., Dasgupta, M., and Marrie, T. J. **Bacterial biofilms in nature and disease.** *Annual Review of Microbiology*, **41**(1):435–464, October 1987.

[41] Costerton, J. W., Lewandowski, Z., Caldwell, D. E., Korber, D. R., and Lappin-Scott, H. M. **Microbial biofilms.** *Annual Review of Microbiology*, **49**(1):711–745, October 1995.

[42] Dao-Thi, M.-H., Van Melderen, L., De Genst, E., Buts, L., Ranquin, A., Wyns, L., and Loris, R. **Crystallization of CcdB in complex with a GyrA fragment**. *Acta Crystallographica D*, **60**(6):1132–1134, June 2004.

[43] de Kievit, T. R. and Iglewski, B. H. **Bacterial quorum sensing in pathogenic relationships**. *Infection and Immunity*, **68**(9):4839–4849, September 2000.

[44] Dehio, C. and Meyer, M. **Maintenance of broad-host-range incompatibility group P and group Q plasmids and transposition of Tn5 in *Bartonella henselae* following conjugal plasmid transfer from *Escherichia coli*.** *Journal of Bacteriology*, **179**(2):538–540, January 1997.

[45] Dethlefsen, L., McFall-Ngai, M., and Relman, D. A. **An ecological and evolutionary perspective on human-microbe mutualism and disease.** *Nature*, **449**(7164):811–818, October 2007.

[46] Dhalla, K., Pallab, K., Rupp, H., RE, B., and NS, D. **Measurement of adrenolutin as an oxidation product of catecholamines in plasma.** *Molecular and Cellular Biochemistry*, **87**(1):85–92, May 1989.

[47] Dimroth, P. **Primary sodium ion translocating enzymes.** *Biochimica et Biophysica Acta (BBA) - Bioenergetics*, **1318**(1–2):11–51, January 1997.

[48] Durham-Colleran, M., Verhoeven, A., and Hoek, M. ***Francisella novicida* forms *in vitro* biofilms mediated by an orphan response regulator**. *Microbial Ecology*, **59**(3):457–465, 2010.

[49] Dzioba, J., Ostroumov, E., Winogrodzki, A., and Dibrov, P. **Cloning, functional expression in *Escherichia coli* and primary characterization of a new NA^+/H^+ antiporter, NhaD, of *Vibrio cholerae***. *Molecular and Cellular Biochemistry*, **229**(1-2):119–124, January 2002.

[50] Fenchel, T. **Microbial behavior in a heterogeneous world**. *Science*, **296**(5570):1068–1071, May 2002.

[51] Ferrières, L., Hèmery, G., Nham, T., Guèrout, A.-M., Mazel, D., Beloin, C., and Ghigo, J.-M. **Silent mischief: Bacteriophage Mu insertions contaminate products of *Escherichia coli* random mutagenesis performed using suicidal transposon delivery plasmids mobilized by broad-host-range RP4 conjugative machinery**. *Journal of Bacteriology*, **192**(24):6418–6427, December 2010.

[52] Finkelstein, R. A. *Cholera,* Vibrio cholerae *O1 and O139, and other pathogenic* Vibrios. Medical Microbiology., Galveston (TX): University of Texas Medical Branch at Galveston, 4th edition edition, 1996.

[53] for Disease Control, C. and Prevention. **Watch: Level1, Practice usual Precautions, Cholera in Haiti**, April 2013.

[54] Freestone, P. P., Williams, P. H., Haigh, R. D., Maggs, A. F., Neal, C. P., and Lyte, M. **Growth stimulation of intestinal commensal *Escherichia coli* by catecholamines: A possible contributory factor in trauma-induced sepsis**. *Shock*, **18**(5):465–470, November 2002.

[55] Freestone, P. P. E., Haigh, R. D., and Lyte, M. **Specificity of catecholamine-induced growth in *Escherichia coli* O157:H7, *Salmonella enterica* and *Yersinia enterocolitica***. *FEMS Microbiology Letters*, **269**(2):221–228, April 2007.

[56] Freestone, P. P. E., Lyte, M., Neal, C. P., Maggs, A. F., Haigh, R. D., and Williams, P. H. **The mammalian neuroendocrine hormone norepinephrine supplies iron for bacterial growth in the presence of transferrin or lactoferrin**. *Journal of Bacteriology*, **182**(21):6091–6098, November 2000.

[57] Freestone, P. P., Haigh, R. D., Williams, P. H., and Lyte, M. **Stimulation of bacterial growth by heat-stable, norepinephrine-induced autoinducers**. *FEMS Microbiology Letters*, **172**(1):53–60, March 1999.

[58] Friedlander, R. S., Vlamakis, H., Kim, P., Khan, M., Kolter, R., and Aizenberg, J. **Bacterial flagella explore microscale hummocks and hollows to increase adhesion**. *Proceedings of the National Academy of Sciences*, **110**(14):5624–5629, April 2013.

[59] Fukuoka, H., Wada, T., Kojima, S., Ishijima, A., and Homma, M. **Sodium-dependent dynamic assembly of membrane complexes in sodium-driven flagellar motors**. *Molecular Microbiology*, **71**(4):825–835, February 2009.

[60] Fukuoka, H., Yakushi, T., Kusumoto, A., and Homma, M. **Assembly of motor proteins, PomA and PomB, in the Na^+-driven stator of the flagellar motor**. *Journal of Molecular Biology*, **351**(4):707–717, August 2005.

[61] Galloway, T. S. and van Heyningen, S. **Binding of NAD^+ by cholera toxin.** *Biochemical Journal*, **244**(1):225–230, May 1987.

[62] Gardel, C. L. and Mekalanos, J. J. **Alterations in *Vibrio cholerae* motility phenotypes correlate with changes in virulence factor expression.** *Infection and Immunity*, **64**(6):2246–2255, June 1996.

[63] Gosink, K. K. and Häse, C. C. **Requirements for conversion of the Na^+-driven flagellar motor of *Vibrio cholerae* to the H^+-driven motor of *Escherichia coli***. *Journal of Bacteriology*, **182**(15):4234–4240, August 2000.

[64] Gray-Owen, S. D. and Schyvers, A. B. **Bacterial transferrin and lactoferrin receptors**. *Trends in Microbiology*, **4**(5):185–191, May 1996.

[65] Halang, P., Leptihn, S., Meier, T., Vorburger, T., and Steuber, J. **The function of the Na^+-driven flagellum of *Vibrio cholerae* is determined by osmolality and pH**. *Journal of Bacteriology*, **195**(21):4888–4899, November 2013.

[66] Hall, T. A. **BioEdit: a user-friendly biological sequence alignment editor and analysis program for Windows 95/98/NT**. *Nucleic Acids Symposium Series*, **41**:95–98, 1999.

[67] Halpern, M., Gancz, H., Broza, M., and Kashi, Y. ***Vibrio cholerae* hemagglutinin/protease degrades chironomid egg masses**. *Applied and Environmental Microbiology*, **69**(7):4200–4204, July 2003.

[68] Hammer, B. K. and Bassler, B. L. **Quorum sensing controls biofilm formation in *Vibrio cholerae***. *Molecular Microbiology*, **50**(1):101–104, October 2003.

[69] Hanahan, D. **Studies on transformation of *Escherichia coli* with plasmids**. *Journal of Molecular Biology*, **166**(4):557–580, June 1983.

[70] Häse, C. C. and Barquera, B. **Role of sodium bioenergetics in *Vibrio cholerae***. *Biochimica et Biophysica Acta (BBA) - Bioenergetics*, **1505**(1):169–178, May 2001.

[71] Häse, C. C., Fedorova, N. D., Galperin, M. Y., and Dibrov, P. A. **Sodium ion cycle in bacterial pathogens: Evidence from cross-genome comparisons**. *Microbiology and Molecular Biology Reviews*, **65**(3):353–370, September 2001.

[72] Häse, C. C. and Mekalanos, J. J. **TcpP protein is a positive regulator of virulence gene expression in *Vibrio cholerae***. *Proceedings of the National Academy of Sciences*, **95**(2):730–734, January 1998.

[73] Häse, C. C. and Mekalanos, J. J. **Effects of changes in membrane sodium flux on virulence gene expression in *Vibrio cholerae***. *Proceedings of the National Academy of Sciences*, **96**(6):3183–3187, March 1999.

[74] Hedge, M., Wood, T. K., and Jayaraman, A. **The neuroendocrine hormone norepinephrine increases *Pseudomonas aeruginosa* PA14 virulence through the las quorum-sensing pathway**. *Applied Microbiology and Biotechnology*, **84**(4):763–776, June 2009.

[75] Heidelberg, J. F., Eisen, J. A., Nelson, W. C., Clayton, R. A., Gwinn, M. L., Dodson, R. J., Haft, D. H., Hickey, E. K., Peterson, J. D., Umayam, L., Gill, S. R., Nelson, K. E., Read, T. D., Tettelin, H., Richardson, D., Ermolaeva, M. D., Vamathevan, J., Bass, S., Qin, H., Dragoi, I., Sellers, P., McDonald, L., Utterback, T., Fleishmann, R. D., Nierman, W. C., White, O., Salzberg, S. L., Smith, H. O., Colwell, R. R., Mekalanos, J. J., Venter, J. C., and Fraser, C. M. **DNA sequence of both chromosomes of the cholera pathogen *Vibrio cholerae***. *Nature*, **406**(6795):477–483, August 2000.

[76] Henikoff, S. and Henikoff, J. G. **Amino acid substitution matrices from protein blocks**. *Proceedings of the National Academy of Sciences*, **89**(22):10915–10919, November 1992.

[77] Henry, J. P. **Biological basis of the stress response**. *Integrative Physiological and Behavioral Science*, **27**(1):66–83, January–March 1992.

[78] Herz, K., Vimont, S., Padan, E., and Berche, P. **Roles of NhaA, NhaB, and NhaD Na^+/H^+ antiporters in survival of *Vibrio cholerae* in a saline environment**. *Journal of Bacteriology*, **185**(4):1236–1244, February 2003.

[79] Hinghofer-Szalkay, H. *Praktische Physiologie Funktionen des menschlichen Körpers*. Blackwell Wissenschaft Verlag, 1999.

[80] Hof, H., örries, R., and Geginat, G. *Duale Reihe: Medizinische Mikrobiologie*. Thieme Verlag, Stuttgart, 2009.

[81] Holmgren, J. **Actions of cholera toxin and the prevention and treatment of cholera**. *Nature*, **292**(5822):413–417, July 1981.

[82] Howard-Jones, N. **Robert Koch and the cholera vibrio: a centenary**. *British Medical Journal (Clinical Resaearch Ed.)*, **288**(6414):379–381, February 1984.

[83] Hughes, D. T. and Sperandio, V. **Inter-kingdom signalling: communication between bacteria and their hosts**. *Nature Reviews Microbiology*, **6**(2):111–120, February 2008.

[84] Huq, A., Small, E. B., West, P. A., Huq, M. I., Rahman, R., and Colwell, R. R. **Ecological relationships between *Vibrio cholerae* and planktonic crustacean copepods.** *Applied Environmental Microbiology*, **45**(1):275–283, January 1983.

[85] Imae, Y. and Atsumi, T. **Na^+-driven bacterial flagellar motors**. *Journal of Bioenergetics and Biomembranes*, **21**(6):705–16, December 1989.

[86] Inglis, T. J. J., Robertson, T., Woods, D. E., Dutton, N., and Chang, B. J. **Flagellum-mediated adhesion by *Burkholderia pseudomallei* precedes invasion of *Acanthamoeba astronyxis***. *Infection and Immunity*, **71**(4):2280–2282, April 2003.

[87] International Centre for Diarrhoeal Diseases Research, C. W. G. Bangladesh, Albert, M. J., Ansaruzzaman, M., Bardhan, P. K., Faruque, A. S. G., Faruque, S. M., Islam, M. S., Mahalanabis, D., Sack, R. B., Salam, M. A., Siddique, A. K., Yunus, M. D., and Zaman, K. **Large epidemic of cholera-like disease in Bangladesh caused by *Vibrio cholerae* 0139 synonym Bengal**. *The Lancet*, **342**(8868):387–390, August 1993.

[88] Islam, M. S., Mahmuda, S., Morshed, M. G., Bakht, H. B. M., Khan, M. N. H., Sack, R. B., and Sack, D. A. **Role of cyanobacteria in the persistence of *Vibrio cholerae* O139 in saline microcosms**. *Canadian Journal of Microbiology*, **50**(2):127–131, February 2004.

[89] Jobling, M. G. and Holmes, R. K. **Characterization of *hapR*, a positive regulator of the *Vibrio cholerae* HA/protease gene *hap*, and its identification as a functional homologue of the *Vibrio harveyi luxR* gene**. *Molecular Microbiology*, **26**(5):1023–1034, December 1997.

[90] Johnson, J. A., Panigrahi, P., and Morris Jr., J. G. **Non-O1 *Vibrio cholerae* NRT36S produces a polysaccharide capsule that determines colony morphology, serum resistance, and virulence in mice**. *Infection and Immunity*, **60**(3):864–869, March 1992.

[91] Johnson, J. A., Salles, C. A., Panigrahi, P., Albert, M. J., Wright, A. C., Johnson, R. J., and Morris Jr., J. G. ***Vibrio cholerae* O139 synonym Bengal is closely related to *Vibrio cholerae* El Tor but has important differences**. *Infection and Immunity*, **62**(5):2108–2110, May 1994.

[92] Kaper, J. B., Morris, J. G., and Levine, M. M. **Cholera.** *Clinical Microbiology Reviews*, **8**(1):48–86, January 1995.

[93] Kaper, J. B. and Sperandio, V. **Bacterial cell-to-cell signaling in the gastrointestinal tract**. *Infection and Immunity*, **73**(6):3197–3209, June 2005.

[94] Karaolis, D. K. R., Johnson, J. A., Bailey, C. C., Boedeker, E. C., Kaper, J. B., and Reeves, P. R. **A *Vibrio cholerae* pathogenicity island associated with epidemic and pandemic strains**. *Proceedings of the National Academy of Sciences*, **95**(6):3134–3139, March 1998.

[95] Kelley, L. A. and Sternberg, M. J. E. **Protein structure prediction on the Web: a case study using the Phyre server**. *Nature protocols*, **4**(3):363–371, February 2009.

[96] Khajanchi, B. K., Kozlova, E. V., Sha, J., Popov, V. L., and Chopra, A. K. **The two-component QseBC signalling system regulates *in vitro* and *in vivo* virulence of *Aeromonas hydrophila***. *Microbiology*, **158**(1):259–271, January 2012.

[97] Kim, E. A., Price-Carter, M., Carlquist, W. C., and Blair, D. F. **Membrane Segment Organization in the Stator Complex of the Flagellar Motor: Implications for Proton Flow and Proton-Induced Conformational Change**. *Biochemistry*, **47**(43):11332–11339, October 2008.

[98] Kinney, K. S., Austin, C. E., Morton, D. S., and Sonnenfeld, G. **Norepinephrine as a growth stimulating factor in bacteria–mechanistic studies**. *Life Sciences*, **67**(25):3075–3085, November 2000.

[99] Klose, K. E. and Mekalanos, J. J. **Distinct roles of an alternative sigma factor during both free-swimming and colonizing phases of the *Vibrio cholerae* pathogenic cycle**. *Molecular Microbiology*, **28**(3):501–520, April 1998.

[100] Kogure, K. **Bioenergetics of marine bacteria**. *Current Opinion in Biotechnology*, **9**(3):278–282, June 1998.

[101] Kojima, S., Shoji, T., Asai, Y., Kawagishi, I., and Homma, M. **A slow-motility phenotype caused by substitutions at residue Asp31 in the PomA channel component of a sodium-driven flagellar motor**. *Journal of Bacteriology*, **182**(11):3314–3318, June 2000.

[102] Kojima, S., Yamamoto, K., Kawagishi, I., and Homma, M. **The polar flagellar motor of *Vibrio cholerae* is driven by an Na^+ motive force**. *Journal of Bacteriology*, **181**(6):1927–1930, March 1999.

[103] Komeda, Y., Kutsukake, K., and Iino, T. **Definition of additional flagellar genes in *Escherichia coli* K12**. *Genetics*, **94**(2):277–290, February 1980.

[104] Kopin, I., Zukowska-Grojec, M. Z nd Bayorh, and Goldstein, D. **Estimation of intrasynaptic norepinephrine concentrations at vascular neuroeffector junctions *in vivo*.** *Naunyn-Schmiedeberg's Archives of Pharmacology*, **325**(4):298–305, April 1984.

[105] Kovach, M. E., Shaffer, M. D., and Peterson, K. M. **A putative integrase gene defines the distal end of a large cluster of ToxR-regulated colonization genes in *Vibrio cholerae***. *Microbiology*, **142**(8):2165–2174, August 1996.

[106] Krah, A., Pogoryelov, D., Langer, J. D., Bond, P. J., Meier, T., and Faraldo-Gómez, J. D. **Structural and energetic basis for H^+ versus Na^+ binding selectivity in ATP synthase F_o rotors**. *Biochimica et Biophysica Acta (BBA) - Bioenergetics*, **1797**(6–7):763–772, June 2010.

[107] Krah, A., Pogoryelov, D., Meier, T., and Faraldo-Gómez, J. D. **On the Structure of the Proton-Binding Site in the F_o Rotor of Chloroplast ATP Synthases**. *Journal of Molecular Biology*, **395**(1):20–27, January 2010.

[108] Krewulak, K. D. and Vogel, H. J. **Structural biology of bacterial iron uptake**. *Biochimica et Biophysica Acta (BBA) - Biomembranes*, **1778**(9):1781–1804, September 2008.

[109] Kutsukake, K., Ohya, Y., Yamaguchi, S., and Iino, T. **Operon structure of flagellar genes in *Salmonella typhimurium***. *Molecular and General Genetics MGG*, **214**(1):11–15, September 1988.

[110] Lagergard, T., Purvén, M., and Frisk, A. **Evidence of *Haemophilus ducreyi* adherence to and cytotoxin destruction of human epithelial cells**. *Microbial Pathogenesis*, **14**(6):417–431, June 1993.

[111] Lauriano, C. M., Ghosh, C., Correa, N. E., and Klose, K. E. **The sodium-driven flagellar motor controls exopolysaccharide expression in *Vibrio cholerae***. *Journal of Bacteriology*, **186**(15):4864–4874, August 2004.

[112] Le Roux, F., Binesse, J., Saulnier, D., and Mazel, D. **Construction of a *Vibrio splendidus* mutant lacking the metalloprotease gene *vsm* by use of a novel counterselectable suicide vector**. *Applied and Environmental Microbiology*, **73**(3):777–784, 2007.

[113] Leake, M. C., Chandler, J. H., Wadhams, G. H., Bai, F., Berry, R. M., and Armitage, J. P. **Stoichiometry and turnover in single, functioning membrane protein complexes**. *Nature*, **443**(7109):355–358, September 2006.

[114] Leinhardt, D., Arnold, J., Shipley, K. A., Mughal, M., RA, L., and Irving, M. **Plasma NE concentrations do not accurately reflect sympathetic nervous system activity in human sepsis.** *American Journal of Physiology*, **265**(2):284–288, August 1993.

[115] Lenard, J. **Mammalian hormones in microbial cells**. *Trends in Biochemical Sciences*, **17**(4):147–150, April 1992.

[116] LeRoith, D., Shiloach, J., Roth, J., and Lesniak, M. A. **Insulin or a closely related molecule is native to *Escherichia coli***. *The Journal of biological chemistry*, **256**(13):6533–6536, July 1981.

[117] Letunic, I., Doerks, T., and Bork, P. **SMART 7: recent updates to the protein domain annotation resource**. *Nucleic Acids Research*, **40**(D1):D302–D305, January 2012.

[118] Li, L., Xu, Z., Zhou, Y., Sun, L., Liu, Z., Chen, H., and Zhou, R. **Global Effects of Catecholamines on *Actinobacillus pleuropneumoniae* Gene Expression**. *PLoS ONE*, **7**(2):e31121, February 2012.

[119] Li, N., Kojima, S., and Homma, M. **Characterization of the periplasmic region of PomB, a Na^+-driven flagellar stator protein in *Vibrio alginolyticus***. *Journal of Bacteriology*, **193**(15):3773–3784, August 2011.

[120] Li, W., Lyte, M., Freestone, P. P., Ajmal, A., Colmer-Hamood, J. A., and Hamood, A. N. **Norepinephrine represses the expression of *toxA* and the siderophore genes in *Pseudomonas aeruginosa***. *FEMS Microbiology Letters*, **299**(1):100–109, October 2009.

[121] Lin, P., Türk, K., Häse, C. C., Fritz, G., and Steuber, J. **Quinone Reduction by the Na^+-Translocating NADH Dehydrogenase Promotes Extracellular Superoxide Production in *Vibrio cholerae***. *Journal of Bacteriology*, **189**(10):3902–3908, May 2007.

[122] Lindl, T. *Zell und Gewebekultur*. Spektrum Akademischer Verlag, 2002.

[123] Liu, J., Lin, T., Botkin, D. J., McCrum, E., Winkler, H., and Norris, S. J. **Intact flagellar motor of *Borrelia burgdorferi* revealed by cryo-electron tomography: Evidence for stator ring curvature and rotor/c-ring assembly flexion**. *Journal of Bacteriology*, **191**(16):5026–5036, August 2009.

[124] Lloyd, S. A., Whitby, F. G., Blair, D. F., and Hill, C. P. **Structure of the C-terminal domain of FliG, a component of the rotor in the bacterial flagellar motor**. *Nature*, **400**(6743):472–475, July 1999.

[125] Lux, R., Munasinghe, V. R. N., Castellano, F., Lengeler, J. W., Corrie, J. E. T., and Khan, S. **Elucidation of a PTS-carbohydrate chemotactic signal pathway in *Escherichia coli* using a time-resolved behavioral assay**. *Molecular Biology of the Cell*, **10**(4):1133–1146, April 1999.

[126] Lyte, M. **Microbial endocrinology and infectious disease in the 21st century**. *Trends in Microbiology*, **12**(1):14–20, January 2004.

[127] Lyte, M. and Bailey, M. T. **Neuroendocrine–Bacterial Interactions in a Neurotoxin-Induced Model of Trauma**. *Journal of Surgical Research*, **70**(2):195–201, July 1997.

[128] Lyte, M. and Ernst, S. **Catecholamine induced growth of gram negative bacteria**. *Life Sciences*, **50**(3):203–212, November 1992.

[129] Macnab, R. M. **How bacteria assemble flagella.** *Annual Review of Microbiology*, **57**(1):77–100, October 2003.

[130] Magariyama, Y., Sugiyama, S., Muramoto, K., Maekawa, Y., Kawagishi, I., Imae, Y., and Kudo, S. **Very fast flagellar rotation**. *Nature*, **371**(6500):752–752, October 1994.

[131] Martinez, R. M., Jude, B. A., Kirn, T. J., Skorupski, K., and Taylor, R. K. **Role of FlgT in anchoring the flagellum of *Vibrio cholerae***. *Journal of Bacteriology*, **192**(8):2085–2092, April 2010.

[132] McCarter, L., Hilmen, M., and Silverman, M. **Flagellar dynamometer controls swarmer cell differentiation of *Vibrio parahaemolyticus***. *Cell*, **54**(3):345–351, July 1988.

[133] McCarter, L. L. **MotX, the channel component of the sodium-type flagellar motor.** *Journal of Bacteriology*, **176**(19):5988–5998, October 1994.

[134] McCarter, L. L. **MotY, a component of the sodium-type flagellar motor.** *Journal of Bacteriology*, **176**(14):4219–4225, July 1994.

[135] McCarter, L. L. **Polar flagellar motility of the *Vibrionaceae***. *Microbiology and Molecular Biology Reviews*, **65**(3):445–462, September 2001.

[136] McCarter, L. L. **Regulation of flagella**. *Current Opinion in Microbiology*, **9**(2):180–186, April 2006.

[137] McLeod, S. M., Kimsey, H. H., Davis, B. M., and Waldor, M. K. **CTXΦ and *Vibrio cholerae*: exploring a newly recognized type of phage-host cell relationship**. *Molecular Microbiology*, **57**(2):347–356, July 2005.

[138] Meier, T., Krah, A., Bond, P. J., Pogoryelov, D., Diederichs, K., and Faraldo-Gómez, J. D. **Complete ion-coordination structure in the rotor ring of Na^+-dependent F-ATP synthases**. *Journal of Molecular Biology*, **391**(2):498–507, August 2009.

[139] Meier, T., Polzer, P., Diederichs, K., Welte, W., and Dimroth, P. **Structure of the rotor ring of F-type Na^+-ATPase from *Ilyobacter tartaricus***. *Science*, **308**(5722):659–662, April 2005.

[140] Meier, T., Matthey, U., von Ballmoos, C., Vonck, J., Krug von Nidda, T., KÃijhlbrandt, W., and Dimroth, P. **Evidence for structural integrity in the undecameric c-rings isolated from sodium ATP synthases**. *Journal of Molecular Biology*, **325**(2):389–397, January 2003.

[141] Mekalanos, J. J., Collier, R. J., and Romig, W. R. **Enzymic activity of cholera toxin. II. Relationships to proteolytic processing, disulfide bond reduction, and subunit composition.** *Journal of Biological Chemistry*, **254**(13):5855–5861, July 1979.

[142] Mekalanos, J. J., Swartz, D. J., Pearson, G. D., Harford, N., Groyne, F., and de Wilde, M. **Cholera toxin genes: nucleotide sequence, deletion analysis and vaccine development.** *Nature*, **306**(5943):551–557, 1983.

[143] Merighi, M., Septer, A., Carroll-Portillo, A., Bhatiya, A., Porwollik, S., McClelland, M., and Gunn, J. **Genome-wide analysis of the PreA/PreB (QseB/QseC) regulon of *Salmonella enterica* Serovar Typhimurium**. *BMC Microbiology*, **9**(1):42, 2009.

[144] Miethke, M. and Skerra, A. **Neutrophil gelatinase-associated lipocalin expresses antimicrobial activity by interfering with l-norepinephrine-mediated bacterial iron acquisition**. *Antimicrobial Agents and Chemotherapy*, **54**(4):1580–1589, April 2010.

[145] Minamino, T., Imada, K., and Namba, K. **Mechanisms of type III protein export for bacterial flagellar assembly**. *Molecular BioSystems*, **4**(11):1105–1115, November 2008.

[146] Minamino, T., Imada, K., and Namba, K. **Molecular motors of the bacterial flagella**. *Current Opinion in Structural Biology*, **18**(6):693–701, December 2008.

[147] Minato, Y., Fassio, S. R., Kirkwood, J. S., Halang, P., Quinn, M. J., Faulkner, W. J., Aagesen, A. M., Steuber, J., Stevens, J. F., and Häse, C. C. **Roles of the sodium-translocationd NADH-quinone oxidoreductase (NQR) on *Vibrio cholerae* metabolism, motility and osmotic stress resistance**. *PLoS ONE*, under submission.

[148] Miroux, B. and Walker, J. E. **Over-production of proteins in *Escherichia coli*: Mutant hosts that allow synthesis of some membrane proteins and globular proteins at high levels**. *Journal of Molecular Biology*, **260**(3):289–298, July 1996.

[149] Misra, H. P. and Fridovich, I. **The Role of Superoxide Anion in the Autoxidation of Epinephrine and a Simple Assay for Superoxide Dismutase**. *Journal of Biological Chemistry*, **247**(10):3170–3175, May 1972.

[150] Moens, S. and Vanderleyden, J. **Functions of bacterial flagella**. *Critical Reviews in Microbiology*, **22**(2):67–100, January 1996.

[151] Moreira, C. G. and Sperandio, V. **Interplay between the QseC and QseE Bacterial Adrenergic Sensor Kinases in *Salmonella enterica* Serovar Typhimurium Pathogenesis**. *Infection and Immunity*, **80**(12):4344–4353, December 2012.

[152] Moreira, C. G., Weinshenker, D., and Sperandio, V. **QseC mediates *Salmonella enterica* Serovar Typhimurium virulence *in vitro* and *in vivo***. *Infection and Immunity*, **78**(3):914–926, March 2010.

[153] Moss, J. and Vaughan, M. **Activation of cholera toxin and *Escherichia coli* heat-labile enterotoxins by ADP-ribosylation factors, a family of 20 kDa guanine nucleotide-binding proteins**. *Molecular Microbiology*, **5**(11):2621–2627, November 1991.

[154] Mulkidjanian, A. Y., Dibrov, P., and Galperin, M. Y. **The past and present of sodium energetics: May the sodium-motive force be with you**. *Biochimica et Biophysica Acta (BBA) - Bioenergetics*, **1777**(7–8):985–992, July 2008.

[155] Nakano, M., Takahashi, A., Sakai, Y., Kawano, M., Harada, N., Mawatari, K., and Nakaya, Y. **Catecholamine-induced stimulation of growth in *Vibrio* species**. *Letters in Applied Microbiology*, **44**(6):649–653, June 2007.

[156] Njoroge, J. and Sperandio, V. **Enterohemorrhagic *Escherichia coli* virulence regulation by two bacterial adrenergic kinases, QseC and QseE**. *Infection and Immunity*, **80**(2):688–703, February 2012.

[157] Novak, E. A., Shao, H., Daep, C. A., and Demuth, D. R. **Autoinducer-2 and QseC control biofilm formation and *in vivo* virulence of *Aggregatibacter actinomycetemcomitans***. *Infection and Immunity*, **78**(7):2919–2926, July 2010.

[158] Ochman, H., Lawrence, J. G., and Groisman, E. A. **Lateral gene transfer and the nature of bacterial innovation**. *Nature*, **405**(6784):299–304, May 2000.

[159] Ochs, S. D., Westfall, T. C., and Macarthur, H. **The separation and quantification of aminochromes using high-pressure liquid chromatography with electrochemical detection**. *Journal of Neuroscience Methods*, **142**(2):201–208, March 2005.

[160] O'Donnell, P. M., Aviles, H., Lyte, M., and Sonnenfeld, G. **Enhancement of *in vitro* growth of pathogenic bacteria by norepinephrine: importance of inoculum density and role of transferrin**. *Applied and Environmental Microbiology*, **72**(7):5097–5099, July 2006.

[161] Ottemann, K. M. and Miller, J. F. **Roles for motility in bacterial-host interactions**. *Molecular Microbiology*, **24**(6):1109–1117, June 1997.

[162] Padan, E., Bibi, E., Ito, M., and Krulwich, T. A. **Alkaline pH homeostasis in bacteria: New insights**. *Biochimica et Biophysica Acta (BBA) - Biomembranes*, **1717**(2):67–88, November 2005.

[163] Panda, D. K., Dasgupta, U., and Das, J. **Transformation of *Vibrio cholerae* by plasmid DNA**. *Gene*, **105**(1):107–111, August 1991.

[164] Pandey, A., Bringel, F., and Meyer, J.-M. **Iron requirement and search for siderophores in lactic acid bacteria**. *Applied Microbiology and Biotechnology*, **40**(5):735–739, 1994.

[165] Paulick, A., Koerdt, A., Lassak, J., Huntley, S., Wilms, I., Narberhaus, F., and Thormann, K. M. **Two different stator systems drive a single polar flagellum in *Shewanella oneidensis* MR-1**. *Molecular Microbiology*, **71**(4):836–850, February 2009.

[166] Pedelacq, J. D., Cabantous, S., Tran, T., Terwilliger, T. C., and Waldo, G. S. **Engineering and characterization of a superfolder green fluorescent protein**. *Nature Biotechnology*, **24**(1):79–88, January 2006.

[167] Peterson, J. W. and Ochoa, L. G. **Role of prostaglandins and cAMP in the secretory effects of cholera toxin**. *Science*, **245**(4920):857–859, August 1989.

[168] Pfaffl, M. W. **A new mathematical model for relative quantification in real-time RT–PCR**. *Nucleic Acids Research*, **29**(9):e45–e45, May 2001.

[169] Postma, P. W., Lengeler, J. W., and Jacobson, G. R. **Phosphoenolpyruvate:carbohydrate phosphotransferase systems of bacteria.** *Microbiological Reviews*, **57**(3):543–594, September 1993.

[170] Pratt, L. A. and Kolter, R. **Genetic analysis of *Escherichia coli* biofilm formation: roles of flagella, motility, chemotaxis and type I pili**. *Molecular Microbiology*, **30**(2):285–293, October 1998.

[171] Pullinger, G. D., van Diemen, P. M., Dziva, F., and Stevens, M. P. **Role of two-component sensory systems of *Salmonella enterica* Serovar Dublin in the pathogenesis of systemic salmonellosis in cattle**. *Microbiology*, **156**(10):3108–3122, October 2010.

[172] Resch, C. T., Winogrodzki, J. L., Patterson, C. T., Lind, E. J., Quinn, M. J., Dibrov, P., and Häse, C. C. **The putative Na^+/H^+ antiporter of *Vibrio cholerae*, Vc-NhaP2, mediates the specific K^+/H^+ exchange *in vivo***. *Biochemistry*, **49**(11):2520–2528, February 2010.

[173] Sambrook, J. and Russell, D. W. *Molecular Cloning: A laboratory manual, 3rd edition.* Cold Spring Harbor Laboratory Press, 2001.

[174] Sandrini, S. M., Shergill, R., Woodward, J., Muralikuttan, R., Haigh, R. D., Lyte, M., and Freestone, P. P. **Elucidation of the mechanism by which catecholamine stress hormones liberate iron from the innate immune defense proteins transferrin and lactoferrin**. *Journal of Bacteriology*, **192**(2):587–594, January 15, 2010.

[175] Sato, K. and Homma, M. **Functional reconstitution of the Na^+-driven polar flagellar motor component of *Vibrio alginolyticus***. *Journal of Biological Chemistry*, **275**(8):5718–5722, February 2000.

[176] Sattler, J., Schwarzmann, G., Knack, I., Röhm, K. H., and Wiegandt, H. **Studies of ligand binding to cholera toxin, III. Cooperativity of oligosaccharide binding.** *Hoppe Seyler's Zeitschrift für Physiologische Chemie*, **359**(6):719–723, June 1978.

[177] Schägger, H. and von Jagow, G. **Tricine-sodium dodecyl sulfate-polyacrylamide gel electrophoresis for the separation of proteins in the**

range from 1 to 100 kDa. *Analytical Biochemistry*, **166**(2):368–379, November 1987.

[178] Schrank, G. D. and Verwey, W. F. **Distribution of cholera organisms in experimental *Vibrio cholerae* infections: proposed mechanisms of pathogenesis and antibacterial immunity.** *Infection and Immunity*, **13**(1):195–203, January 1976.

[179] Schultz, J., Milpetz, F., Bork, P., and Ponting, C. P. **SMART, a simple modular architecture research tool: Identification of signaling domains**. *Proceedings of the National Academy of Sciences*, **95**(11):5857–5864, May 1998.

[180] Schulz, H., Fabianek, R. A., Pellicioli, E. C., Hennecke, H., and Thöny-Meyer, L. **Heme transfer to the heme chaperone CcmE during cytochrome c maturation requires the CcmC protein, which may function independently of the ABC-transporter CcmAB**. *Proceedings of the National Academy of Sciences*, **96**(11):6462–6467, May 1999.

[181] Sharp, L. L., Zhou, J., and Blair, D. F. **Features of MotA proton channel structure revealed by tryptophan-scanning mutagenesis**. *Proceedings of the National Academy of Sciences*, **92**(17):7946–7950, August 1995.

[182] Shea, M. E., Juarez, O., Cho, J., and Barquera, B. **Aspartic acid 397 in subunit B of the Na^+-pumping NADH: quinone oxidoreductase from *Vibrio cholerae* forms part of a sodium binding site, is involved in cation selectivity and affects cation binding site cooperativity**. *Journal of Biological Chemistry*, **288**(43):31241–9, September 2013.

[183] Simpson, L. M. and Oliver, J. D. **Regulation of proteolytic activity of *Vibrio vulnificus* by iron-containing compounds**. *Microbial Pathogenesis*, **14**(3):249–252, March 1993.

[184] Sitnikov, D. M., Schineller, J. B., and Baldwin, T. O. **Transcriptional regulation of bioluminesence genes from *Vibrio fischeri***. *Molecular Microbiology*, **17**(5):801–812, September 1995.

[185] Skulachev, V. P. **The sodium cycle: A novel type of bacterial energetics**. *Journal of Bioenergetics and Biomembranes*, **21**(6):635–647, December 1989.

[186] Smith, P. K., Krohn, R. I., Hermanson, G. T., Mallia, A. K., Gartner, F. H., Provenzano, M. D., Fujimoto, E. K., Goeke, N. M., Olson, B. J.,

and Klenk, D. C. **Measurement of protein using bicinchoninic acid**. *Analytical Biochemistry*, **150**(1):76–85, October 1985.

[187] Sowa, Y., Hotta, H., Homma, M., and Ishijima, A. **Torque-speed relationship of the Na^+-driven flagellar motor of *Vibrio alginolyticus***. *Journal of Molecular Biology*, **327**(5):1043–1051, April 2003.

[188] Sowa, Y. and Berry, R. M. **Bacterial flagellar motor**. *Quarterly Reviews of Biophysics*, **41**(2):103–132, May 2008.

[189] Sowa, Y., Rowe, A. D., Leake, M. C., Yakushi, T., Homma, M., Ishijima, A., and Berry, R. M. **Direct observation of steps in rotation of the bacterial flagellar motor**. *Nature*, **437**(7060):916–919, October 2005.

[190] Spangler, B. D. **Structure and function of cholera toxin and the related *Escherichia coli* heat-labile enterotoxin.** *Microbiological Reviews*, **56**(4):622–647, December 1992.

[191] Speelmans, G., Poolman, B., Abee, T., and Konings, W. N. **Energy transduction in the thermophilic anaerobic bacterium *Clostridium fervidus* is exclusively coupled to sodium ions**. *Proceedings of the National Academy of Sciences*, **90**(17):7975–7979, September 1993.

[192] Sperandio, V., Torres, A. G., and Kaper, J. B. **Quorum sensing *Escherichia coli* regulators B and C (QseBC): a novel two-component regulatory system involved in the regulation of flagella and motility by quorum sensing in *E. coli***. *Molecular Microbiology*, **43**(3):809–821, February 2002.

[193] Staroń, A., Sofia, H. J., Dietrich, S., Ulrich, L. E., Liesegang, H., and Mascher, T. **The third pillar of bacterial signal transduction: classification of the extracytoplasmic function (ECF) σ factor protein family**. *Molecular Microbiology*, **74**(3):557–581, November 2009.

[194] Stevens, A. M. and Greenberg, E. P. **Quorum sensing in *Vibrio fischeri*: essential elements for activation of the luminescence genes.** *Journal of Bacteriology*, **179**(2):557–562, January 1997.

[195] Stock, A. M., Robinson, V. L., and Goudreau, P. N. **Two-component signal transduction**. *Annual Review of Biochemistry*, **69**(1):183–215, June 2000.

[196] Stoebner, J. A. and Payne, S. M. **Iron-regulated hemolysin production and utilization of heme and hemoglobin by *Vibrio cholerae***. *Infection and Immunity*, **56**(11):2891–2895, November 1988.

[197] Stolz, B. and Berg, H. C. **Evidence for interactions between MotA and MotB, torque-generating elements of the flagellar motor of *Escherichia coli*.** *Journal of Bacteriology*, **173**(21):7033–7037, November 1991.

[198] Sudo, Y., Kitade, Y., Furutani, Y., Kojima, M., Kojima, S., Homma, M., and Kandori, H. **Interaction between Na^+ ion and carboxylates of the PomAPomB stator unit studied by ATR-FTIR spectroscopy**. *Biochemistry*, **48**(49):11699–11705, November 2009.

[199] Syed, K. A., Beyhan, S., Correa, N., Queen, J., Liu, J., Peng, F., Satchell, K. J. F., Yildiz, F., and Klose, K. E. **The *Vibrio cholerae* flagellar regulatory hierarchy controls expression of virulence factors**. *Journal of Bacteriology*, **191**(21):6555–6570, November 2009.

[200] Takekawa, N., Li, N., Kojima, S., and Homma, M. **Characterization of PomA mutants defective in the functional assembly of the Na^+-driven flagellar motor in *Vibrio alginolyticus***. *Journal of Bacteriology*, **194**(4):1934–1939, February 2012.

[201] Tang, H., Braun, T. F., and Blair, D. F. **Motility protein complexes in the bacterial flagellar motor.** *Journal of Molecular Biology*, **261**(2):209–221, August 1996.

[202] Tao, Z., Wang, G., Goodisman, J., and Asefa, T. **Accelerated oxidation of epinephrine by silica nanoparticles**. *Langmuir*, **25**(17):10183–10188, May 2009.

[203] Terahara, N., Sano, M., and Ito, M. **A *Bacillus* flagellar motor that can use both Na^+ and K^+ as a coupling ion is converted by a single mutation to use only Na^+**. *PLoS ONE*, **7**(9):e46248, September 2012.

[204] Terashima, H., Koike, M., Kojima, S., and Homma, M. **The flagellar basal body-associated protein FlgT is essential for a novel ring structure in the sodium-driven *Vibrio* motor**. *Journal of Bacteriology*, **192**(21):5609–5615, November 2010.

[205] Terashima, H., Li, N., Sakuma, M., Koike, M., Kojima, S., Homma, M., and Imada, K. **Insight into the assembly mechanism in the supramolecular rings of the sodium-driven *Vibrio* flagellar motor from the structure of FlgT**. *Proceedings of the National Academy of Sciences*, **110**(15):6133–6138, April 2013.

[206] Terauchi, T., Terashima, H., Kojima, S., and Homma, M. **A conserved residue, PomB-F22, in the transmembrane segment of the flagellar stator complex, has a critical role in conducting ions and generating torque**. *Microbiology*, **157**(8):2422–2432, August 2011.

[207] Thompson, J. D., Higgins, D. G., and Gibson, T. J. **CLUSTAL W: improving the sensitivity of progressive multiple sequence alignment through sequence weighting, position-specific gap penalties and weight matrix choice**. *Nucleic Acids Research*, **22**(22):4673–4680, November 1994.

[208] Thormann, K. M. and Paulick, A. **Tuning the flagellar motor**. *Microbiology*, **156**(5):1275–1283, May 2010.

[209] Tusnády, G. and Simon, I. **Principles governing amino acid composition of integral membrane proteins: application to topology prediction**. *Journal of Molecular Biology*, **283**(2):489–506, October 1998.

[210] Tusnády, G. and Simon, I. **The HMMTOP transmembrane topology prediction server**. *Bioinformatics*, **17**(9):849–850, September 2001.

[211] Ulrich, L. E., Koonin, E. V., and Zhulin, I. B. **One-component systems dominate signal transduction in prokaryotes**. *Trends in Microbiology*, **13**(2):52–56, February 2005.

[212] Ünal, C. M., Singh, B., Fleury, C., Singh, K., Chávez de Paz, L., Svensäter, G., and Riesbeck, K. **QseC controls biofilm formation of non-typeable *Haemophilus influenzae* in addition to an AI-2-dependent mechanism**. *International Journal of Medical Microbiology*, **302**(6):261–269, November 2012.

[213] Van Way, S. M., Hosking, E. R., Braun, T. F., and Manson, M. D. **Mot protein assembly into the bacterial flagellum: a model based on mutational analysis of the *motB* gene**. *Journal of Molecular Biology*, **297**(1):7–24, March 2000.

[214] Vance, R. E., Zhu, J., and Mekalanos, J. J. **A constitutively active variant of the quorum-sensing regulator LuxO affects protease production and biofilm formation in *Vibrio cholerae***. *Infection and Immunity*, **71**(5):2571–2576, May 2003.

[215] Verbrugghe, E., Boyen, F., Gaastra, W., Bekhuis, L., Leyman, B., Van Parys, A., Haesebrouck, F., and Pasmans, F. **The complex interplay between stress and bacterial infections in animals**. *Veterinary Microbiology*, **155**(2–4):115–127, March 2012.

[216] Vgenopoulou, I., Gemperli, A. C., and Steuber, J. **Specific modification of a Na^+ binding site in NADH:quinone oxidoreductase from *Klebsiella pneumoniae* with Dicyclohexylcarbodiimide**. *Journal of Bacteriology*, **188**(9):3264–3272, May 2006.

[217] Vimont, S. and Berche, P. **NhaA, an Na^+/H^+ antiporter involved in environmental survival of *Vibrio cholerae***. *Journal of Bacteriology*, **182**(10):2937–2944, May 2000.

[218] von Ballmoos, C., Cook, G. M., and Dimroth, P. **Unique rotary ATP synthase and its biological diversity**. *Annual Review of Biophysics*, **37**(1):43–64, May 2008.

[219] von Heijne, G. **Proline kinks in transmembrane α-helices**. *Journal of Molecular Biology*, **218**(3):499–503, April 1991.

[220] Vorburger, T., Stein, A., Ziegler, U., Kaim, G., and Steuber, J. **Functional role of a conserved aspartic acid residue in the motor of the Na^+-driven flagellum from *Vibrio cholerae***. *Biochimica et Biophysica Acta (BBA) - Bioenergetics*, **1787**(10):1198–1204, October 2009.

[221] Wadhams, G. H. and Armitage, J. P. **Making sense of it all: bacterial chemotaxis**. *Nature Reviews Molecular Cell Biology*, **5**(12):1024–1037, December 2004.

[222] Waldor, M. K. and Mekalanos, J. J. **Lysogenic conversion by a filamentous phage encoding cholera toxin**. *Science*, **272**(5270):1910–1914, June 1996.

[223] Wang, Q., Suzuki, A., Mariconda, S., Porwollik, S., and Harshey, R. M. **Sensing wetness: a new role for the bacterial flagellum.** *The EMBO Journal*, **24**(11):2034–42, June 2005.

[224] Wang, X., Wang, Q., Yang, M., Xiao, J., Liu, Q., Wu, H., and Zhang, Y. **QseBC controls flagellar motility, fimbrial hemagglutination and intracellular virulence in fish pathogen *Edwardsiella tarda***. *Fish & Shellfish Immunology*, **30**(3):944–953, March 2011.

[225] Watnick, P. I. and Kolter, R. **Steps in the development of a *Vibrio cholerae* El Tor biofilm**. *Molecular Microbiology*, **34**(3):586–595, November 1999.

[226] Watnick, P. I., Lauriano, C. M., Klose, K. E., Croal, L., and Kolter, R. **The absence of a flagellum leads to altered colony morphology, biofilm development and virulence in *Vibrio cholerae* O139**. *Molecular Microbiology*, **39**(2):223–235, January 2001.

[227] Weinberg, E. D. **The *Lactobacillus* anomaly: total iron abstinence**. *Perspectives in biology and medicine*, **40**(4):578–583, Summer 1997.

[228] West, A. H. and Stock, A. M. **Histidine kinases and response regulator proteins in two-component signaling systems**. *Trends in Biochemical Sciences*, **26**(6):369–376, June 2001.

[229] Williams, P., Rabsch, W., Methner, U., Voigt, W., Tschäpe, H., and Reissbrodt, R. **Catecholate receptor proteins in *Salmonella enterica*: role in virulence and implications for vaccine development**. *Vaccine*, **24**(18):3840–3844, May 2006.

[230] Williams, S. G., Carmel-Harel, O., and Manning, P. A. **A functional homolog of *Escherichia coli* NhaR in *Vibrio cholerae***. *Journal of Bacteriology*, **180**(3):762–765, February 1998.

[231] Wilson, D. R. and Beveridge, T. J. **Bacterial flagellar filaments and their component flagellins**. *Canadian Journal of Microbiology*, **39**(5):451–472, May 1993.

[232] Yakushi, T., Maki, S., and Homma, M. **Interaction of PomB with the third transmembrane segment of PomA in the Na^+-driven polar flag-**

ellum of *Vibrio alginolyticus*. *Journal of Bacteriology*, **186**(16):5281–5291, August 2004.

[233] Yildiz, F. H., Dolganov, N. A., and Schoolnik, G. K. **VpsR, a member of the response regulators of the two-component regulatory systems, is required for expression of *vps* biosynthesis genes and EPS^{ETr}-associated phenotypes in *Vibrio cholerae* O1 El Tor**. *Journal of Bacteriology*, **183**(5):1716–1726, March 2001.

[234] Yildiz, F. H. and Schoolnik, G. K. ***Vibrio cholerae* O1 El Tor: Identification of a gene cluster required for the rugose colony type, exopolysaccharide production, chlorine resistance, and biofilm formation**. *Proceedings of the National Academy of Sciences*, **96**(7):4028–4033, March 1999.

[235] Yorimitsu, T. and Homma, M. **Na^+-driven flagellar motor of *Vibrio***. *Biochimica et Biophysica Acta (BBA) - Bioenergetics*, **1505**(1):82–93, May 2001.

[236] Yorimitsu, T., Mimaki, A., Yakushi, T., and Homma, M. **The conserved charged residues of the C-terminal region of FliG, a rotor component of the Na^+-driven flagellar motor**. *Journal of Molecular Biology*, **334**(3):567–583, November 2003.

[237] Yorimitsu, T., Sato, K., Asai, Y., Kawagishi, I., and Homma, M. **Functional interaction between PomA and PomB, the Na^+-driven flagellar motor components of *Vibrio alginolyticus***. *Journal of Bacteriology*, **181**(16):5103–5106, August 1999.

[238] Yoshida, S., Sugiyama, S., Hojo, Y., Tokuda, H., and Imae, Y. **Intracellular Na^+ kinetically interferes with the rotation of the Na^+-driven flagellar motors of *Vibrio alginolyticus*.** *Journal of Biological Chemistry*, **265**(33):20346–20350, November 1990.

[239] Zhang, R. G., Scott, D. L., Westbrook, M. L., Nance, S., Spangler, B. D., Shipley, G. G., and Westbrook, E. M. **The three-dimensional crystal structure of cholera toxin**. *Journal of Molecular Biology*, **251**(4):563–573, August 1995.

[240] Zhou, J. and Blair, D. F. **Residues of the cytoplasmic domain of MotA essential for torque generation in the bacterial flagellar motor**. *Journal of Molecular Biology*, **273**(2):428–439, October 1997.

[241] Zhou, J., Lloyd, S. A., and Blair, D. F. **Electrostatic interactions between rotor and stator in the bacterial flagellar motor**. *Proceedings of the National Academy of Sciences*, **95**(11):6436–6441, May 1998.

[242] Zhu, J. and Mekalanos, J. J. **Quorum sensing-dependent biofilms enhance colonization in *Vibrio cholerae***. *Developmental Cell*, **5**(4):647–656, October 2003.

[243] Zhu, S., Homma, M., and Kojima, S. **Intragenic suppressor of a plug deletion nonmotility mutation in PotB, a chimeric stator protein of sodium-driven flagella**. *Journal of Bacteriology*, **194**(24):6728–6735, December 2012.

[244] Zhulin, I. B., Rowsell, E. H., Johnson, M. S., and Taylor, B. L. **Glycerol elicits energy taxis of *Escherichia coli* and *Salmonella typhimurium*.** *Journal of Bacteriology*, **179**(10):3196–3201, May 1997.

Acknowledgements

First of all, my sincere thanks go to Prof. Dr. Julia Fritz-Steuber, who gave me the opportunity to perform my PhD thesis in her work group.

I want to thank Prof. Dr. Hanke for his disposition to attend as second reviewer.

Special thanks also go to Dr. Thomas Vorburger for his advices.

I also want to thank Dr. Birgit Flauger, Bernadette Geißel, Yasmin Kolar and Manuel Müller for their experimental support.

My thanks also go to the former and current members of the Steuber Lab for the inspiring coffee breaks, balcony and after work meetings.

I want to thank my parents, who gave me the opportunity and their support to begin my studies in the first place.

Last but not least, I want to thank Stephan for being there.

Curriculum vitae

Surname	Halang
First name	Petra
Born	17. July 1983
City	Munich

Education

07/2010 – 09/2013	Research associate at the Institute of Microbiology, University of Hohenheim, Stuttgart „Stressful environments: Motility and catecholamine response in *Vibrio cholerae*
09/2004 – 03/2010	University studies at the KIT, Karlsruhe Diploma thesis at the Institute for Applied Biosciences, Department Microbiology, KIT „Physiology and Regulation of the Extracytoplasmic Function σ Factor EcfI from *Bacillus licheniformis* “
09/1994 – 06/2003	Abitur at the Edith-Stein-Gymnasium, Munich

Publications

1. „The function of the Na^+-driven flagellum of *Vibrio cholerae* is determined by osmolality and pH“, P. Halang, S. Leptihn, T. Meier, T. Vorburger, J. Steuber; Journal of Bacteriology, 195(21): 4888-4899, 2013
2. „Serine 26 in the PomB subunit of the flagellar motor is essential for hypermotility of *V. cholerae*“, P. Halang, T. Vorburger, J. Steuber; manuscript under revision, PLOS ONE
3. „Roles of the sodium-translocating NADH-quinone oxidoreductase (NQR) on *Vibrio cholerae* metabolism, motility and osmotic stress resistance“, Y. Minato, S. R. Fassio, J. S. Kirkwood, P. Halang, M. J. Quinn, W. J. Faulkner, A. M. Aagesen, J. Steuber, J. F. Stevens, C. C. Häse; PLOS ONE, 9(5): e97083, 2014